TURUN
YLIOPISTO
UNIVERSITY
OF TURKU

The Network of C/N Balancing, Photosynthesis and Flavodiiron Proteins in the Cyanobacterium *Anabaena* sp. PCC 7120

Towards Bioengineering Strategies

Elisa Werner

TURUN YLIOPISTON JULKAISUJA – ANNALES UNIVERSITATIS TURKUENSIS

SARJA – SER. AI OSA – TOM. 762 | ASTRONOMICA – CHEMICA – PHYSICA – MATHEMATICA | TURKU 2026

TURUN
YLIOPISTO
UNIVERSITY
OF TURKU

THE NETWORK OF C/N BALANCING, PHOTOSYNTHESIS AND FLAVODIIRON PROTEINS IN THE CYANOBACTERIUM ANABAENA SP. PCC 7120

Towards Bioengineering Strategies

Elisa Werner

TURUN YLIOPISTON JULKAISUJA – ANNALES UNIVERSITATIS TURKUENSIS
SARJA – SER. AI OSA – TOM. 762 | ASTRONOMICA - CHEMICA - PHYSICA – MATHEMATICA | TURKU 2026

University of Turku

Faculty of Technology
Department of Life Technologies
Molecular Plant Biology
Doctoral Programme in Technology

Supervised by

Prof. Yagut Allahverdiyeva-Rinne
PhotoMicrobes Group
Molecular Plant Biology
Department of Life Technologies
University of Turku
Turku, Finland

Dr. Tuomas Huokko
Photomicrobes group
Molecular Plant Biology
Department of Life Technologies
University of Turku
Turku, Finland

Dr. Lauri Nikkanen
Molecular Plant Biology
Department of Life Technologies
University of Turku
Turku, Finland

Reviewed by

Prof. Amel Latifi
Aix Marseille Université,
Laboratoire de Chimie Bactérienne
Marseille, France

Prof. Giorgio Perin
Department of Biology
University of Padova
Padova, Italy

Opponent

Dr. Szilvia Tóth
Institute of Plant Biology
HUN-REN Biological Research Centre, Szeged
Szeged, Hungary

ISBN 978-952-02-0695-6 (PRINT)
ISBN 978-952-02-0696-3 (PDF)
ISSN 0082-7002 (Print)
ISSN 2343-3175 (Online)
Painosalama, Turku, Finland 2026

“In Hac Spe Vivo”
-Shakespeare, Pericles

UNIVERSITY OF TURKU
Faculty of Technology
Department of Life Technologies
Molecular Plant Biology
ELISA WERNER: The network of C/N balancing, photosynthesis and flavodiiron proteins in the cyanobacterium Anabaena sp. PCC 7120 – Towards Bioengineering Strategies
Doctoral Dissertation, 122 pp.
Doctoral Programme in Technology
June 2026

ABSTRACT

The heterocyst-forming cyanobacterium *Anabaena* sp. PCC 7120 can perform oxygenic photosynthesis in vegetative cells and simultaneously O_2-sensitive N_2 fixation in heterocysts. In Paper I, deletion mutants of the photoprotective flavodiiron proteins *flv1A* and *flv3A* were characterized. The deletion of the vegetative cell-specific *flv3A* leads to downregulation of the heterocyst-specific Hup uptake hydrogenase gene. This leads to enhanced H_2 production, suggesting a connection between photosynthetic e^- sinks and N_2 fixation. Moreover, Paper I demonstrates that both Flv1A and Flv3A are required under fluctuating light similar to *Synechocystis*. However, in contrast to *Synechocystis*, where Flv1 and Flv3 are mutually dependent, Flv3A can moderately catalyse the Mehler-like reaction independent from Flv1A. Still, this function of Flv3A requires the presence of Flv2 and Flv4, suggesting some level of cooperation under air-level CO_2. The formation of heterocysts is a transcriptional response to cellular C/N imbalance which is mainly signalled by the central metabolite 2-OG. Paper II demonstrates that deletion of the global transcription factor PacR, an important regulator of C-metabolism, FDPs, and photosynthesis, leads to enhanced heterocyst formation after shifting the N source from NH_4^+ to NO_3^-, most likely due to internal N shortage. This was primarily attributed to the downregulation of NO_3^- uptake, which is directly regulated by PacR. Moreover, impaired regulation of photosynthetic components in the absence of PacR may have led to the slight decrease in the size of the photo-reducible Fed-pool, thereby decreasing the availability of reducing equivalents required for NO_3^- reduction. Additionally, NH_4^+ assimilation was disrupted due to GS/GOGAT-cycle impairment. Thus, these findings indicate that PacR functions as a regulator of N metabolism and C/N balancing and confirm the regulation of flavodiiron proteins.

KEYWORDS: Anabaena sp. PCC 7120, heterocysts, photosynthesis, flavodiiron proteins, PacR, carbon–nitrogen balance

TURUN YLIOPISTO
Teknillinen tiedekunta
Elämäntekniikan laitos
Molekyylikasvibiologia
ELISA WERNER: C/N-tasapainon, fotosynteesin ja flavodiironiproteiinien verkosto syanobakteerissa Anabaena sp. PCC 7120– kohti biotekniikan strategioita
Väitöskirja, 122 s.
Teknologian tohtoriohjelma
Kesäkuu 2026

TIIVISTELMÄ

Syanobakteeri *Anabaena* sp. PCC 7120 muodostaa erikoistuneita soluja, heterokystejä, vasteena solunsisäiseen hiili–typpiepätasapainoon. Tämän ansiosta se pystyy yhdistämään happea vapauttavan fotosynteesin vegetatiivisissa soluissa ja hapelle herkän typen sidonnan heterokysteissä. Näiden kahden solutyypin aineenvaihdunta ja säätelyverkostot ovat tiiviissä vuorovaikutuksessa. Väitöskirjassani karakterisoin *flv1A*- ja *flv3A*-deleetiomutantteja. Nämä geenit koodaavat flavodiironiproteiineja, jotka toimivat fotosynteesin valosuojaavina elektroninieluina. Tulokseni osoittavat, että vegetatiivisissa soluissa ilmentyvän *flv3A*-geenin poisto heikentää heterokysteissä toimivan Hup-hydrogenaasin ilmentymistä. Tämä lisäsi vedyn tuotantoa jopa normaalissa ilman kaasukoostumuksessa ja osoittaa yhteyden fotosynteesin elektroninielujen ja suuren elektronimäärän vaativan typen sidonnan välillä. Lisäksi transkriptiotekijä FurA saattaa säädellä raudan jakautumista näiden prosessien välillä. Tulokseni osoittavat myös, että Flv1A- ja Flv3A-proteiinit ovat välttämättömiä vaihtelevissa valo-olosuhteissa. Toisin kuin syanobakteeri *Synechocystiksessä*, jossa Flv1 ja Flv3 toimivat yhdessä, *Anabaenassa* Flv3A voi katalysoida Mehler-tyyppisen reaktion ilman Flv1A:ta, mutta tämä riippuu Flv2- ja Flv4-proteiinien toiminnasta. Lisäksi osoitin, että globaalin transkriptiotekijän PacR:n poisto lisää heterokystien muodostumista siirryttäessä ammoniumista nitraattiin, todennäköisesti solunsisäisen typenpuutteen seurauksena. Tämä johtuu nitraatinoton voimakkaasta vähenemisestä sekä häiriöistä fotosynteesin ja GS/GOGAT-syklin säätelyssä. Yhteenvetona tulokseni osoittavat PacR:n keskeiseksi säätelijäksi typen aineenvaihdunnassa, solunsisäisen hiili–typpitasapainon ylläpidossa sekä flavodiironiproteiinien ilmentymisessä.

AVAINSANAT: Anabaena sp. PCC 7120, heterokystit, fotosynteesi, flavodiironiproteiinit, PacR, hiili–typpitasapaino

Table of Contents

Abbreviations

Acetly-CoA	Acetyl coenzyme A
ADH	Alanine dehydrogenase
ADP	Adenosine diphosphate
AET	Alternative e- transport
Ala	Alanine
APC	Allophycocyanin
Ar	Argon
Arg	Arginine
ARTO	Alternative respiratory terminal oxidase
Asp	Aspartate
ATP	adenosine triphosphate
C	Carbon
CBB	Calvin Benson Bassham
CCM	Carbon Concentration Mechanism
CET	Cyclic e- transport
Chl	Chlorophyll
C_i	Inorganic carbon
CO_2	Carbon dioxide
Cox	Cytochrome c oxidase
CS	Control strain
Cyd	Cytochrome *bd* quinol oxidase
Cyt b_6f	Cytochrome b_6f
Cyt c_6	Cytochrome c_6
Cyt *f*	Cytochrome *f*
D_2	Deuterium
DIRKs	Dark interval relaxation kinetics
DNA	Desoxyribonucleic acid
e^-	Electron
ECS	Electrochromic shift
ED	Entner-Doudoroff
EMP	Embden-Meyerhof-Parnas

FAD	Flavin adenine dinucleotide
Fe	Iron
FDP	Flavodiiron proteins
Fed	Ferredoxin
Flv	A-type flavoprotein
F_m^D	Maximal fluorescence under dark adaptation
FMN	Flavin-mononucleotide
FNR	Ferredoxin-NAD(P)H oxidoreductase
F_0 rise	Transient post-illumination fluorescence
F_s	Steady-state-level fluorescence
Ga	billion years ago
GAP	Glyceraldehyde-3-Phosphate
gH^+	Conductivity of the thylakoid membrane
Gln	Glutamine
Glu	Glutamate
GOE	Great oxygenation event
GOGAT	Glutamate synthetase
GS	Glutamine synthetase
H_2	Hydrogen
H^+	proton
HC	High CO_2 concentration
HCO_3^-	Bicarbonate
Hep	Heterocyst envelope polysaccharides
Hgl	Heterocyst-specific glycolipids
HL	High light
H_2O	Water
Hox	Bidirectional hydrogenase
HPLC	High pressure liquid chromatography
Hup	Uptake hydrogenase
IDH	Isocitrate dehydrogenase
IF	Inactivation factor
LC	Atmospheric CO_2 concentration
LET	Linear electron transport
LTTR	LysR type transcriptional regulator
MIMS	Membrane Inlet Mass Spectrometry
MT	Multiple turnover
N	Combined nitrogen
N_2	Atmospheric nitrogen
NAD(P)H	Nicotinamide adenine dinucleotide (phosphate)
NAGK	N-acetyl glutamate kinase

NDH-1	NAD(P)H:quinone oxidoreductase
NH_3	Ammonia
NH_4^+	Ammonium
Nm	Neomycin
NO_2^-	Nitrite
NO_3^-	Nitrate
NO	Nitric oxide
NOE	Neoproterozoic oxygenation event
nPG	*n*-propyl gallate
O_2	Oxygen
OAC	Ornithine-Ammonia-Cycle
OCP	Orange Carotenoid Protein
OD_{750}	Optical density at 750 nm
OEC	Oxygen Evolving Complex
2-OG	2-Oxoglutarate
OPP	Oxidative pentose phosphate
PAM	Pulse amplitude modulated
PBS	Phycobilisomes
PC	Phycocyanin
Pc	Plastocyanine
PCR	Polymerase chain reaction
PE	Phycoerythrin
PEC	Phycoerythrocyanin
PETC	Photosynthetic e- transport chain
2-PG	2-Phosphoglycolate
3-PGA	3-Phosphoglyceric acid
ΔpH	Proton concentration gradient
Pheo	Pheophytin
P_i	Inorganic phosphate
pmf	Proton motive force
PQ	Plastoquinone
PQH_2	Plastoquinol
PSI	Photosystem I
PSII	Photosystem II
Ptox	Plastid terminal oxidase
Pyr	Pyruvate
RC	Reaction center
Redox	Reduction/oxidation
RETC	Respiratory e- transport chain
RIN	RNA integrity number

RNA	Ribonucleic acid
RNA-seq	RNA sequencing
ROS	Reactive oxygen species
rRNA	ribosomal RNA
RTO	Respiratory terminal oxidase
RT-qPCR	Reverse transcription quantitative PCR
RuBisCO	Ribulose bisphosphate carboxylase/oxygenase
RuBP	Ribulose-1,5-bisphosphate
SP	Saturating pulse
Spec	Spectinomycin
TCA	Tricarboxylic acid
Trx	Thioredoxin
$v\mathrm{H}^{+}$	Thylakoid proton flux
WT	Wild type
Y(I)	effective quantum yield of PSI
Y(II)	effective quantum yield of PSII
Y(NA)	Acceptor side limitation of PSI
Y(ND)	Donor side limitation of PSI

List of Original Publications

This dissertation is based on the following original publications, which are referred to in the text by their Roman numerals:

I Santana-Sánchez A, Nikkanen L, Werner E, Tóth G, Ermakova M, Kosourov S, Walter J, He M, Aro EM, Allahverdiyeva Y. Flv3A facilitates O2 photoreduction and affects H2 photoproduction independently of Flv1A in diazotrophic Anabaena filaments. New Phytologist. 2023; 237(1):126-39. https://doi.org/10.1111/nph.18506

II Werner E, Huokko T, Santana-Sánchez A, Picossi S, Nikkanen L, Herrero A, Allahverdiyeva Y. The role of the LysR-type transcription factor PacR in regulating nitrogen metabolism in Anabaena sp. PCC7120. Physiologia Plantarum. 2025; 177(3):e70248. https://doi.org/10.1111/ppl.70248

1 Introduction

1.1 The cyanobacterium *Anabaena*: Evolution, diversity and ecological role of multicellularity and atmospheric nitrogen (N_2) fixation

1.1.1 Evolution

The emergence of cyanobacteria is placed during the Archean Eon between 3.5-2.0 billion years ago (Ga) (Flores & Herrero, 2010; Och & Shields-Zhou, 2012; Sánchez-Baracaldo et al., 2022; Schirrmeister et al., 2013, 2016). They spread and diversified at the end of the Archean (Sánchez-Baracaldo et al., 2022; Schirrmeister et al., 2016), probably causing rising oxygen (O_2) levels, leading to the great oxygenation event (GOE) (Sánchez-Baracaldo et al., 2022; Schirrmeister et al., 2013, 2016). The emergence of multicellularity in cyanobacteria substantially increased diversification rates. Most extant cyanobacterial lineages (both multi- and unicellular) appear to have evolved from an ancient multicellular lineage (Schirrmeister et al., 2016). Multicellularity provided several adaptive advantages, including improved biofilm formation by improving motility and allowing optimal positioning and surface attachment (Sánchez-Baracaldo et al., 2022; Schirrmeister et al., 2016). Moreover, adopting a cooperative strategy could have increased fitness due to economies of scale and metabolic advantages (Schirrmeister et al., 2013). Biofilms containing filamentous cyanobacteria were widespread during the Proterozoic and likely played a major role in global primary production (Sánchez-Baracaldo et al., 2022).

Possibly simultaneously with the emergence of multicellularity (2.45-2.1 Ga), the capability to fix N_2 and form heterocysts - specialized microoxic cells that fix N_2 (described in detail in chapter 1.6.), emerged in cyanobacteria (Flores, Arévalo, et al., 2019; Gallego et al., 2025). The ability of some vegetative cells to differentiate into heterocysts, interspersed among to vegetative cells, emerged only once during evolution, giving rise to the monophyletic group of heterocystous cyanobacteria (Flores, Arévalo, et al., 2019; Gallego et al., 2025), which includes the orders *Nostocales* (including *Anabaena* sp. PCC7120) and *Stigonematales* (Sánchez-Baracaldo et al., 2022; Zeng & Zhang, 2022). Nitrogenase, the O_2 sensitive enzyme responsible for N_2 fixation in heterocysts, was acquired early in cyanobacterial

evolution and occurs in both unicellular and filamentous taxa (Sánchez-Baracaldo et al., 2022). Since nitrogenase is inactivated by O_2, the evolutionary pressure to limit O_2 diffusion to nitrogenase was likely driven by rising O_2 levels during the GOE (Flores, Arévalo, et al., 2019; Gallego et al., 2025). This led to the evolution of various strategies to protect nitrogenase, including: 1) temporal separation (alternating N_2 fixation and oxygenic photosynthesis in time), 2) spatial separation (compartmentalizing the two processes, e.g., in heterocysts, whose outer layers limit O_2 diffusion, and vegetative cells), or 3) symbiotic specialization (genome reduction and loss of oxygenic photosynthesis in a symbiotic relationship (Cumino et al., 2007; Gallego et al., 2025; Sánchez-Baracaldo et al., 2022; Stal, 2015). In the Neoproterozoic, cyanobacteria, including N_2 fixing cyanobacteria, also started colonizing the open ocean as part of the phytoplanktonic expansion that followed extreme changes of biogeochemical cycles (Sánchez-Baracaldo et al., 2022; Schirrmeister et al., 2016). This transition may have significantly increased the biogeochemical impact of oxygenic photosynthesis and led to cyanobacteria becoming the major primary producers in the oceans during the Proterozoic. The phytoplankton mediated carbon (C) and N cycling in the open ocean led to increased C sedimentation, which in turn increased O_2 availability. This established a positive feedback loop between nutrient cycling and O_2 generation, leading to the development of the O_2 rich Phanerozoic biosphere (Hohmann-Marriott & Blankenship, 2011; Sánchez-Baracaldo et al., 2022). This Neoproterozoic oxygenation event (NOE) occurred during the Neoproterozoic – Phanerozoic transition between 0.85-0.54 Ga and likely raised O_2 levels near present levels (Och & Shields-Zhou, 2012).

1.1.2 Diversity

Classification. Cyanobacteria are gram negative bacteria (Hoiczyk & Hansel, 2000), that are, despite being monophyletic, one of the morphologically most diverse groups of procaryotic organisms (Stal, 2015) with an estimated number of up to 8,000 species (Allaf & Peerhossaini, 2022). They vary in size from < 0.5 to 30 µm, may be unicellular or multicellular (Stal, 2015), can reversibly or terminally differentiate cells into e.g. akinetes, heterocysts or aerotopes and form (endo-)symbiotic relationships. Due to diversified growth strategies, cyanobacteria can grow in the majority of terrestrial and aquatic habitats, including also those with extreme conditions (Kaštovský, 2024; Schirrmeister et al., 2013), like hot springs and Antarctic rocks (Malatinszky et al., 2017).

To classify cyanobacteria, three different systems can be applied: a botanical/procaryotic code (Pinevich & Averina, 2024) a bacteriological system and a phylogenetic system. In the bacteriological system, Rippka et al., 1979, classified cyanobacteria into subsections based on structural and developmental

characteristics. Subsections I (binary fission) and II (multiple fission) include unicellular species, whereas subsections III (no cellular differentiation), IV (presence of heterocysts), and V (presence of heterocysts and true branching) comprise multicellular forms. Notably, species in subsections IV and V can form terminally differentiated cells. However, none of these morphological subsections are monophyletic and multiple evolutionary transitions between uni- and multicellularity have taken place (Schirrmeister et al., 2013; Stal, 2015). The phylogenetic system is based on evolutionary relationships determined by molecular markers e.g. 16S ribonucleic acid (RNA) (Pinevich & Averina, 2024).

Currently, the taxonomy of cyanobacteria is based on a polyphasic approach, integrating e.g., morphology and ultrastructure, metabolism, chemical composition (e.g., photosynthetic pigment composition) and genetic data (e.g., ribosomal RNA (rRNA)) (Badger & Price, 2003; Pinevich & Averina, 2024). The most common approach is based on the phylogenetically distinct protein components of different carboxysome types and different Ribulose bisphosphate carboxylase/oxygenase (RuBisCO) types (Badger & Price, 2003; Rae, 2013). α-cyanobacteria possess α-carboxysomes and the 1A form of RuBisCO and are predominantly found in the oceans (e.g. the marine picocyanobacteria *Synechococcus* and *Prochlorococcus*) (Badger & Price, 2003; Rae, 2013). Recent global freshwater metagenomics show that, contrary to previous findings, α-picocyanobacteria are also widespread in these habitats and can dominate the picocyanobacterial community in freshwater (Cabello-Yeves et al., 2022). In contrast, β-cyanobacteria, which represent the majority of species, have β-carboxysomes and the 1B form of RuBisCO, and are found mainly in freshwater and estuarine environments (Badger & Price, 2003; Rae, 2013).

Anabaena sp. PCC 7120. The genus *Anabaena* belongs to the order *Nostocales* and family *Nostocaceae*, following the procaryotic code. *Anabaena* is classified as subsection IV in the bacteriological system (Flores, Picossi, et al., 2019; Rajaniemi et al., 2005) and as a β-cyanobacterium (Herrero & Flores, 2008; Price et al., 2008) in the polyphasic approach (Prasanna et al., 2006). Members of the order of *Nostocales* are characterized by their ability to form the specialized heterocyst cell type under N deprivation (Flores, Picossi, et al., 2019). They form filaments, consisting of many cells, sometimes extending to hundreds (Flores, Picossi, et al., 2019). Species classified as *Anabaena* are dominant in the planktonic composition of freshwater lakes, ponds and reservoirs as well as in brackish water bodies globally and in some lineages also occur in terrestrial habitats (Halinen et al., 2008). In addition to free-living forms, *Anabaena* are found as symbionts of the water fern *Azolla* (Prasanna et al., 2006).

The cells within *Anabaena* filaments can differentiate into at least four different cell types: vegetative cells that perform photosynthesis and carbon dioxide (CO_2) fixation, heterocysts responsible for N_2 fixation forming in response to diazotrophic

conditions, akinetes with a spore-like function which form in response to energy limitation, and hormogonia which are short motile filaments involved in reproduction and dispersal, formed in response to environmental cues such as combined nitrogen (N) deprivation or a plant hormogonium-inducing factor (Flores & Herrero, 2010). While the genus *Anabaena* is environmentally important, it is also widely used for genetic manipulation (Prasanna et al., 2006). due to a highly efficient conjugation system available for gene transfer (Kaneko et al., 2001). Thus, *Anabaena* is frequently used to study cellular differentiation, pattern formation and N_2 fixation (Kaneko et al., 2001). The freshwater *Anabaena* sp. PCC7120 (hereafter *Anabaena*) (Kaneko et al., 2001; Kaštovský, 2024; Pereira et al., 2005) is a widely used model organism for the order of *Nostocales* and to study heterocyst differentiation (Flores, Picossi, et al., 2019; Nicolaisen, Hahn, et al., 2009; Nieves-Morión et al., 2021).

Anabaena is a truly pluricellular and pluripotent bacterium with multiple functionally distinct cell types performing specialized roles with the entire filament operating as an organism unit. This integration is reflected in coordinated behaviours such as circadian rhythm in the exchange of nutrients and regulatory molecules (e.g., morphogens) between different cell types (Flores & Herrero, 2010; Valladares & Herrero, 2025). While individual vegetative cells of a filament have a cytoplasmic membrane and peptidoglycan layer(s), the filament shares a continuous outer membrane and a common periplasmic space. This shared periplasm is proposed to facilitate intercellular communication and metabolic exchange (Flores, Picossi, et al., 2019) although evidence remains inconclusive (Zeng & Zhang, 2022; L. C. Zhang et al., 2008). At the cell poles, *Anabaena* forms specialized multiprotein complexes, the septal junctions. These connect adjacent cells by traversing through nanopores formed in the septal peptidoglycan (Kieninger & Maldener, 2021). There is sufficient evidence that an exchange of molecules with the cytoplasm of adjacent cells takes place via these septal junctions (Nicolaisen, Mariscal, et al., 2009; Valladares & Herrero, 2025; K. Wang et al., 2024; Zeng & Zhang, 2022).

Under nitrogen (N)- deprived conditions, where combined N sources such as nitrate (NO_3^-) or ammonium (NH_4^+)) are absent in the medium (diazotrophic conditions), *Anabaena* differentiates specialized heterocysts (Flores & Herrero, 2010). These heterocysts are intercalated along the filament, usually spaced at intervals of ∼10-15 cells, although occasionally terminal heterocyst positions can also occur depending on the species (Flores, Picossi, et al., 2019; Nieves-Morión et al., 2021). The process of heterocyst differentiation involves tightly regulated structural, biochemical and genetic modifications, which result in some marked physiological features: Heterocysts possess a specialized cell envelope, which is composed of an inner heterocyst-specific glycolipid (Hgl) layer to reduce O_2 diffusion, and an outer heterocyst envelope polysaccharide (Hep) layer to provide mechanical protection for the fragile Hgl layer (Flores, Picossi, et al., 2019;

Nicolaisen, Hahn, et al., 2009). The interface between heterocysts and neighbouring vegetative cells is narrowed into a "neck" (Flores, Picossi, et al., 2019) where septal junctions enable exchange of metabolites with vegetative cells (Flores et al., 2016). Here, O_2 and N_2 may enter the heterocyst across the periplasm in a regulated manner – however there is also limited diffusion of gases through the cell envelope (Stal, 2017; Walsby, 2007). It is also here where cyanophycine granules, a storage polymer for N, are found (Flores, Arévalo, et al., 2019). Heterocyst thylakoid membranes are organized into "honeycomb membranes", which are only found at heterocyst poles and are only dedicated to respiration (Flores, Picossi, et al., 2019) to maintain microoxic conditions by consuming residual O_2 together with other processes e.g. the Mehler-like reaction (Flores, Picossi, et al., 2019; Harish & Seth, 2020).

Heterocyst differentiation is primarily regulated via the intracellular C/N ratio, which in cyanobacteria, including *Anabaena*, is indicated by 2-oxoglutarate (2-OG) levels (see chapter 1.5.2. for more details). However, the presence of heterocysts does not guarantee active N_2 fixation, which may be downregulated even when heterocysts are formed. Moreover, in some cases, heterocysts persist in the presence of N. Likely, heterocystous cyanobacteria can only outperform other species under N limiting conditions, indicated by the observation that in natural environments heterocysts are almost always present (Stal, 2015).

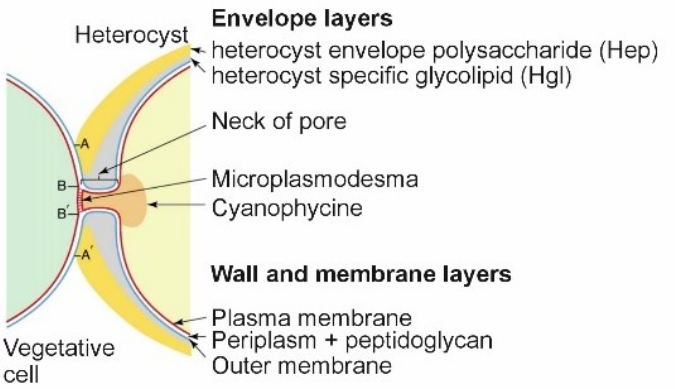

Figure 1. Longitudal section through the heterocyst-vegetative cell junction in filamentous cyanobacteria. Heterocysts contact the cell membrane of vegetative cells via the pore structure, which consists of the following components: A narrow channel of cytoplasm, which often contains cyanophycine; it is surrounded by the heterocyst plasma membrane which is in contact with the vegetative cell plasmamembrane; the contact area forms a microplasmodesma (or septal junction: B, B'), this is where O_2 and N_2 may enter the heterocyst across the periplasm in a regulated manner (next to diffusion through the cell envelope); the periplasmic space including the peptidoglycan layer, which is shared with the vegetative cell; as well as the outer membrane which is shared by all cells of the filament. The pore is constricted by the thick layers of the heterocyst envelope, consisting of the Hep and Hgl layers, which is in contact with the vegetative cell from A to A' (Stal, 2017; Walsby, 2007; K. Wang et al., 2024). Image adapted from Walsby et al., 2007 (Elsevier license: 6202090348159, doi:10.1016/j.tim.2007.06.007)

1.1.3 Ecological Significance

Cyanobacteria and Microalgae are the main primary producers in aquatic ecosystems, where they are known as phytoplankton, which makes up less than 1 % of the photosynthetic biomass on earth. Still, phytoplankton activity amounts to about 50 % of global primary production (Falkowski, 2012; Thoré et al., 2023). Cyanobacteria (principally the genera *Prochlorococcus* and *Synechococcus*) account for approximately 25 % of global marine primary production, due to their widespread distribution across the world's marine ecosystems (Lucius & Hagemann, 2024; Renström-Keliner et al., 1990). In addition to producing O_2, cyanobacteria play a key role in shaping global cycles of C, N/N_2, iron (Fe), reduction/oxidation (redox) sensitive trace metals and sulphur (Sánchez-Baracaldo et al., 2022; Schirrmeister et al., 2016). Because bioavailability of N is a key limiting factor, its supply influences global primary productivity (Sánchez-Baracaldo et al., 2022). It is estimated that 60 % of the fixed N input into the global N cycle and 80-90 % of N available to terrestrial plants originates from biological N_2 fixation. This process is restricted to diazotrophic microorganisms, including cyanobacteria, and some archea (Alleman & Peters, 2023; Cumino et al., 2007). These diazotrophs are found in most ecological niches and in symbiotic relationships e.g. with crops (Alleman & Peters, 2023). Cyanobacteria alone fix 200 million tons of N_2 per year (Perin et al., 2021; Picossi et al., 2015; Schirrmeister et al., 2016). For example, the free-floating *Anabaena* sp. significantly contributes to C and N economy of multiple ecosystems (Perin et al., 2021) as one of the dominant species in freshwater and brackish water ecosystems (Halinen et al., 2008).

Another key factor contributing to the ecological and evolutionary significance of cyanobacteria is their ability to form endosymbiotic relationships (Schirrmeister et al., 2016). Due to an endosymbiotic event between a basal cyanobacterium (closely related to *Gloeomargarita*) and a protist, the clade of photosynthetic eukaryotes (including glaucophytes, red algae, green algae, and land plants) was formed around 1.9-1.25 Ga (Hohmann-Marriott & Blankenship, 2011; Sánchez-Baracaldo et al., 2022). Moreover, cyanobacteria form a wide range of symbiotic relationships with taxonomically diverse hosts. Symbiotic cyanobacteria include unicellular, filamentous, diazotrophic (N_2 fixing) and non-diazotrophic species. The capability to fix N_2 is a particularly common trait among cyanobacterial (endo-) symbionts, since it enables hosts to grow in areas deficient in bioavailable N (Mishra et al., 2021; Ran et al., 2010; Sánchez-Baracaldo et al., 2022) and may also enable the maintenance of microoxic conditions in the symbionts needed for N_2 fixation by nitrogenase (A. Mishra et al., 2021).

1.2 Photosynthesis in cyanobacteria

1.2.1 Photosynthesis – an overview

Oxygenic photosynthesis is the process by which CO_2 is converted into carbohydrates using photosynthetically active radiation (400-700 nm) as the energy source to drive water (H_2O) splitting and electron (e^-) transfer. The overall reaction of photosynthesis can be summarized as: $6\ H_2O + 6\ CO_2 \rightarrow C_6H_{12}O_6 + 6\ O_2$. In the light-reactions of photosynthesis, solar energy is captured and harnessed to drive the production of nicotinamide adenine dinucleotide (NADPH) and adenosine triphosphate (ATP), which are subsequently used to power the downstream metabolism e.g. CO_2 fixation (see chapter 1.3.). H_2O serves as the e^- donor, resulting in the evolution of O_2 as a byproduct. The light reactions take place in the thylakoid membrane through a series of coupled redox-reactions which make up the photosynthetic e^- transport chain (PETC) (Schmidt-Rohr, 2021; Vermaas & Fj, 2001).

The four major protein complexes that drive the light reactions are the photosynthetic pigment protein complexes photosystem II (PSII) and photosystem I (PSI), the cytochrome b_6f (Cyt b_6f) complex and ATP synthase. After splitting of H_2O at PSII, electrons are passed via plastoquinones (PQ) to Cyt b_6f and then via e.g. plastocyanine (Pc) or cytochrome c_6 (Cyt c_6) in cyanobacteria to PSI. During linear e^- transport (LET), PSI reduces ferredoxin (Fed), which subsequently donates electrons to ferredoxin-NAD(P)H oxidoreductase (FNR), which then reduces NADPH, the carrier of reducing power for downstream metabolic processes. During the flow of electrons through the thylakoid membrane, a proton motive force (*pmf*) is generated, which is harnessed by ATP synthase to produce ATP, the energy carrier for downstream metabolic processes. The PETC is described in more detail below.

1.2.2 The LET

In cyanobacteria, light harvesting is initiated/mediated by antennae complexes called phycobilisomes (PBS) (Stadnichuk et al., 2015). PBS are attached to the surface of the thylakoid membrane at the cytoplasmatic side (Saenger et al., 2002), where they function as the primary antennae of PSII (Calzadilla & Kirilovsky, 2020). However, PBS can transfer energy to both PSII and PSI (Mullineaux, 2014). PBS mainly consist of phycobiliproteins, which covalently bind different kinds of linear tetrapyrroles chromophores called phycobilins (Stadnichuk et al., 2015; Sui, 2021). There are four primary types of phycobiliproteins, containing distinct phycobilins with absorption capacities between 500-670 nm: allophycocyanin (APC), phycocyanin (PC), phycoerythrin (PE) and phycoerythrocyanin (PEC). APC and PC

are universally present in PBS, while PEC is utilized only by a subset of cyanobacteria (Calzadilla & Kirilovsky, 2020). In *Anabaena*, APC, PC and PEC are found (Ducret et al., 1996). The PBS occurs in a variety of configurations, which were described previously (Calzadilla & Kirilovsky, 2020; GLAUSER et al., 1992; Grettenberger et al., 2024; Sui, 2021). In cyanobacteria, PBSs are typically of the hemidiscoidal type, with a central triangular core from which six peripheral rods radiate (Ducret et al., 1996). In *Anabaena* a variant of the hemidiscoidal PBS is found (described in Ducret et al., 1996 and Glauser et al., 1992).

Excitation energy in the PBS is transmitted via Förster-Resonance-Energy-Transfer (FRET). Transfer starts from the phycobiliprotein absorbing at shorter wavelengths, thus PE and PEC (if present), and then continues via PC and then APC in the PBS core. Finally, the energy is funnelled to the terminal emitters (ApcD/ApcE), which channel the excitation energy to the reaction center (RC) chlorophyll (Chl) *a* special pair (P680) of PSII, initiating the PETC (Adir et al., 2020).

PSII is prevalently found as a homodimer *in vivo*. Each monomer consists of 20 protein subunits and 77 cofactors. It contains a Q type/type II RC where the terminal e^- acceptor is a quinone. A recent cryo e^- microscopy (EM) structure of cyanobacterial PSII is available (Gisriel et al., 2022). The most important protein subunits of the PSII monomer are the heterodimeric RC core proteins D1 and D2, Chl binding inner antenna subunits CP43 and CP47. Moreover, the Oxygen Evolving Complex (OEC) is integrated into the RC (Hohmann-Marriott & Blankenship, 2011), and sits at the membrane-lumen interface, to provide PSII with e^- from H_2O (Raymond & Blankenship, 2008). The PSII core complex also contains a large number of low-molecular-weight intrinsic proteins, which play roles e.g., in assembly, stabilization, and photoprotection. However, all redox-active cofactors are bound to the RC proteins D1 and D2 (Hankamer et al., 2001).

Upon excitation energy transfer from the inner antenna complexes, the primary e^- donor P680 is excited, generating the P680* state (Schmidt-Rohr, 2021). This enables charge separation, where pheophytin (Pheo) accepts the excited e^- from P680*, forming $Pheo^{-}\bullet$ and leaving behind the highly oxidizing energy $P680^{+}\bullet$. This is an energetically downhill process, which reduces the probability of direct charge recombination of $P680^{+}\bullet$ and $Pheo^{-}\bullet$ into the ground state of P680 (Schmidt-Rohr, 2021). However, the precise mechanism of primary charge separation is still under debate (Nguyen et al., 2023). The high-energy e^- deficient $P680^{+}\bullet$ can now take up one e^- from the redox-active TyrZ, regenerating P680 and producing high-energy e^- deficient TyrZ•/ proton (H+), which is subsequently reduced by an e^- deriving from H_2O splitting (Loll et al., 2005; Schmidt-Rohr, 2021). In one Kok-cycle, the Mn_4CaO_5 cluster of the OEC accumulates four oxidizing equivalents (corresponding to the different s states) driven by charge separation at P680. These oxidizing

equivalents are then used for H_2O oxidation resulting in two molecules of H_2O being split and four protons and one O_2 being generated (Guo et al., 2024; Schmidt-Rohr, 2021). Following primary charge separation in PSII, Pheo-• is oxidized back to Pheo by the first PQ e^- acceptor Q_A in a spontaneous redox-reaction. Q_A-• is then oxidized back to Q_A via a redox-reaction with the second PQ Q_B. After two sequential reductions (electrons from two turnovers of PSII) and protonations via H^+ from the cytoplasmatic side, plastoquinol Q_BH_2 is released from the Q_B site as PQH_2 and is replaced by a new PQ (Loll et al., 2005; Schmidt-Rohr, 2021). Thus, PSII formally pumps four protons from the cytosol to the lumen via splitting of H_2O molecules in the lumen and generating two Q_BH_2 at the cytosolic side of the thylakoid membrane (Schmidt-Rohr, 2021). PQH_2 next delivers e^- to the Cyt b_6f complex.

The Cyt *b6f* complex is a dimeric integral membrane-protein complex. It has four major subunits: Cyt *f*, Cyt b_6, the Rieske protein and subunit IV and four minor subunits (Baniulis et al., 2008). It performs the Q cycle, where it oxidizes PQH_2 and reduces PQ. In the first Q half-cycle, PQH_2 binds at the Qp site of Cyt b_6f and transfers one e^- onto the high and one e^- onto the low potential branches of Cyt b_6f, while the protons enter the lumenal space. In the high-potential branch an e^- is transferred to Fe^{3+} in the $[Fe_2S_2]$ (or 2Fe-2S) cluster of the Rieske protein. The reduced Fe-S-cluster of the Rieske-protein is oxidized by Fe^{3+} in Cyt *f*. On the low-potential branch e^- are transferred through heme b_p to heme b_n (and possibly heme c_n) and then to the Q_n PQ binding site proximal to the cytoplasm, where PQ takes up one H^+ from the stroma, forming PQH•. The energetically uphill proton-pumping redox reaction is possible since it is coupled with the energetically downhill reduction of the Rieske protein. In the second half-cycle, another PQH_2 molecule is oxidized at the Q_p site, which adds two more protons to the lumen. This reduces another Fe^{3+} in a $[Fe_2S_2]$-cluster and PQH• at the stroma side gets fully reduced to PQH_2, which removes another H^+ from the stroma contributing further to the proton concentration gradient (Malone et al., 2021).

Then, e^- are transported from the Cyt *f* subunit of Cyt b_6f via a soluble e^- carrier (Fedorov et al., 2019). Cyt c_6 and Pc both fulfil a similar function as the soluble e^- donor from Cyt b_6f to PSI (in photosynthesis) and to Cyt *c* oxidase (in respiration) in all known cyanobacteria. Cyt c_6 is highly expressed under copper deficiency, and Pc is expressed under copper sufficient conditions. While Cyt c_6 is downregulated in the presence of copper in vegetative cells of *Anabaena*, it remains expressed in heterocysts where it fulfils an essential role independent of Pc (Torrado et al., 2019). The soluble e^-carriers then donate electrons to PSI.

PSI is a multi-subunit Chl-protein complex with an FeS type (Type I) reaction centre, where the terminal e^- acceptor is an FeS cluster (Saenger et al., 2002). PSI may however also utilize the PBS for light harvesting (Santabarbara et al., 2024). PSI is mostly trimeric in cyanobacteria (Santabarbara et al., 2024). However,

tetrameric PSI is widespread among heterocyst-forming cyanobacteria such as *Anabaena* (Santabarbara et al., 2024; Watanabe et al., 2011) where it consists of a dimer of a dimers (Kato et al., 2019). The PSI monomer of *Anabaena* is similar to the monomeric unit in the *Synechocystis* trimer (Nagao et al., 2020). The functional unit of PSI is comprised of a core complex and its peripheral light harvesting antennae (Santabarbara et al., 2024) containing about 90 Chl molecules (Saenger et al., 2002). A crystal structure of PSI is available (Malavath et al., 2018). PSI has a highly conserved heterodimeric core, PsaA/PsaB, which coordinates the components of the PETC (Saenger et al., 2002). The primary charge separation takes place upon excitation at special RC Chl_{1A}/Chl_{1B} pair (P700) (Cherepanov et al., 2022). Then, P700* donates one electron to the PETC forming $P700^{+}$•, and thus initiates e^- flow through the PETC (Santabarbara et al., 2024). $P700^{+}$• then received an e^- from Cyt c_6 or Pc. The transfer of electrons towards the cytoplasmatic side occurs via Chl A_0 (primary e^- acceptor), a phylloquinone pair A_1 and the three Fe_4S_4 clusters from which electrons are transferred onto the soluble e^- carrier Fed and from there onto FNR, which reduces $NADP^+$ to NADPH (Hohmann-Marriott & Blankenship, 2011).

The *pmf*, which is build up by the e^- flow through the respiratory e^- transport chain (RETC) and the PETC, is mainly utilized by ATP synthetase to drive ATP production. ATP synthase catalyses ATP generation through proton-driven rotation of rotor subunits. Depending on the size of the c-ring in the F_o subunit, about 4.33-5 protons are needed to synthesize one ATP. Cyanobacterial ATP synthase is classified as a F-type ATP-synthase. F-type ATP synthases have two subcomplexes, F_1 and F_o. F_o is hydrophobic and membrane-embedded and the hydrophilic F_1 protrudes into the cytoplasm. The F_o complex converts the potential energy of the *pmf* into a rotary force. The F_1 complex uses the rotary force to catalyse the synthesis of ATP from adenosine diphosphate (ADP) + inorganic phosphate (P_i), thus converting electrochemical energy into biologically useable chemical energy (Yi et al., 2024).

1.2.3 Alternative e^- transport (AET) pathways

In addition to the main PETC, cyanobacteria possess multiple AET pathways. These include cyclic e^- transport (CET) to adjust ATP/NADPH ratios to match the metabolic demand (Moore & Vermaas, 2024), as well as pathways that protect the cells from an excess of electrons (Lea-Smith et al., 2016), which can lead to ROS production, decrease the photosynthetic efficiency and/or alter the redox state of the cell (Lea-Smith et al., 2016; Moore & Vermaas, 2024; Mullineaux, 2014).

Under fluctuating light or nutrient levels, e.g. if the e^- sink capacity of the Calvin Benson Bassham (CBB) cycle becomes saturated, the PETC may become over-reduced, potentially leading to the generation of reactive oxygen species (ROS), which can severely damage the photosynthetic machinery (Nikkanen et al., 2021).

AETs for photoprotection include e.g. flavodiiron proteins (FDPs), hydrogenases and respiratory terminal oxidases (RTOs) (Lea-Smith et al., 2016). Adaption may also take place via state transitions and non-photochemical quenching via the Orange Carotenoid Protein (OCP) (Kerfeld et al., 2017; Kirilovsky, 2015).

CET. Balancing the ATP/NADPH ratio is extremely important to maintain metabolic homeostasis, as this ratio determines the energy budget of the cells, their energy utilization and their efficiency in CO_2 fixation (Erdrich et al., 2014; Theune et al., 2021). LET in cyanobacteria generates an ATP/NADPH ratio of about 1.28. However, fixation of one CO_2 molecule in the CBB consumes three ATP and two NADPH, thus requiring a ratio of 1.5 (Erdrich et al., 2014). Moreover, different metabolic pathways under different physiological circumstances may have deviating optimal ATP/NADPH ratios (Lucius & Hagemann, 2024).

This imbalance is addressed by CET, which recycles e^- around PSI, generating a *pmf* and driving ATP production without NADPH generation (Erdrich et al., 2014). CET is estimated to make up 35 % of total e^- flow in cyanobacteria, which is twice as much as in plants. This is probably due to cyanobacteria needing additional energy to drive their CCM (Carbon Concentration Mechanism) (Theune et al., 2021). The NAD(P)H:quinone oxidoreductase (NDH-1) is the main CET route in cyanobacteria (Miller et al., 2021). There are four distinct NDH-1 complexes with different physiological roles (also see chapter 1.3.4.). All four NDH-1 types shuttle e^- from reduced Fed to the PQ pool (Z. He et al., 2015; Laughlin et al., 2019; Saura & Kaila, 2019; Schuller et al., 2019).

This increases the *pmf* by pumping three (NDH-$1_{3–4}$)- four (NDH-$1_{1–2}$) protons per two electrons from the cytosol (Schuller et al., 2019, 2020). Taking into account H^+ pumping by the Cyt b_6f complex in the Q cycle (S. Zhang et al., 2023) , the CET thus results in the transport of four protons/e^-. At the same time, the LET and the H_2O-H_2O cycle (mediated by FDP activity, see below) move only three H^+/e^- across the membrane (Theune et al., 2021).

FDPs. A crucial mechanism to protect the PETC from overreduction involves FDPs formerly known as A-type flavoproteins (Flvs). This large protein family is widely found in strict or facultative anaerobic bacteria and archaea as well as some anaerobic pathogenic protozoa (Allahverdiyeva, Isojärvi, et al., 2015). It is also found in all oxygenic photosynthesizers except red and brown algae and angiosperms (Alboresi et al., 2019). The function of FDPs is detoxification of O_2 and/or nitric oxide (NO) during oxidative and/or nitrosative stress (Allahverdiyeva et al., 2013). FDPs transfer excess e^- in the PETC onto O_2, forming H_2O. This is known as the Mehler-like reaction, which avoids ROS production (Vicente et al., 2002).

Under specific conditions, RTOs (see below) can also contribute to O_2 photoreduction, however under standard growth conditions this task falls almost entirely to FDPs (Allahverdiyeva, Isojärvi, et al., 2015). The contribution of FDPs to the *pmf* is that they enable a higher rate of linear e^- transfer via the cytosolic consumption of protons in O_2 photoreduction (Nikkanen et al., 2021). It is likely, that FDP activity is tightly regulated to avoid competing for reducing power with the CBB cycle (Nikkanen et al., 2021). For example, FDP heterooligomers reversibly associate with the thylakoid membrane, which determines their activity. This depends on changes in their net surface charges, releasing FDPs from the membrane with a time-delay after gradual alkalization under light. This enables FDP activity only directly after high-light illumination (with Flv2/4 staying associated longer than Flv1/3 in *Synechocystis* sp. PCC 6803) (Nikkanen et al., 2025). Although not confirmed yet in cyanobacteria, another possible mode of regulation is the redox-dependent formation of heterotetramers as found recently in *Physcomitrium patens* (Beraldo et al., 2024).

Two structural domains are conserved in all FDPs: 1) N-terminal metallo-β-lactamase-like domain that contains a non-heme diiron centre, which performs O_2 and/or NO reduction (Fe-Fe domain) and 2) C terminal flavodoxin-like domain that contains a flavin-mononucleotide (FMN) moiety (FMN-domain) (Allahverdiyeva et al., 2015; Vicente et al., 2008). FDPs are grouped into four classes (A-D) depending on their subunit composition (Allahverdiyeva, Isojärvi, et al., 2015). Class C FDPs, which are found in oxygenic phototrophs including cyanobacteria, have a C terminal NAD(P)H:flavin oxidoreductase –like domain in addition to the core Fe-Fe- and FMN-domains. This makes it possible for NAD(P)H to be used as an e^- donor (Allahverdiyeva, Isojärvi, et al., 2015). However, it has been demonstrated, that reduced Fed-1 is the direct e^- donor to the Flv1, Flv2 and Flv3 heterooligomers in *Synechocystis* sp. PCC 6803 (Nikkanen et al., 2025; Sétif et al., 2020). FDPs typically function as hetero-oligomer arranged in a “head-to-tail" configuration. This is essential for e^- transfer to take place since the diiron-center of each monomer is now in close contact (about six Angström) with the FMN moiety of the partner-monomer, forming two independent catalytic sites per dimer (Vicente et al., 2008). β-cyanobacteria have four-six isoforms of FDPs (Flv1-4, Flv1B, Flv3B) grouped into cluster A (Flv1 and Flv2) and cluster B (Flv3 and Flv4) (Allahverdiyeva et al., 2015; P. Zhang et al., 2009). Flv1A, Flv3A, Flv1B and Flv3B belong to subclusters and are only found in heterocystous filamentous β-cyanobacteria, with Flv1B and Flv3B being heterocyst-specific (Allahverdiyeva, Isojärvi, et al., 2015; Ermakova et al., 2013). In cyanobacteria, Flv1 and Flv3 likely operate as a hetero-oligomer (Eckardt et al., 2024; Mustila et al., 2016).

Anabaena possesses Flv1A, Flv3A, Flv2, and Flv4, which are homologous to FDPs in *Synechocystis* sp. PCC 6803 (Allahverdiyeva, Isojärvi, et al., 2015) as well

as Flv1B and Flv3B (Ermakova et al., 2013). In *Anabaena*, Flv1A and Flv3A are indispensable under severe fluctuating light in both LC (atmospheric CO_2 concentration) and HC (high CO_2 concentration) as well as diazotrophic and non-diazotrophic conditions (Allahverdiyeva et al., 2013; Santana-Sánchez et al., 2023). In *Anabaena*, Flv1B and Flv3B are only transcribed in N_2 fixing conditions and only in heterocysts. Flv3B functions as a homo-oligomer and is crucial in maintaining anoxia for nitrogenase function, while the role of Flv1B remains unknown (Ermakova, 2014).

The unicellular non-N_2 fixing cyanobacterium *Synechocystis* sp. PCC 6803 possesses four different FDPs (Flv1-4) (Allahverdiyeva, Isojärvi, et al., 2015). In *Synechocystis* sp. PCC 6803 Flv1 and Flv3 are indispensable as a strong e^- sink, protecting PSI under fluctuating light (Allahverdiyeva et al., 2013). They are rapidly but transiently activated at the onset of illumination Flv2/4 hetero oligomers contribute to a slower and weaker, but steady-state O_2 photoreduction under LC in *Synechocystis* sp. PCC 6803 (Santana-Sanchez et al., 2019). Expression of *flv2* and *flv4* transcripts is strongly inhibited in high inorganic carbon (C_i) - HC - and alkaline pH in *Synechocystis* (Santana-Sanchez et al., 2019). Under HC conditions, Flv1/3 activity is sufficient to provide strong steady-state O_2 photoreduction in *Synechocystis* sp. PCC 6803 (Santana-Sanchez et al., 2019).

Homologues of both Flv1 and Flv3 have also been found to play important roles in other species such as in the moss *p. patens* (Gerotto et al., 2016), where they are also indispensable under fluctuating light, and in the microalgae *Chlamydomonas reinhardtii* (Jokel et al., 2015).

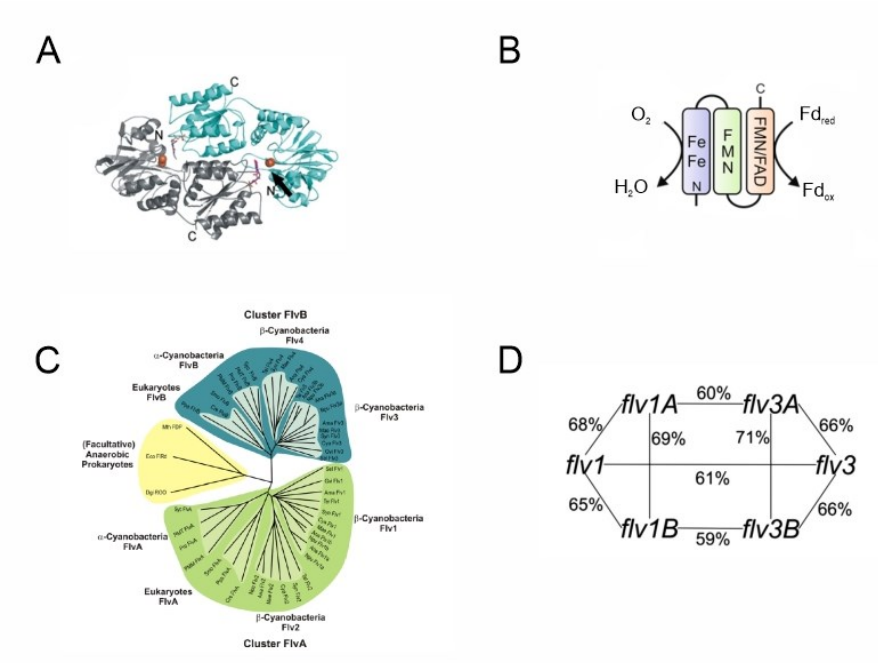

Figure 2. FDPs, structure and phylogeny. A) Overall fold of the Flv2/Flv4 heterodimer of *Synechocystis* in its head-to-tail arrangement. The Fe binding site of the Flv2 monomer faces the FMN binding site of the Flv4 monomer and vice versa. FMN is shown in magenta and Fe as orange spheres, adapted from Zhang et al., 2012 (Oxford University press licence: 6202091056284) (P. Zhang et al., 2012) B) Modular arrangement of Class C FDPs found in oxygenic photosynthetic organisms (cyanobacteria and photosynthetic eukaryotes). Fe-Fe: beta-lactamase like domain; FMN: flavodoxin domain; FMN/Flavin adenine dinucleotide (FAD): Flavin reductase domain, adapted from Allahverdiyeva et al., 2015 (Allahverdiyeva, Isojärvi, et al., 2015) C) Phylogenetic analysis of FDPs in photosynthetic organisms, adapted from Zhang et al., 2009 (P. Zhang et al., 2009) D) Values of nucleotide sequence identity in % between *flv1 (sll1521)* and *flv3* (*sll0217*) from *Synechocystis* and *flv1A* (*all3891*), *flv1B* (*all0177*), *flv3A* (*all3895*) and *flv3B* (*all0178*) from *Anabaena* (Ermakova et al., 2013). Adapted from Ermakova et al., 2013 (John Wiley and Sons license: 6202130371288)

Hydrogenases. Hydrogen (H_2) photoproduction in cyanobacteria mainly relies on two O_2 sensitive enzymes: the bidirectional hydrogenase (Hox) (Eckert et al., 2012) and nitrogenase (see chapter 1.6.1.) (A. K. Mishra et al., 2019). Hox is a NiFe hydrogenase (Ludwig et al., 2006), that takes e^- from the acceptor side of PSI and reversibly transfers them onto two protons, producing H_2 (Appel et al., 2000; Tamagnini et al., 2007). Its activity depends on the redox state of the cell (Tamagnini et al., 2007). Hox is found in N_2 fixing and non N_2 fixing strains (Sjöholm et al., 2007; Tamagnini et al., 2007). It has previously only been found to be active under the following conditions: dark anaerobic growth (Carrieri et al., 2011), for a short time during dark-light-transitions (Appel et al., 2000) or after a sudden increase in

light-intensity (Burgstaller et al., 2022). Thus, Hox has been classified as an e^- valve that protects the PETC from overreduction during transition states (Ludwig et al., 2006). Hox may transfer electrons between Fd, flavodoxin and NADPH pools (Artz et al., 2020) and may be important as an anaerobic alternative to FDPs (Mullineaux, 2014). Moreover, Hox takes part in fermentation metabolism (Ludwig et al., 2006). Thus, three main functions for Hox have been defined: removal of excess reductants during anaerobic fermentation or photosynthetic activity and to deliver e^- to the RETC via oxidation of H_2 (Marques et al., 2011). The role of Hox in heterocysts is still under debate, however it is thought to function as an e^- valve downstream of the PETC and the RETC and other energy metabolic routes (Pernil & Schleiff, 2019).

Another cyanobacterial NiFe hydrogenase is the uptake hydrogenase (Hup), which is found exclusively in N_2 fixing strains and mainly fulfils the function of H_2 recycling to regain reduction equivalents (described in chapter 1.6.1.) (Tamagnini et al., 2007).

RTOs. In cyanobacteria, at least eight types of RTOs are found, which all facilitate the reduction of O_2 to H_2O and have been described previously. During respiration in cyanobacteria, O_2 is the only known terminal e^- acceptor, however different RTOs receive e^- from different sources (Schmetterer, 2016), including Pc and Cyt c_6 (Navarro et al., 2005).

Anabaena has five different RTOs: a genuine cytochrome *c* oxidase (Cox), two alternative respiratory terminal oxidases (ARTOs) also termed Cox, a quinol oxidase (Qox) and another quinol oxidase, the plastid terminal oxidase (Ptox) (Schmetterer, 2016; Stebegg R, 2011). Except for the ARTOs (Cox2 and Cox3), which are found in heterocysts, all RTOs in *Anabaena* are located in the vegetative cells (Stebegg R, 2011). Cox2 and Cox3 proteins are located in the honeycomb membranes, where they are required to maintain a microoxic environment (Harish & Seth, 2020; Schmetterer, 2016) and have been found essential for heterocyst formation and function (Valladares et al., 2007; Valladares, Herrero, Pils, Schmetterer, Flores, et al., 2003)(see chapter 1.6).

Anabaena also contains a Cytochrome *bd* quinol oxidase (Qox), which takes up electrons from the PQ pool and probably functions to prevent its over-reduction (Stebegg R, 2011).

1.2.4 Regulation of photosynthesis

Photosynthetic control

The *pmf* is the main factor determining photosynthetic control and is formed through the following processes:

During LET in cyanobacteria, the reduction of one $NADP^+$ to NADPH requires the transfer of two electrons. For these two electrons, (i) two protons are released into the lumen by the OEC during water oxidation, and (ii) the Cyt b_6f complex operating the Q-cycle contributes an additional four protons to the lumen. At the same time, two protons are taken up from the cytosolic side during PQ reduction at PSII. Thus, per NADPH formed, LET results in a net translocation of 6 protons to the lumen, thereby building *pmf* that drives ATP synthesis. Moreover, during CET, the NDH-1 complex pumps more protons across the membrane (Miller et al., 2021). By analogy with respiratory complex I, this may be the pumping of 4 protons per two electrons (C. Zhang et al., 2020).

Other processes contributing to the H^+ gradient are e.g. oxidation of PQH_2 by RTOs and the consumption of protons in the cytosol, mainly by the CBB (Nikkanen et al., 2021). This proton translocation leads to acidification of the lumen and generation of the *pmf*. It consists of two components: the H^+ concentration gradient (ΔpH) and the electric potential (Δψ), which arises from charge separation at the photosystems (Lyu & Lazár, 2017) as well as H^+ and other ion gradients across the thylakoid membrane (Armbruster et al., 2017; Nikkanen et al., 2021). Regulation of the *pmf* takes place via ATP synthase (Nikkanen et al., 2021) and thylakoid ion transporters (Checchetto et al., 2013; Tsujii et al., 2024). Photosynthetic control occurs through acidification of the lumen which limits PQH_2 oxidation in the Q cycle and thus restricts e^- transport from Cytb_6f to protect PSI from overreduction (Degen & Johnson, 2024; Malone et al., 2021). Most likely this mechanism also functions in cyanobacteria (Checchetto et al., 2012; Nikkanen et al., 2021). However, photosynthetic control in cyanobacteria is likely less essential for photoprotection of PSI than in angiosperms, due to the high PSI/PSII ratio (2:1-4:1) (Moore & Vermaas, 2024) and the presence of FDPs (Nikkanen et al., 2021).

State Transitions. A central strategy of cyanobacteria to adapt to changing light conditions are state transitions (Calzadilla & Kirilovsky, 2020). In state II, light is preferentially absorbed by PSII, resulting in higher fluorescence from PSI, since PBS is preferentially associated with PSI. In state I, light is preferentially absorbed by PSI, resulting in higher PSII fluorescence since the PBS is preferentially associated with PSII. However, an alternative model has been proposed where PBS disassociates from the thylakoid membrane in state I and associates with PSII in state II. Thus, altered association of PBS with the photosystems adjusts the relative activities of the photosystems under e.g. fluctuating light (Calzadilla & Kirilovsky, 2020; Mullineaux, 2014). Different states may also influence the LET/CET-ratio (Mullineaux, 2014). CET dominates in state 2, while LET is predominant in state I (Elanskaya et al., 2021; Mullineaux, 2014).

1.3 Carbon Metabolism

1.3.1 The CBB cycle

In all oxygenic phototrophs, the CBB cycle is the principal anabolic pathway for the reduction of CO_2 to organic sugars and metabolic intermediates (Lucius & Hagemann, 2024). It utilizes the reducing power of NADPH and the chemical energy provided by ATP, both of which are synthesized via photosynthetic light reactions. In this cascade of chemical reactions 12 NADPH and 12 H^+ reduce six molecules of CO_2 to form glucose ($C_6H_{12}O_6$).

In all photosynthetic organisms, the CBB cycle is comprised of 11 enzymes and two regulatory proteins (RuBisCO activase and the CP12 scaffold). It can be divided into a carboxylation phase, reduction phase and regeneration phase with the initial carboxylation reaction via RuBisCO, the major C fixing enzyme, as the rate-limiting step and ribulose-1,5-bisphosphate (RuBP) regeneration as the co-limiting step. In the carboxylation phase, RuBisCO fixes one molecule of CO_2 onto the C5 sugar RuBP. This reaction yields two molecules of 3-Phosphoglyceric acid (3-PGA). In the reduction phase, 3-PGA is reduced to Glyceraldehyde-3-Phosphate (GAP), which is used in gluconeogenesis (Lucius & Hagemann, 2024; Meloni et al., 2023). The canonical CBB cycle uses nine ATP and six NADPH per GAP (Hudson, 2024). In the regeneration phase, GAP is metabolized for the regeneration of the precursor molecule RuBP (Lucius & Hagemann, 2024; Meloni et al., 2023). The RuBP regeneration phase is catalysed by eight enzymes, some of which also participate in the oxidative pentose phosphate (OPP) pathway, which functions in the reverse direction (Meloni et al., 2023).

It should be noted that the activation of the CBB cycle after a dark-to-light transition depends on the elevation of the cytoplasmic pH after photosynthesis commences (Elanskaya et al., 2021; Mangan et al., 2016). Also, in cyanobacteria including *Anabaena*, the thioredoxin (Trx) system is essential in activating the CBB cycle after light activation and depends on photosynthetic reduction equivalents (Mallén-Ponce et al., 2024).

1.3.2 Photorespiration

RuBisCO is an inefficient enzyme since it has a low catalytic turnover number and low selectivity between CO_2 and O_2 (Flamholz et al., 2019). When O_2 is more abundant than CO_2, the oxygenase activity of RuBisCO yields 1 x 3-PGA and 1x 2-phosphoglycolate (2-PG) from one RuBP (Bauwe et al., 2010; Flamholz et al., 2019). 2-PG is metabolically costly and inhibits photosynthesis in higher concentrations. It is recycled via photorespiration, which provides C-intermediates for the CBB cycle.

Variations of the photorespiration pathway are found in cyanobacteria, including one which entails loss of CO_2 and NH_4^+ and is also found in *Anabaena* (Bauwe et al., 2010; Montgomery et al., 2016) Here, 3-PGA is recovered from two molecules of 2-PG, with one out of four 2-PG carbon atoms being lost. This photorespiration pathway also releases one NH_4^+ from glutamate (Glu) per two 2-PG molecules (Bauwe et al., 2010). Due to the action of the CCM and FDPs (see chapters 1.3.4.; 1.2.3.), the e^- sink capacity of photorespiration under C_i limitation is probably not frequently used at full capacity in cyanobacteria (Allahverdiyeva, Isojärvi, et al., 2015; Bolay et al., 2022). It is however a relevant e^- valve under low C_i and high-light conditions (Allahverdiyeva et al., 2011; Hackenberg et al., 2009).

1.3.3 Downstream C metabolism and storage

Most of the photosynthetically fixed C is directed towards biomass production. Under conditions of C surplus, such as macronutrient limitation, excess C is diverted into the synthesis of ADP-glucose, which serves as a precursor for glycogen biosynthesis. The resulting glycogen reserves can be catabolized during darkness or other starvation conditions, providing a critical energy and C source (Gründel et al., 2012; Lucius & Hagemann, 2024; Makowka et al., 2020). However, glycogen is also being constantly synthesized and degraded even under constant light and photoautotrophic conditions (Hudson, 2024; Lucius & Hagemann, 2024), where it functions as a metabolic buffer to maintain homeostasis and prevent metabolic imbalance (Lucius & Hagemann, 2024; Ortega-Martínez et al., 2024).

Autocatalytic open cycles, such as the CBB cycle, require stable fluxes sustained by anaplerotic and cataplerotic reactions. Glycolytic routes play a significant role in fine-tuning central C metabolism under photoautotrophic conditions, where they form anaplerotic shunts that replenish the CBB cycle, using carbohydrate reservoirs. This may be necessary during transition states and under fluctuating light conditions (Makowka et al., 2020).

The CBB cycle is thus part of a broader network of anaplerotic and cataplerotic reactions of C compounds. It intersects with the three main catabolic routes for C in cyanobacteria, which have glucose-6-phosphate as their common entry point: The Embden-Meyerhof-Parnas (EMP) pathway (“classical glycolysis”), the OPP pathway, possibly the Entner-Doudoroff (ED) pathway (Chen et al., 2016; Lucius & Hagemann, 2024; Makowka et al., 2020) and additionally also a phosphoketolase-mediated pathway (Makowka et al., 2020). In these pathways, glucose is oxidized, providing ATP, NAD(P)H and GAP, which can then enter lower glycolysis. Funneling of C into lower glycolysis is also possible directly from the CBB cycle, via 3-PGA, which happens especially under a low C/N ratio (Lucius & Hagemann, 2024).

The pentose-phosphate pathway can run in the oxidative mode (OPP pathway), oxidizing carbohydrates and producing C5 sugars essential for nucleic acid biosynthesis, or in reductive mode (as a part of the CBB) to fix CO_2 (Chen et al., 2016; Lucius & Hagemann, 2024). The OPP pathway is regarded as the main route for glycogen and glucose catabolism during photoautotrophic growth in cyanobacteria (Lucius & Hagemann, 2024; Shinde et al., 2020) and it is the only metabolic source of NADPH in the dark (Lucius & Hagemann, 2024; Makowka et al., 2020). Like the CBB cycle, the OPP pathway is also Trx regulated (Mallén-Ponce et al., 2022).

The end product of glycolysis, pyruvate (Pyr), is directly funnelled into the tricarboxylic acid (TCA) cycle, with 2-OG as an intermediate product (Lucius & Hagemann, 2024). The TCA cycle is a series of catabolic reactions that generate reducing equivalents for ATP formation as well as important precursor-molecules for the biosynthesis of cellular compounds (Steinhauser et al., 2012; You et al., 2024). In cyanobacteria, the TCA has two main roles: (a) oxidation of acetyl coenzyme A (acetly-CoA) to generate NADH/FADH which supply e^- to oxidative phosphorylation and (b) the formation of metabolic intermediates such as oxaloacetate, 2-OG and succinate (Katayama et al., 2022; You et al., 2024). The cyanobacterial TCA differs from the conventional TCA cycle due to the absence of 2-OG dehydrogenase (Lucius & Hagemann, 2024; You et al., 2024). Instead 2-OG decarboxylase and succinate semialdehyde dehydrogenase transform 2-OG into succinate (You et al., 2024; S. Zhang, 2011). Moreover, several bypass pathways exist (You et al., 2024) that vary in their release of NAD(P)H and CO_2 and do not produce ATP (Knoop et al., 2013; S. Zhang, 2011). Since the CBB plays the main role in delivering C_i to the cell and the photosystems are responsible for energy production, the TCA is less critical for maintaining cellular energy balance in cyanobacteria as opposed to heterotrophs. In cyanobacteria, the rate of metabolic flux through the TCA cycle is thus low (Wan et al., 2017; You et al., 2024).

1.3.4 CCM

To sustain high rates of oxygenic photosynthesis, it is crucial to maintain high levels of C_i in the vicinity of RuBisCO (Badger & Price, 2003; Daley et al., 2012). Cyanobacteria have evolved a sophisticated CCM to acquire C_i for photosynthesis and avoid photorespiration. It encompasses bicarbonate (HCO_3^-) accumulation in the cytosol via several light-energy dependent HCO_3^- transporters as well as NDH complexes, which convert CO_2 (entering through diffusion) into HCO_3^-, to which the cell is impermeable (Badger et al., 2006; Badger & Price, 2003; De Araujo et al., 2014).

Cyanobacteria can actively take up HCO_3^- or convert atmospheric CO_2 into HCO_3^- (Badger & Price, 2003). There are several C_i uptake systems which can be broadly classified into two functional categories: low-affinity/high-flux systems, typically expressed under C replete conditions, and high-affinity/low-flux systems, which are induced in response to C limitation (Daley et al., 2012). The low affinity/high flux transporters BicA (Na^+ dependent, for HCO_3^-) and NDH-1$_4$ (redox-driven, converting CO_2 to HCO_3^-) are constitutively expressed. High-affinity C_i transporters induced under limited C availability are the HCO_3^- transporters BCT1 (ATP dependent) and SbtA/B (Na^+-dependent) as well as the high-affinity/low flux NDH-1$_3$, a redox-driven enzyme using Fed to convert CO_2 into HCO_3^- (Badger et al., 2006; Kurkela & Tyystjärvi, 2024).

RuBisCO is compartmentalized within the carboxysome. The carboxysome is a specialized protein microcompartement localized in the cytoplasm, which has a protein shell that is selectively permeable to HCO_3^- (Badger et al., 2006; Daley et al., 2012). Next to RuBisCO, carboxysomes possess carbonic anhydrase, responsible for the conversion of accumulated HCO_3^- into CO_2 (Badger et al., 2006; De Araujo et al., 2014). RuBisCO from cyanobacteria exhibit a reduced affinity for both CO_2 and O_2 than its algae or plant counterpart, however it achieves much higher turnover rates per unit protein (Badger et al., 2006), since the CCM allows RuBisCO to operate under a near-saturating substrate concentration (Badger et al., 2006; Cameron, 2014).

1.4 Nitrogen metabolism in cyanobacteria

1.4.1 Types of N sources

Cyanobacteria can utilize several N sources in a hierarchical manner: NH_4^+, NO_3^-, nitrite (NO_2-), urea, several amino acids and, for some species, N_2 (E. Flores; A. Herrero, 2005; Perin et al., 2021). Independent of the initial N source, all are converted to NH_4^+ and then assimilated through the glutamine synthetase/glutamate synthetase (GS/GOGAT) cycle. When environmental N sources are scarce, cyanobacteria can consume internal N storages, mainly cyanophycin (in diazotrophic cyanobacteria) and PBS to sustain N metabolism (H. Zhang et al., 2018; H. Zhang & Yang, 2019).

1.4.2 N import

NH_4^+ can be assimilated at the lowest metabolic cost as uncharged ammonia (NH_3) readily diffuses across cell membranes. Also, NH_4^+ is the most reduced N source and thus does not require reducing equivalents and additional conversion steps

(Forchhammer & Selim, 2020; Perin et al., 2021; C. C. Zhang et al., 2018). However, as NH_4^+ availability is low in most habitats, high-affinity NH_4^+ transporters of the Amt family function as scavengers which can take up NH_4^+ at submicromolar levels. In *Anabaena*, Amt1 functions as the primary NH_4^+ permease involved in this high-affinity uptake (Herrero & Flores, 2019; Paz-Yepes et al., 2008; Perin et al., 2021). NH_4^+ transport needs to be, however, tightly controlled, as elevated intracellular NH_4^+ concentrations are toxic (Watzer et al., 2019). In *Anabaena* and other freshwater cyanobacteria, NO_3^- is imported via the high-affinity ATP binding cassette (ABC) type NO_3^-/ NO_2^- transporter NRT. Once inside the cell, NO_3^- is reduced to NO_2^- by nitrate reductase (NR, encoded by *narB*) and then NO_2^- is reduced to NH_4^+ via nitrite reductase (NiR, encoded by *nirA*). In *Anabaena*, these genes constitute the *nirA* operon (n*irA-nrtABCD-narB*) (Flores et al., 2005; Frías et al., 1997; Herrero et al., 2001). In *Anabaena*, both NR and NiR use PSI-reduced Fed (encoded by the vegetative cell specific *petF*) as an e^- donor (Floß et al., 1997; Mondal & Bruce, 2018; Schmitz & Böhme, 1995; Watzer et al., 2019), thus coupling NO_3^-/ NO_2^- fixation directly to photosynthesis/the PETC (Shimakawa, 2023). Expression of the *nirA* operon is repressed in the presence of NH_4^+ and is induced by NO_3^- or NO_2^- (see chapter 1.5.2) (Herrero et al., 2001).

1.4.3 GS/GOGAT cycle

GS (*glnA*) and GOGAT constitute the GS/GOGAT cycle, which is the main route of incorporation of NH_4^+ into the metabolism and connects C and N metabolism (Yutthanasirikul et al., 2024). GS catalyzes the ATP and NH_4^+ dependent amidation of Glu, synthesizing glutamine (Gln) (Galmozzi et al., 2010; Yutthanasirikul et al., 2024). Two molecules of Glu are in turn synthesized from Gln and 2-OG by GOGAT (Galmozzi et al., 2010; M. I. Muro-Pastor et al., 2001; Yutthanasirikul et al., 2024). Glu/Gln are then the primary N donors for anabolic reactions, including amino acid and nucleotide biosynthesis (Forchhammer & Selim, 2020; C. C. Zhang et al., 2018). Most cyanobacterial GOGAT enzymes, including the only GOGAT enzyme from *Anabaena*, use reduced Fed as an e^- donor, thereby linking the GS/GOGAT cycle to photosynthesis (Galmozzi et al., 2010; Herrero & Flores, 2019; Schmitz et al., 1996; Yutthanasirikul et al., 2024).

1.4.4 Arginine (Arg) synthesis

The anabolic pathway of Arg takes place in vegetative cells and heterocysts of *Anabaena* and consists of two parts: First the production of ornithine from Glu and secondly the transformation of ornithine into Arg via the OAC (Flores, Arévalo, et al., 2019). Thus, the OAC is coupled to the GS/GOGAT cycle via Arg synthesis from

Glu and enables a high rate of N assimilation, mobilization and storage (in form of cyanophycin) and thus adaptation to fluctuating N conditions (H. Zhang et al., 2018; H. Zhang & Yang, 2019). Thus, when N becomes available, the OAC is activated, simultaneously synthesizing and degrading Arg as a first reaction to N availability (H. Zhang & Yang, 2019).

1.4.5 N storage

Cyanophycin is produced by many β-cyanobacteria as a dynamic N reservoir (Flores, Arévalo, et al., 2019). It accumulates when there is excessive N relative to other nutrients, or in response to light limitation or low temperature (Flores, Arévalo, et al., 2019; H. Zhang et al., 2018), and is degraded when balanced growth resumes. Cyanophycin is especially relevant in N_2 fixing cyanobacteria, where newly fixed N_2 can be transiently stored in this polymer. In heterocysts, cyanophycin provides a source of β-aspartyl-arginine, which can be transferred to vegetative cells as N source. While not essential in all cyanobacteria, *Anabaena* shows a clear dependence for cyanophycin biogenesis to maintain N metabolism (Flores, Arévalo, et al., 2019). In addition to cyanophycin, PBS can serve as a N reservoir, mobilized through their controlled degradation (H. Zhang et al., 2018).

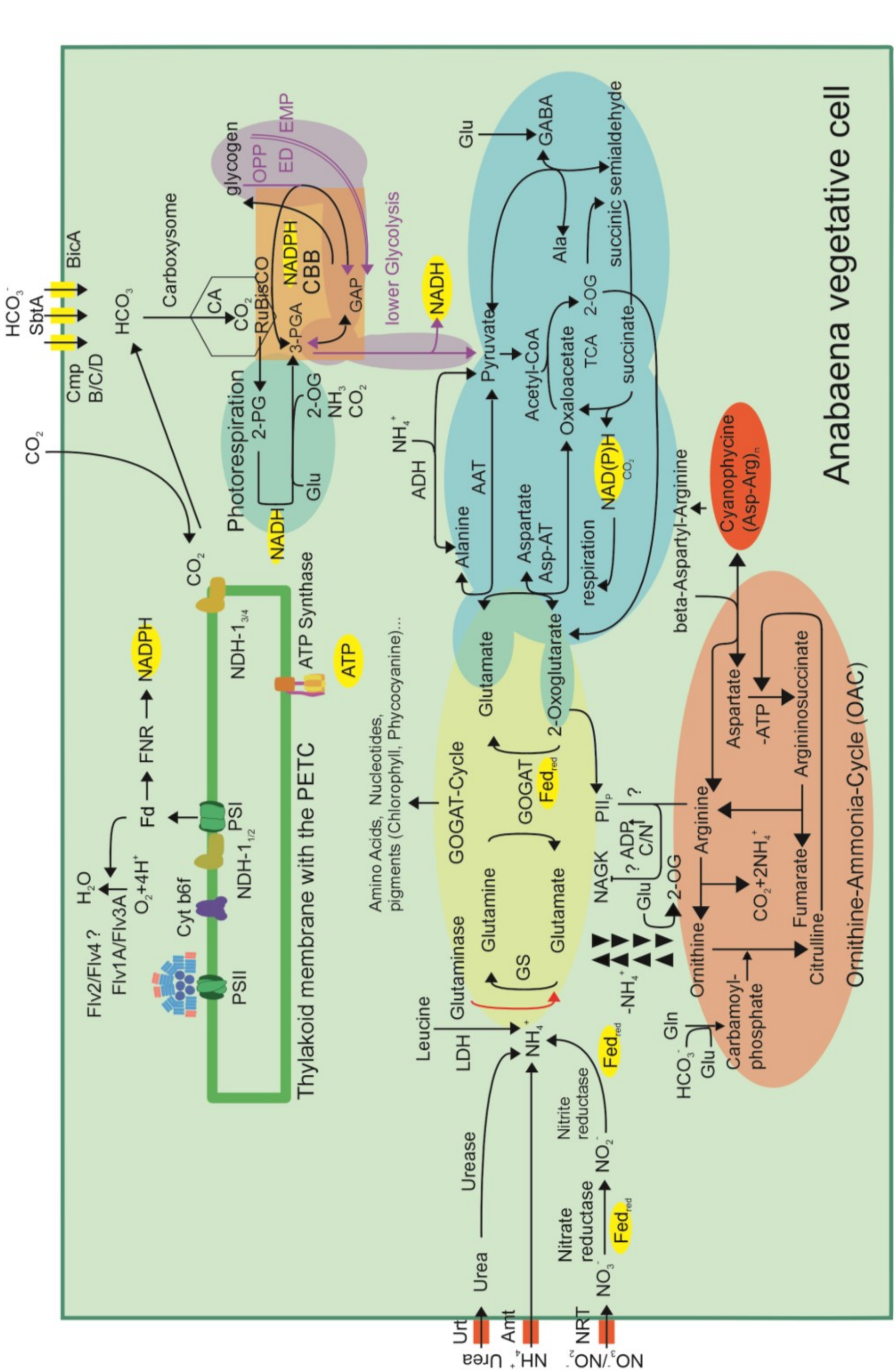

Anabaena vegetative cell
Thylakoid membrane with the PETC
PSII
Cyt b6f
PSI
NDH-1 1/2
NDH-1 3/4
ATP Synthase
ATP
Fd → FNR → NADPH
Flv2/Flv4 ?
Flv1A/Flv3A
O2+4H+
H2O
CO2
HCO3-
Cmp B/C/D
SbtA
BicA
HCO3
Carboxysome
CA
CO2
RuBisCO
3-PGA
NADPH
CBB
GAP
glycogen
OPP
ED
EMP
lower Glycolysis
NADH
Photorespiration
2-PG
2-OG
NH3
CO2
Glu
NADH
Pyruvate
Acetyl-CoA
Oxaloacetate
TCA
2-OG
succinate
succinic semialdehyde
GABA
Glu
Ala
NAD(P)H
CO2
respiration
Alanine
AAT
ADH
NH4+
Aspartate
Asp-AT
Glutamate
2-Oxoglutarate
GOGAT-Cycle
GOGAT
Fedred
Glutamine
GS
Glutaminase
Amino Acids, Nucleotides, pigments (Chlorophyll, Phycocyanine)...
NAGK
PIIp
ADP
C/N
?
Glu
2-OG
-NH4+
Leucine
LDH
Urea
Urease
Nitrate reductase
Nitrite reductase
NO3-
NO2-
Fedred
Urt
Amt
NRT
Urea
NH4+
NO3-/NO2-
beta-Aspartyl-Arginine
Cyanophycine (Asp-Arg)n
Aspartate
-ATP
Argininosuccinate
Arginine
Fumarate
Citrulline
Ornithine
CO2+2NH4+
Carbamoyl-phosphate
Gln
HCO3-
Glu
Ornithine-Ammonia-Cycle (OAC)

◄ **Figure 3. Central metabolic pathways of the *Anabaena* vegetative cell.** In cyanobacteria, photosynthesis and C and N metabolism are tightly coupled. The PETC captures light energy via the PBS (Ducret et al., 1996) and provides ATP and reduction equivalents to the metabolism (C. C. Zhang et al., 2018). FDPs serves as an e^- valve in case of PETC overreduction (Allahverdiyeva, Isojärvi, et al., 2015). N is taken up in form of e.g. NH_4^+, NO_3^- or urea and enters the central metabolism via the GS/GOGAT cycle. Intermediates of the cycle, Gln and Glu, serve as precursors for e.g. amino acids, nucleotides and photosynthetic pigments (Yutthanasirikul et al., 2024) The GS/GOGAT cycle is connected to the OAC, which directly assimilates N in form of Gln and Aspartate (Asp) to synthesize Arg, which can be used to generate cyanophycin (H. Zhang et al., 2018). In *Synechocystis*, flow of N from Glu to ornithine is regulated via regulation of feedback inhibition of NAGK by Arg with a dependency on 2-OG and ADP levels mediated by PII (Forchhammer & Selim, 2020). C is taken up in form of CO_2 and HCO_3^- via the CCM, which includes transporters, NDH-$1_{3/4}$ and the carboxysome. The CBB cycle assimilates CO_2 into 3-PGA, which enters gluconeogenesis via GAP or the TCA cycle via lower glycolysis. Photorespiration in cyanobacteria is comprised of overlapping pathways, which regenerate the sideproduct of RuBisCO activity, 2-PG, and one of which consumes Glu and releases 2-OG, NH_3 and CO_2 (Bauwe et al., 2010; Montgomery et al., 2016). There are three main catabolic routes for C in cyanobacteria, which have glucose-6-phosphate as their common entry-point and all feed into GAP: The EMP pathway, OPP pathway, which intersects with the CBB and possibly the ED pathway (Chen et al., 2016; Lucius & Hagemann, 2024; Makowka et al., 2020). The TCA cycle in cyanobacteria has several variations which are described in Steinhauser et al. (2012) and You et al. (2024).

1.5 C/N balance in cyanobacteria

1.5.1 Coupling of C and N metabolic pathways

C and N metabolism are tightly interconnected, as they constitute the two most abundant cellular elements, forming e.g. carbohydrates, proteins and nucleic acids. Moreover, N assimilation requires a C skeleton. Thus, limitation or excess of either nutrient strongly affects the metabolism of the other (B. Li et al., 2024; C. C. Zhang et al., 2018).

The C/N ratio of different organisms varies in a relatively narrow range (C. C. Zhang et al., 2018) to prevent metabolic imbalance (Gollan et al., 2020). In cyanobacteria the C/N ratio is close to 5:1 (Forchhammer & Selim, 2020; Wolk, 1973). N metabolic pathways intersect in the GS/GOGAT cycle (see chapter 1.4.3.), where 2-OG provides the C skeleton for N assimilation. To control uptake and assimilation of various N and C sources under changing environmental conditions, cyanobacteria employ different levels of regulation, acting at both the metabolic and transcriptional levels (Forchhammer & Selim, 2020; B. Li et al., 2024; C. C. Zhang et al., 2018).

1.5.2 The N starvation signal 2-OG and its signalling cascade

Although cyanobacteria possess at least three bypasses in the TCA cycle, which allow for 2-OG conversion to succinate despite 2-OG dehydrogenase missing in

cyanobacteria, fluctuations in 2-OG levels are determined by its formation via isocitrate dehydrogenase (IDH) in the TCA cycle and its consumption through the GS/GOGAT cycle (Forchhammer & Selim, 2020; S. Zhang, 2011). Since C and N metabolism are directly linked via 2-OG in the GS/GOGAT cycle (see chapter 1.4.3.) (Lucius & Hagemann, 2024), 2-OG levels increase under N deprivation (Yutthanasirikul et al., 2024) making it the signal transducer for N-control in cyanobacteria (Flores, Arévalo, et al., 2019; Herrero & Flores, 2019; Robles-Rengel et al., 2019). Also in *Anabaena*, 2-OG accumulates rapidly upon N limitation (C. C. Zhang et al., 2018). Moreover, via a non-metabolizable 2-OG analogue, Laurent et al. (2005) were able to trigger heterocyst formation in *Anabaena* under repressive conditions, providing in vivo evidence for the signalling role of 2-OG. A similar conclusion was also reached by Li et al., 2003, utilizing 2-OG directly to trigger heterocyst development. Additionally, in *A.variabilis* Gln is an adequate N source for cyanobacterial growth but cannot repress heterocyst development, underlining the intrinsic role of 2-OG in triggering heterocyst formation (Laurent et al., 2005). Currently, four 2-OG sensors have been identified in cyanobacteria: Ntca, FurA, PII and NdhR (CcmR) (Guío et al., 2020; Jiang et al., 2018; Tanigawa et al., 2002; Y. Zhang & Zhao, 2008).

Ntca. NtcA is a global transcriptional regulator of C and N metabolism in cyanobacteria, including *Anabaena*. It regulates a wide range of processes e.g. cellular regulation, transport, translation, biosynthesis and central metabolism, Fe acquisition, photosynthesis and respiration. NtcA was originally discovered as a N regulator and indeed, the widest range of regulated genes fall under that category such as NO_3^- and NH_4^+ assimilation systems and the urea uptake system, as well as heterocyst differentiation and N_2 fixation by nitrogenase (see chapter 1.6.) (Picossi et al., 2014). NtcA binds 2-OG directly, leading to an increase in the binding affinity of NtcA to some of its target promoters, including its own promoter, triggering or suppressing transcription (Flores, Picossi, et al., 2019; Herrero & Flores, 2019; M. I. Muro-Pastor et al., 2001). Under low 2-OG conditions, basal NtcA binding to desoxyribonucleic acid (DNA) may be important for its repressive role (Flores, Picossi, et al., 2019).

N control describes a common mechanism in microorganisms, where the assimilation of an inferior N source is repressed when another, more easily assimilated source of N is available (Herrero et al., 2001). For example, uptake of NO_3^-, the second most preferred N source in Anabaena, only takes place when NH_4^+ is no longer available in the medium (Watzer et al., 2019; Xing & Zhang, 2019; C. C. Zhang et al., 2018). N control is achieved primarily on the transcriptional but also on the post transcriptional level. On the transcriptional level, NtcA is the primary regulator (Flores, Picossi, et al., 2019; Galmozzi et al., 2010; Herrero & Flores, 2019). The different affinities of NtcA to different promoters could play an important role in the order of promoter activation after a change in N source and for N control (Flores, Picossi, et al., 2019; Galmozzi et al., 2010; Herrero & Flores, 2019; Perin et

al., 2021). The expression of NH_4^+ repressible genes commonly requires NtcA (Flores et al., 1999; Herrero et al., 2001; Vega-Palas et al., 1992). The role of NtcA in NH_4^+ acclimation remains to be investigated (S. Lin et al., 2025). For example, when NH_4^+ becomes depleted in the environment, cellular 2-OG levels are transiently increased due to reduced consumption (B. Li et al., 2024). 2-OG binds to NtcA, activating the transcription of the previously repressed *nirA* operon together with NtcB (Aichi et al., 2001; Ohashi et al., 2011; C. C. Zhang et al., 2018). NtcB is a LysR type transcriptional regulator (LTTR), which is specifically involved in activation of the NO_3^- assimilation genes (Ohashi et al., 2011). In *Anabaena*, NtcB appears to be essential for the expression of the *nirA* operon, independent of NO_3^- availability (Aichi et al., 2001).

Regulation of the GS/GOGAT cycle is essential for the C/N balance in cyanobacteria and regulated by enzymatic activity (Yutthanasirikul et al., 2024) and at the transcriptional level (Galmozzi et al., 2010; Reyes et al., 1997). GS is a key regulator of the GS/GOGAT cycle (Yutthanasirikul et al., 2024) and its regulation is described in the following.

Posttranslational regulation of GS in cyanobacteria was first described in *Synechocystis* sp. PCC 6803, where GS interacts reversibly with two small proteins, inactivation factor 7 (IF7, *gifA*) and IF17 (*gifB*). Most cyanobacteria have IF7-like proteins. In *Anabaena* there is only one *gif* gene which is homologous to *gifA* in *Synechocystis* sp. PCC 6803 and codes for IF7A (Galmozzi et al., 2010). Transcription of *gifA* in *Anabaena* is partially repressed by NtcA under all N regimes, however more strongly when NH_4^+ is not the N source. When NH_4^+ is the N source, *gifA* expression is basal in *Anabaena*. In contrast to *Synechocystis* sp. PCC 6803, NH_4^+ mediated upregulation of *gifA* is not transitory and *gifA* expression remains high during NH_4^+ treatment. The reason for this may be slower GS inactivation in *Anabaena.* In *Synechocystis* sp. PCC 6803, *gifA* and *gifB* are downregulated under N limitation, which leads to IF7 and IF17 proteins being degraded, activating GS (Galmozzi et al., 2007, 2010; García-Domínguez et al., 2000). This results in higher GS activity under N limitation/when N_2 is the N source (Flores & Herrero, 1994; Forchhammer & Selim, 2020; Galmozzi et al., 2010). After NH_4^+ addition, similar to *Synechocystis* sp. PCC 6803, *Anabaena gifA* expression is partially derepressed, leading to IF7A synthesis and thus GS inactivation (Galmozzi et al., 2010). In a second level of regulation in *Anabaena* and other cyanobacteria, GS is controlled at the transcriptional level via NtcA. *GlnA* translation is low when N levels are high and when NH_4^+ is available in the environment. In turn, in the absence of N, *glnA* is expressed at higher levels (Frías et al., 1994; Herrero et al., 2001; Tumer et al., 1983).

PII. The small signal-transducing protein PII regulates multiple C and N metabolic processes by sensing the intracellular C/N ratio via 2-OG and the energy status via

the ATP/ADP ratio (Forchhammer et al., 2022; Watzer et al., 2019; C. C. Zhang et al., 2018). In unicellular cyanobacteria, PII regulates NtcA through the binding of the NtcA co-activator PipX (Espinosa et al., 2007) , as well as NH_4^+, NO_3^- and urea uptake directly (Espinosa et al., 2007; Watzer et al., 2019), including e.g. the short-term NH_4^+ mediated inhibition of NO_3^- import (H. M. Lee et al., 2000) and NO_3^- uptake in response to light availability (Kloft & Forchhammer, 2005). Moreover, PII participates in the regulation of N storage formation/Arg biosynthesis (via N-acetyl glutamate kinase, NAGK, *argB*) (Flores, Arévalo, et al., 2019; Forchhammer & Lüddecke, 2016; Maheswaran et al., 2006), fatty acid synthesis (via acetyl-CoA carboxylase) (Hauf et al., 2016) and C_i uptake (Hisbergues et al., 1999).

PII is integrating and relaying this information via changing interactions with various target proteins of the central metabolic pathways depending on covalent modifications (phosphorylation/nitrisylation) and the combination of metabolites (e.g. ATP/ADP and 2-OG) it has bound. Importantly, binding of partner proteins may change the affinity of effectors (Forchhammer et al., 2022; Forchhammer & Selim, 2020; B. Li et al., 2024; Watzer et al., 2019; Y. Zhang & Zhao, 2008). PII functions in the NtcA-PipX-PII regulatory axis. When NtcA is activated, it enhances transcription of the PII-encoding gene (H.-M. Lee et al., 1999). In turn PII modulates NtcA gene expressions by sequestering the NtcA co-activator PipX (Espinosa et al., 2006, 2007). E.g. PII switches off PipX-activated NtcA gene expression at high ADP and intermediate 2-OG levels (Zeth et al., 2014).

The PII protein is also a central regulator of N control on the posttranscriptional level. In unicellular strains the activity of the NH_4^+, NO_3^- and urea transporter system is regulated by PII on the protein level, depending on its phosphorylation levels which are determined by the C/N balance (Forchhammer & Selim, 2020; B. Li et al., 2024; Watzer et al., 2019). In unicellular cyanobacteria, PII also controls N storage metabolism through regulation of NAGK, a rate limiting-enzyme of Arg- and thus also cyanophycin-synthesis, leading to enhanced N storage under N sufficiency (high intracellular ATP and low 2-OG levels) (Forchhammer, 2008; Forchhammer & Selim, 2020; Watzer et al., 2019; C. C. Zhang et al., 2018).

In heterocystous cyanobacteria, the role of PII is less well understood. Here, PII may have distinct functions since e.g. *glnB*, coding for PII, is essential in *Nostoc punctiforme* ATCC 29133 (Hanson et al., 1998). In *Anabaena*, PII is known to change its modification state depending on the N regime and cell type and play a role in regulating N metabolism. While PII is not needed for heterocyst differentiation (Laurent et al., 2004; Y. Zhang et al., 2007), the PipX gene is mainly expressed during heterocyst differentiation as described in chapter 1.6.2. (Valladares et al., 2011). At least in *Anabaena variabilis* NAGK inhibition at increased Arg levels has been demonstrated (Hoare & Hoare, 1966), thus, NAGK may also be feedback-inhibited by Arg possibly via PII in *Anabaena* sp. PCC7120.

1.5.3 2-PG as a signal for C starvation

2-PG is derived from the oxygenase activity of RuBisCO and thus serves as a metabolic signal of C starvation (see chapter 1.3.2.) (C. C. Zhang et al., 2018). 2-PG relays this signal via various transcription factors (TFs), as described below.

The LysR-type TF subfamily CbbR (proteobacterial Calvin Cycle regulator) regulates CO_2-responsive genes, including genes encoding enzymes of the CBB cycle. It is regulating CO_2 fixation and the adaptation to C_i limitation and is found in many autotrophic microorganisms including β-cyanobacteria (Dangel & Tabita, 2015; Price et al., 2008).

Anabaena possesses three CbbR-like LTTRs, CmpR, NdhR (also known as CcmR), and PacR (also known as RbcR, *all3953*) (Kaneko et al., 2001). CmpR activates the *cmp* operon *(alr2877-alr2880*) and also autoregulates its own expression in response to C_i limitation. CmpR activates the *cmp* operon and positively autoregulates its own expression in response to C_i limitation (López-Igual et al., 2012; C. C. Zhang et al., 2018). CmpR may have 2-PG as a positive effector (Nishimura et al., 2008).

NdhR is a sensor of 2-OG and 2-PG (Jiang et al., 2018) and acts as a repressor of C_i uptake under HC conditions and negatively regulates its own transcription (Figge et al., 2001; López-Igual et al., 2012; H. L. Wang et al., 2004; C. C. Zhang et al., 2018).

PacR. The LysR-type, RbcR-like transcription factor PacR globally regulates C_i assimilation and photosynthesis-related genes in *Anabaena*. It has been found to adjust the formation of reductive power depending on C_i availability while providing protection form oxidative damage to photosynthetic components. Remarkably, PacR was the first CbbR-like TF described in cyanobacteria to activate RuBisCo encoding genes and the first TF that was found to be able to fine-tune photosynthetic gene expression (e.g. the core PSI RC *psaA* gene) to the availability of C_i. Under C_i limiting conditions, PacR predominantly upregulates its target genes. Interestingly, PacR appears not to autoregulate its own transcription, which is also not regulated by NtcA, and its expression appears independent of the intracellular C/N balance (Picossi et al., 2015).

It has been demonstrated that PacR is a truly global TF, which positively or negatively regulates genes in various parts of the metabolism (e.g. biosynthesis of aminoacids, cofactors, prosthetic groups, carriers and the cell envelope as well as central- and energy-metabolism, DNA replication, recombination and repair, translation, transport and binding proteins, photosynthesis and respiration and other regulatory proteins). A particularly high number of PacR-regulated genes are involved in photosynthesis and C_i assimilation (e.g. the CCM) or encode regulatory proteins. Photosynthetic genes targeted by PacR are in general regulated depending on C_i availability. For example, their products function in ROS protection or are structural components of both PSI and PSII (Picossi et al., 2015).

PacR shares an 82 % sequence identity with RbcR (*sll0998*) from *Synechocystis* sp. PCC 6803 (Bolay et al., 2022). In contrast to *Anabaena*, RbcR is essential in *Synechocystis* sp. PCC 6803 (Figge et al., 2001) probably due to its role as positive regulator of C_i acquisition genes, e.g. *rbcLS*, coding for RuBisCO (Bolay et al., 2022; Figge et al., 2001). Moreover, expression of *rbcR* is induced under low C_i conditions in *Synechocystis* (H. L. Wang et al., 2004), whereas in *Anabaena*, *pacR* expression appears constitutive and independent of C_i availability (Picossi et al., 2015). Despite these regulatory differences, PacR and RbcR seem to both play roles in regulating genes involved in C_i acquisition and concentration and appear to share a certain target set (e.g. *rbcLXS*, *sbtAB*, carboxysome-component coding genes (e.g. *ccmK*) and stress-response genes such as *sigB* and *flv4* (*flv2* only in *Synechocystis* sp. PCC 6803) as well as *ndhF3*) (Bolay et al., 2022; Picossi et al., 2015). However, in contrast to other autotrophic microorganisms, RbcR of *Synechocystis* sp. PCC 6803, does not function as a global master-regulator of all CBB cycle genes (Bolay et al., 2022).

1.5.4 The integration of 2-OG and 2-PG signals enables C/N balancing

The intracellular 2-PG and 2-OG levels are inversely correlated, and their ratio reflects the C/N balance. The mechanisms by which cells sense and readjust their C/N status involve a complex network of interdependent signalling proteins and TFs. These regulatory pathways respond not only to 2-OG and 2-PG but also to other key metabolites such as ATP, NADP(H), and RuBP (C. C. Zhang et al., 2018). Some central signalling networks are highlighted below. Under N limitation, the NtcA/2-OG complex activates transcription of N uptake and assimilation related genes, while the NdhR/2-OG complex represses CCM related genes. In contrast, the apo form of NtcA has a low DNA-binding affinity under C_i limitation, leading to downregulation of N uptake and assimilation genes. Simultaneously, the NdhR/2-PG complex is unable to bind DNA and act as a repressor, thereby allowing the expression of CCM genes. Thus, the joint action of NtcA and NdhR helps regulating C and N uptake and assimilation genes to regain C/N balance (C. C. Zhang et al., 2018).

Additional TF are also involved in integrating C/N signalling. As an example, in *Synechocystis*, it has been proposed that under C_i limitation the PacR homologue RbcR, together with the TF CyAbrB2, may activate C_i assimilation genes after alleviation of NdhR mediated repression (Bolay et al., 2022).

Another example of C/N involves the regulation of CO_2 import via the CmpR TF. CmpR may activate the *cmp* operon in response to 2-PG binding, promoting CO_2 import under C_i limitation (Nishimura et al., 2008). While CmpR in *Anabaena* is expressed under low C_i, its expression under these conditions is boosted when N is

absent via coregulation of its expression by NtcA (López-Igual et al., 2012), allowing coordination between C_i uptake and N availability, as reflected by 2-OG levels.

1.6 Heterocyst metabolism and differentiation

1.6.1 Characteristics of heterocysts

The distinguishing characteristic of a heterocyst is its microoxic environment, which protects nitrogenase from O_2 and provides it with ATP and reducing equivalents in form of Fed (e.g. the heterocyst-specific *fdxH*, the main nitrogenase e^- donor (Masepohl et al., 1997) and *fdxB* (Kourpa 2019). Low O_2 levels in heterocysts are maintained through a combination of mechanisms: 1) A specialized cell envelope restricts O_2 diffusion (Chapter 1.1.) 2) O_2 production is minimized by the presence of non-O_2 producing PSII (Magnuson, 2019; Nagao et al., 2022). 3) Active respiration is mediated by NtcA-dependent expression of the heterocyst specific RTOs Cox2 and Cox3 which are located in the honeycomb membranes (Jones & Haselkorn, 2002; Valladares et al., 2003, 2007). 4) The cytoplasmic heterocyst-specific Flv3B homo-oligomer enables microoxic conditions by performing light-induced O_2 reduction (Ermakova, 2014).

Heterocyst lack CCM, glycogen granules, and functional PSII and are therefore limited to photoheterotrophic metabolism. Thus, vegetative cells provide them reduced C in form of e.g. sucrose, alanine (Ala) and Glu (Cumino et al., 2007; Flores, Picossi, et al., 2019; Harish & Seth, 2020; Nieves-Morión et al., 2021). Sucrose then enters the OPP pathway or glycolysis, producing NADPH (Cumino et al., 2007; Curatti et al., 2002). There have been conflicting reports of this NADPH directly reducing Fed and then nitrogenase, or rather electrons being transported to nitrogenase via PSI (Magnuson, 2019; Schrautemeier et al., 1984). More recently, an e^- transport network has been proposed, where NADPH originating from the OPP pathway reduces Fed via FNR and subsequently Fed may directly reduce nitrogenase or contribute to LET via NDH-1. In this model, Fed also donates e^- to RTO or FDP activity (Alleman & Peters, 2023). Moreover, the CET is active in heterocysts to enhance ATP production, which is mainly produced through photosynthetic light reactions. This ATP is vital for nitrogenase activity (Alleman & Peters, 2023; Bandyopadhyay et al., 2021; Thomas, 1970). Compared to vegetative cells, heterocysts contain higher levels of NDH-1, ATP synthase, PSI, and the Cyt b_6f complex (Ow et al., 2008).

N_2 fixation in heterocysts is carried out by the heterocyst specific nitrogenase enzyme, a multiprotein enzyme complex that catalyses N_2 fixation, with unidirectional H_2 production as an inevitable side-product (Bothe et al., 2010; Khetkorn et al., 2012; Tsygankov, 2007; W.D. Steward, 1996). Nitrogenase

functions as a heterodimer, with each dimer composed of three subunits: one NifH and two NifDK (Alleman & Peters, 2023; A. K. Mishra et al., 2019). NifDK forms the MoFe dinitrogenase component (*nifD* codes for the α- and *nifK* for the β-subunit), which reduces N_2 in an ATP dependent reaction. NifH is the Fe dinitrogenase reductase that accepts e^- from Fed. In this energy and e^- intensive reaction, N_2 and protons are simultaneously reduced to NH_4^+ and H_2, respectively, as shown in the equations below (Burgess & Lowe, 1996; Christiansen et al., 2001; A. K. Mishra et al., 2019; Ross D. Milton, 2016):

Under N_2 atmosphere:

$$N_2 + 8\ H^+ + 8\ e^- + 16\ ATP \rightarrow 2\ NH_3 + H_2 + 16\ ADP + 16\ P_i$$

When N_2 is not available, all e^- are directed towards protons, which reduces the ATP requirement (Mohan & Pandey, 2013; Wilson et al., 2021):

$$2\ H^+ + 2\ e^- + 4\ ATP \rightarrow H_2 + 4\ ADP + 4\ P_i$$

To recycle H_2 produced by nitrogenase (Khanna & Lindblad, 2015; Tamagnini et al., 2007), *Anabaena* possesses Hup which is expressed exclusively in the heterocysts (Houchins & Burris, 1981).

The heterocyst-specific Hup consists of at least two subunits: the large subunit, HupL, which contains the active site NiFe cluster and a small subunit, HupS, which contains the FeS clusters that transport e^- between the active center and the e^- acceptor/donor (Albracht, 1994; Tamagnini et al., 2002, 2007).

Hup is likely membrane-bound, however the existence of a soluble form cannot be ruled out (Houchins & Burris, 1981). H_2 recycling has been suggested to have at least four different beneficial functions: 1) It provides ATP via the oxyhydrogen reaction, minimizing the loss of energy 2) It removes O_2 from nitrogenase, protecting it from inactivation 3) It supplies reducing equivalents to N fixation, photosynthesis and other reductive processes and 4) It prevents feedback inhibition of nitrogenase by H_2 buildup (Khanna & Lindblad, 2015; Tamagnini et al., 2007). In *Anabaena*, the contiguous *hupL* and *hupS* genes undergo rearrangement during heterocyst differentiation (see chapter 1.6.2.). The promoter of the *hup* operon contains a putative NtcA binding site, for which NtcA binding could be demonstrated, at least in *N. punctiforme* (Pia Lindberg, 2003; Tamagnini et al., 2007).

In heterocysts, at least parts of the NO_3^- uptake system and GOGAT are not expressed (A. K. Mishra et al., 2019). NH_4^+ generated by nitrogenase is incorporated into vegetative cell-provided Glu by GS, producing Gln. Gln is transferred to the adjacent vegetative cells (Martín-Figueroa et al., 2000; Thomas et al., 1977; Wolk et al., 1976). Accordingly, in heterocystous *Anabaena*, 2-OG metabolism mainly takes place in vegetative cells (Galmozzi et al., 2010). However, 2-OG levels remain high

in the heterocysts due to the activity of the NADH-IDH, which generates NADPH for Fed reduction (Galmozzi et al., 2010; Martín-Figueroa et al., 2000). This 2-OG is then exported to the vegetative cell (Böhme, 1998; Malatinszky et al., 2017; Martín-Figueroa et al., 2000). In *Anabaena*, only one Fed-dependent GOGAT (encoded by *glsF*) is found, and transcription levels remain constant regardless of the N source. Expression is restricted to vegetative cells (Martín-Figueroa et al., 2000). In heterocysts, accumulation of 2-OG represses *gifA* transcription via NtcA, thus leading to GS activation (see chapters 1.4.3.; 1.5.2.). Moreover, the *gifA* promoter is not de-repressed in heterocysts, possibly due to higher 2-OG levels influencing NtcA activity. Thus, the GS inactivation system is repressed in heterocysts but not in vegetative cells in *Anabaena* (Galmozzi et al., 2010), allowing for a splitting of the GS/GOGAT cycle between cell types.

If Gln is not exported from the heterocyst, it is converted to Arg and perhaps also exported in this form (Böhme, 1998; Martín-Figueroa et al., 2000). Arg is the most N rich amino acid and has a role both as a protein building block, and in a wide range of N metabolism, including N storage (Forchhammer & Selim, 2020). Arg together with Asp, can be used to synthesize cyanophycin (Flores, Arévalo, et al., 2019). In the heterocyst, and to a lesser degree also in the vegetative cell, cyanophycin is stored as a dynamic N reservoir (Flores, Arévalo, et al., 2019; Gupta & Carr, 1981; Picossi et al., 2004; H. Zhang & Yang, 2019). In heterocysts, cyanophycin accumulates at the heterocyst poles adjacent to vegetative cells as cyanophycin granules (Flores, Picossi, et al., 2019; Lang et al., 1972; Sherman et al., 2000) which appear to function as a transient N storage before transfer to the vegetative cell in form of β-aspartyl-arginine (Burnat et al., 2014; Flores, Arévalo, et al., 2019; N. G. Carr, 1989; Sherman et al., 2000).

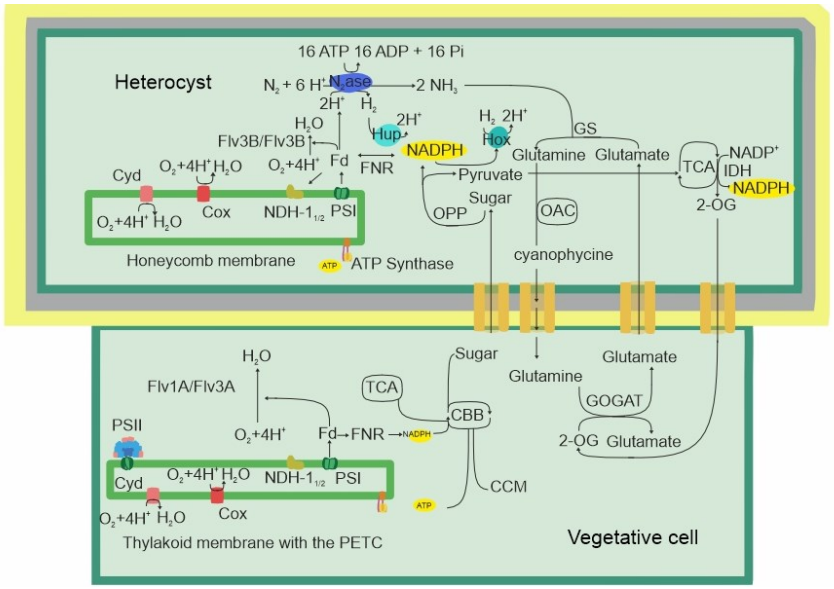

Figure 4. Difference in metabolic pathways and exchange in metabolites between the vegetative cell and heterocyst. In contrast to the vegetative cell, the heterocyst doesn't have an active PSII and it utilizes RTOs like Cox and Cyd as well as Flv3B to maintain a microoxic environment. Fd-I and FNR(long) possibly perform classic e^- transfer, while FxdH is specific for CET and nitrogenase and FNR (short) is specific for shuttling of e^- from the OPP to FdxH. Hox may function as an e^- valve. Photosynthetic reducing equivalents are donated to nitrogenase for N_2 fixation. Nitrogenase produces H_2 as a sideproduct from which reducing equivalents are recycled via Hup. The GS/GOGAT cycle is split between the cell types, allowing for transport of N fixed in the heterocyst via Gln. 2-OG is produced in the heterocyst to generate reducing equivalents and is also transported to the vegetative cell (Ermakova, 2014; Khetkorn et al., 2012; Malatinszky et al., 2017; Perin et al., 2021; Pernil & Schleiff, 2019).

1.6.2 Heterocyst differentiation

Anabaena filaments require approximately 48 h to fully switch to atmospheric N_2 fixation (Perin et al., 2021). It has been suggested that more than one round of heterocyst differentiation may occur within this period (Nieves-Morión et al., 2021). Other sources however state that heterocyst differentiation is typically completed within 18-24 h after N deprivation (Flores, Picossi, et al., 2019; Santamaría-Gómez et al., 2018; Valladares et al., 2011), with protoheterocysts already detectable after six-eight hours (Harish & Seth, 2020; A. M. Muro-Pastor & Hess, 2012). During heterocyst differentiation, the photoautotrophic metabolism of the vegetative cell is switched to heterotrophic mode (Harish & Seth, 2020), the O_2 impenetrable outer layer is synthesized, and key enzymes such as RTOs, FDPs and nitrogenase are expressed. Central to the regulation of heterocyst differentiation in cyanobacteria are the global regulatory transcription factor NtcA and PipX, which mediate responses

to C/N balance, as well as HetR, which is only found in filamentous cyanobacteria and functions in cell differentiation (Flores, Picossi, et al., 2019).

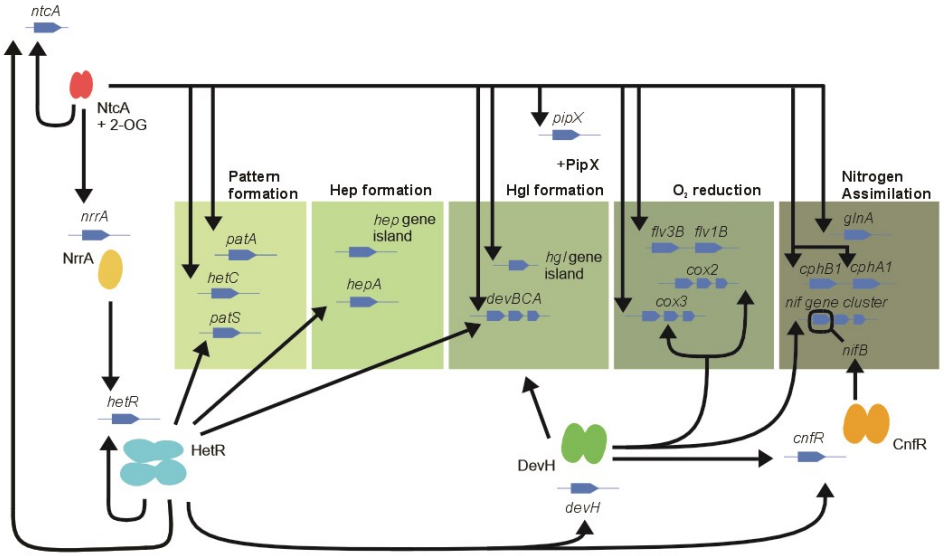

Figure 5. Timeline of gene activation during heterocyst formation. A subset of genes are shown as examples. Heterocyst differentiation takes 18-24 h to complete after N stepdown. No precise timings are intended to be shown in the figure. However, genes represented further left are expressed at earlier stages of differentiation than genes represented to the right. NtcA-NrrA-HetR interactions initiate heterocyst differentiation, however NtcA as well as HetR also influence gene expression at later stages as indicated by arrows. Grey boxes group genes implicated in the indicated activities. Genes are shown as blue arrows. Proteins are represented by the other shapes (ovals, squares, triangles etc...). Solid arrows = direct regulation (i.e. the direct binding of the regulator to the promoter has been demonstrated), grey arrows = direct regulation is hypothetical and dashed arrows = indirect regulation/reglation not known. Abbreviations: HK=Histidine Kinase; RR= Response regulator; STK=Serine/Threonine Kinase; HTH=Helix-Turn-Helix-Motive; -P= Phosphorylation possible or demonstrated. Image adapted after Flores, Picossi et al. 2019 (Flores, Picossi, et al., 2019; Harish & Seth, 2020; Kurio et al., 2020; A. M. Muro-Pastor & Hess, 2012; Zeng & Zhang, 2022)

Heterocyst differentiation is terminal process and encompasses four major processes (does not reflect the sequence of events): (a) sensing the differentiation signal and initiating differentiation (b) spatial pattern determination along the filament (c) formation of heterocyst envelope and (d) assembly of the N_2 fixing machinery. After triggering of heterocyst formation via NtcA, NrrA and HetR, the spatial distribution pattern of heterocysts is first established, and then the final commitment to terminal heterocyst differentiation is initiated. First, protoheterocysts are formed by degrading PBS, reorganizing thylakoid membranes into honeycomb membranes and synthesizing Hep and Hgl layers. However, protoheterocysts do not

yet have a microoxic environment and lack rearrangement of *nifHD*. Thus, in the second/maturation stage, Pipx is activated and first O_2 consuming processes are established (e.g. expression of FDP and Cox encoding genes). Nitrogenase encoding genes can then be expressed and N_2 assimilation can commence. Remodelling of C and N metabolism accompanies this process, including the suppression of C_i fixation by e.g. binding of NtcA at the translation start site of the *rbcLXS* operon, thereby downregulating production of RuBisCO. (Flores, Picossi, et al., 2019; Harish & Seth, 2020; A. M. Muro-Pastor & Hess, 2012; Zeng & Zhang, 2022). The developmental steps of heterocyst formation are shown in Figure 4 and described in more detail in the following.

Heterocyst formation in *Anabaena* is triggered by C/N imbalance and relies on a precise sensing of the internal C/N ratio. While N deprivation is the primary cue, elevated CO_2 levels can also trigger heterocyst formation, demonstrating the central regulatory role of the C/N balance (C. C. Zhang et al., 2018).

Here, N starvation as the main driver of heterocyst formation is discussed. Following the principle of N control, heterocyst differentiation only takes place when no combined N source is available, as N_2 fixation is the most energy-demanding form of N (E. Flores; A. Herrero, 2005; Herrero et al., 2001). N starvation is signalled by rising intracellular levels of 2-OG, which links C and N metabolism through the GS/GOGAT cycle (see chapter 1.4.3.). 2-OG is considered the primary metabolic trigger for heterocyst formation (see chapter 1.5.2.) (Harish & Seth, 2020; Zeng & Zhang, 2022; C. C. Zhang et al., 2018). Increased intracellular levels of 2-OG have been shown to increase heterocyst frequency and accelerate commitment to heterocyst differentiation in *Anabaena* (J. H. Li et al., 2003). In *Anabaena*, 2-OG levels peak one hour after removal of N, triggering the heterocyst differentiation process, and then gradually return to basal levels within 16 h (Laurent et al., 2005; Videau et al., 2015). This may be due to 2-OG being consumed as a C skeleton during the breakdown of N reserves (Laurent et al., 2005; Meeks & Elhai, 2002). In accordance with this, heterocyst frequency usually peaks shortly after N deprivation and then decreases gradually (J. H. Li et al., 2003; Zulkefli & Hwang, 2020).

Fluctuations in basal *hetR*/HetR and *patS*/PatS levels even in the presence of NH_4^+ within individual cells lead to a latent pattern, which results in heterocyst pattering after N stepdown (Corrales-Guerrero et al., 2015; Flores, Picossi, et al., 2019; Yoon & Golden, 2001). PatS is a 17-amino acid peptide that, when expressed after activation by HetR, diffuses to neighbouring cells and establishes a concentration gradient, acting as a morphogen and inducing the posttranslational degradation of HetR, inhibiting heterocyst formation in neighbouring cells, thus determining heterocyst pattering (Flores, Picossi, et al., 2019; Harish & Seth, 2020; J. H. Li et al., 2003).

In heterocystous cyanobacteria, 2-OG binds to and activates NtcA. This N starvation signal is amplified by positive autoregulation of NtcA until *ntcA* transcription reaches a maximal level, enabling the activation of alternative N metabolism and heterocyst formation genes (Herrero et al., 2001; J. H. Li et al., 2003). *hetR* codes for the master regulator of heterocyst formation and its expression is activated indirectly by NtcA through the response regulator-like factor NrrA (Ehira & Ohmori, 2006; María Muro-Pastor et al., 2006; Zeng & Zhang, 2022). After NtcA induces *hetR* expression, both TFs positively regulate their own expression by binding to their own and each other's promoters (A. M. Muro-Pastor et al., 2002). In protoheterocysts, NtcA also upregulates *furA* expression. FurA may negatively regulate NtcA expression depending on 2-OG levels as well as HetR expression. This partially suppresses heterocyst differentiation since morphogenesis is impaired early in the process as an additional safeguard against premature differentiation (González et al., 2013; Guío et al., 2020). HetR is an NtcA co-activator (Camargo et al., 2012) and regulates *hetP*, which is involved in the irreversible commitment to heterocyst formation, directly (Higa & Callahan, 2010; Videau et al., 2016). After commitment to heterocyst differentiation, FurA induces other heterocyst formation genes, such as *hetC* and *patA* and modulates *patS* expression (González et al., 2014). Expression of the HepA gene, which enables synthesis of the Hep layer (Harish & Seth, 2020; Zhu et al., 1998) requires HetR binding (Flores, Picossi, et al., 2019). Likewise, genes involved in Hgl layer formation are activated by NtcA/HetR directly (Camargo et al., 2012; Picossi et al., 2014) or indirectly via the TF DevH (Hebbar & Curtis, 2000; Kurio et al., 2020).

During the late phase of heterocyst differentiation, HetN regulates pattern maintenance (Callahan & Buikema, 2001; Casanova-Ferrer et al., 2022). PipX is a late NtcA coactivator, directly activated by NtcA and required to achieve the activation of late heterocyst differentiation genes (e.g. FDPs and Cox encoding genes to establish microoxic conditions) as well as mature heterocyst genes (Flores, Picossi, et al., 2019; Valladares et al., 2011). DevH also regulates late heterocyst-specific genes including the *cox2* and *cox3* operons and the *nif* gene cluster (Zeng & Zhang, 2022).

In *Anabaena* (as well as other diazotrophic bacteria), *cnfR* (previously *patB*) is expressed only in heterocysts via NtcA regulation and probably activates *nif* gene expression due to low O_2 tension. The kinase PknE, whoes transcription is activated by HetR and NtcA, inhibits HetR in a later stage of differentiation via phosphorylation (Flores, Picossi, et al., 2019; Harish & Seth, 2020). During mid-to-late heterocyst differentiation, FurA also contributes to shutting down NtcA activity together with PknE or HetR (González et al., 2013).

2 Aims of the study

Flavodiiron proteins are of major importance as auxiliary e^- sinks in photosynthetic organisms. By harmlessly dissipating excess reducing power, FDPs protect the photosynthetic apparatus under fluctuating light intensities. Interest in FDPs has grown substantially due to their major role in cellular bioenergetics, as well as their biotechnological potential: Redirecting e^- flux away from FDPs towards reductive bio-transformations could enhance the efficiency of photosynthetic production systems. To this end, it is imperative to gain a deeper understanding of the role of FDPs within regulatory mechanisms and endogenous networks. Here, the impact of FDP deletion on the photosynthetic performance and N_2 fixation capacity is investigated in the N_2-fixing cyanobacterium *Anabaena*.

To place FDP function within a broader regulatory context, the role of PacR, a global transcription factor that also affects FDP expression, was explored. PacR plays a major role in regulating photosynthesis and the C metabolism, thereby most likely adjusting C_i assimilation to the photosynthetic capacity.

Thus, by deepening the understanding of the global regulator PacR and of FDPs as part of the PacR regulon as well as a vital redox buffering system, I aim at understanding better how *Anabaena* balances C/N and photosynthesis. These insights will inform bioengineering strategies aiming at utilizing reductive power and/or the N_2 fixation and H_2 producing capabilities of *Anabaena*.

Therefore, my thesis has two main objectives:

- Elucidate the role of vegetative-cell specific Flv1A and Flv3A proteins in *Anabaena,* and determine how they are linked to photosynthetic performance and heterocyst metabolism.
- Elucidate how PacR regulates the crosstalk between photosynthesis and C/N balancing and coordinates metabolism between heterocyst and vegetative cells in *Anabaena* with particular emphasis on its role in regulating the expression of flavodiiron proteins at a transcriptional level.

3 Materials and Methods

3.1 Cyanobacterial strains and growth conditions

First paper. Strains used in the first paper were the *Anabaena sp.* PCC 7120 wild type (WT) as well as the Δ*flv1A,* Δ*flv3A* (Allahverdiyeva et al., 2013) and Δ*hupL* (Masukawa et al., 2002) mutants which were described previously. A second Δ*flv3A* clone was constructed as previously described by inserting a neomycin (Nm) cassette into the *all3895* gene (Allahverdiyeva et al., 2013). The double-mutant Δ*flv1A*/Δ*flv3A* was constructed as follows: The Nm resistance cassette of the Δ*flv1A* construct was replaced with a Spectinomycin (Spec)/Streptomycin (Strep) resistance cassette. This construct was then used to mutate a Δ*flv3A* strain. Selection for new clones was done by adding sucrose, the respective antibiotic(s) (Cai & Wolk, 1990) and segregation was checked via polymerase chain reaction (PCR). Δ*flv1A* and Δ*flv3A* were maintained in BG11 medium supplemented with 40 µg ml^{-1} Nm and Δ*flv1A*/Δ*flv3A* double mutants were supplemented with 40 µg ml^{-1} Nm and 15 µg ml^{-1} Spec. Δ*hupL* was maintained in BG11 medium with 20 µg ml^{-1} Spec. Precultures were grown without antibiotics in Z8x medium (Z8 medium without N sources, pH 7.0-7.3, (Kotai, 1972)) and at 30 °C. Cells were illuminated under constant white light (50 µmol photons m^{-2} s^{-1}) and the starting optical density at 750 nm (OD_{750}) was 0.1. Cells were grown in a total volume of 200 ml with continuous bubbling with air with LC or air supplemented with 1 % CO_2 (HC) unless mentioned otherwise. The precultures were harvested at the logarithmic growth phase and inoculated in fresh Z8x medium at an OD_{750} of 0.1. The experimental cultures were grown in the same way as the pre-cultures and harvesting was conducted after four days.

Second paper. The Δ*pacR* knockout mutant of *Anabaena* sp. PCC 7120 (strain CSS74) and the control strain (CS), CSS77, were previously characterized by Picossi et al., 2015. Initial cultures were cultivated in BG11 medium containing 20 mM HEPES-NaOH buffer (pH 7.5) and 25 µg ml^{-1} Spec. These cultures were maintained at 30 °C with continuous shaking at 80 rpm, under HC and illuminated at 50 µmol photons m^{-2} s^{-1}.

To prepare precultures, cells were collected from four-day old initial cultures and diluted to an OD_{750} of 0.1 in BG11-0 medium, which was also buffered with 20 mM HEPES-NaOH (pH 7.5). After setup, 6 mM NH_4Cl were added to the medium, followed by an additional 3 mM NH_4Cl after two and three days. Experimental cultures were set up in the same way as the precultures but were grown in BG11-0 medium at pH 7.5, supplemented either with 3 mM NH_4^+ (added on days 1, 2, and 3 for growth assays) or with 17.6 mM NO_3^- as the N source.

3.2 Chl *a* and total sugar determination

Chl extraction. For extraction of Chl *a* from cyanobacteria cells, they were treated with 90 % methanol and heated at 65 °C for 10 min. Cells were spun down and the supernatant used for analysis. After spectroscopic measurement, the Chl *a* concentration was determined using the extinction coefficient factor of 12.7 (Meeks & Castenholz, 1971).

Determination of total sugar content. Total sugar, including simple sugars, oligosaccharides and polysaccharides) was determined via a colorimetric method described previously (Dubois et al., 1956).

3.2.1 Gas exchange measurements

Membrane Inlet Mass Spectrometry (MIMS). For Paper I, cells were harvested after four days and resuspended in fresh Z8x medium. For paper II, cells were grown for 48 h, harvested and resuspended in fresh BG11 medium. A total Chl *a* concentration of 10 µg mL^{-1} was adjusted. Prior to measurements, cells were acclimated for one hour under growth conditions. In case of LC samples, the dissolved inorganic C was saturated with 1.5 mM $NaHCO_3$ prior to measurements. *In vivo* measurements were then conducted using MIMS as described previously (Mustila et al., 2016), monitoring $^{16}O_2$ (m/z = 32), $^{18}O_2$ (m/z = 36), CO_2 (m/z = 44) and H_2 (m/z = 2) fluxes. Gas exchange was measured for four minutes in darkness, then five minutes under HL (500 µmol photons m^{-2} s^{-1}) and then two minutes in the dark. The CCM coefficients were determined as described previously (Douchi et al., 2019). For measurement of deuterium (D_2) uptake, the medium was flushed with argon (Ar) for 15 min, then, pure D_2 was injected (2 % D_2 in total in headspace). Two hours and 24 h after injection, changes in H_2 (m/z = 2), D_2 (m/z = 4) and HD (m/z = 3) content in the gas phase were measured via injection of 250 µl gaseous samples into the gastight MIMS chamber. The maximal response after background subtraction, served as an estimate for H_2, D_2 and HD content.

The activities of Hup and Hox (total hydrogenase activity) determine the consumption of D_2 from the headspace. HD was formed in very low amounts compared to H_2 and D_2 signals, which indicates that the N_2 dependent hydrogenase activity of the nitrogenase, which is needed for the H/D exchange reaction (Vignais, 2005), is negligible and thus also doesn't significantly contribute to D_2 uptake. Thus, it was possible to simply analyse D_2 as a proxy for total H_2 recycling capacity. Calibration was conducted by measuring the signal for known D_2 concentrations into the chamber.

3.2.2 Spectroscopy

Chl fluorescence and absorbance. Chl *a* fluorescence and P700 absorbance were measured simultaneously using a pulse amplitude modulated (PAM) fluorometer (Dual-PAM-100, Walz). For the first paper, cells were grown under diazotrophic conditions in LC for four days and were then harvested and resuspended in fresh Z8x medium. For the second paper, after harvesting, cells were resuspended in fresh BG11 medium. A Chl *a* concentration of 15 µg mL^{-1} was adjusted, and cells were acclimated under growth conditions for one hour. Before the measurement, samples were dark adapted for 10 min. The effective quantum yield of PSII [Y(II)] and PSI [Y(I)], as well as the acceptor side limitation of PSI [Y(NA)] and donor side limitation of PSI [Y(ND)] were measured and calculated as described previously (Huokko et al., 2017). For Paper I, a saturating pulse (SP, 5 000 µmol photons m^{-2} s^{-1}, 400 ms) was applied in darkness, determining maximal fluorescence under dark adaptation (F_m^D). This was followed by 380 s long illumination with red actinic light at 50 µmol photons m^{-2} s^{-1} while SPs were given every minute (SP1-SP9). For Paper II, a SP (300 ms, 5 000 µmol photons m^{-2} s^{-1}) was given in darkness, followed by application of strong far red light (720 nm, 75 W m^{-2}), during which a SP was given, followed by actinic light (630 nm, 50 µmol photons m^{-2} s^{-1}) for 250 sec, during which time four more SPs were given.

Determination of model spectra for the determination of P700 and Fed redox changes from near infrared absorbance. To determine changes in the redox state of Fed via absorbance differences at 780–820, 820–870, 840–965 and 870–965 nm, a Dual-KLAS-NIR spectrophotometer (Walz) was used. Cultures were grown in 50 µmol photons m^{-2} s^{-1} under LC conditions in Z8x medium for four days. After harvesting, cells were resuspended in fresh Z8x medium. After adjusting a Chl *a* concentration of 20 µg mL^{-1} and acclimation of one hour under growth conditions, cells were dark adapted for 10 minutes.

The redox change kinetics of P700 and Fed are deconvoluted from the four absorbance differences using differential model plots. Model plots were measured

from *Anabaena* as described for *Synechocystis* by Theune et al., 2021, with the exception that to measure Fed model spectra the Δ*flv1A*/Δ*flv3A* mutant was used instead of anaerobic conditions to impair the Mehler-like reaction and sufficiently slow down the reoxidation of Fed. To measure P700 and Pc model spectra, WT *Anabaena* was used. Probably, P700 and Pc signals are closely related in *Anabaena*, which makes it difficult to extract a Pc signal of large magnitude.

Determination of P700 and Fed redox changes. To determine changes in the redox state of Fed via absorbance differences at 780–820, 820–870, 840–965 and 870–965 nm, a Dual-KLAS-NIR spectrophotometer (Walz) was used. For the first paper, cultures were grown in 50 µmol photons m^{-2} s^{-1} under LC conditions in Z8x medium for four days. After harvesting, cells were resuspended in fresh Z8x medium. For the second paper, after harvesting cells were resuspended in fresh BG11 medium. After adjusting a Chl *a* concentration of 20 µg mL^{-1} and acclimation of one hour under growth conditions, cells were dark adapted for 10 min. For most of the strains used in the first paper, absorbance differences of the wavelength pairs were measured during application of five seconds of actinic illumination at 500 µmol photons m^{-2} s^{-1}, followed by a dark period. The maximal levels of P700 oxidation and Fed reduction were determined using the NIRMAX script as described below.

For the second paper (and the *Synechocystis* Δ*flv1A* mutant from the first paper), the absorbance differences between the aforementioned wavelength pairs were measured using the NIRMAX script (Klughammer & Schreiber, 2016; Schreiber, 2017): First, three seconds of red actinic illumination (3000 µmol photons m^{-2} s^{-1} or 200 µmol photons m^{-2} s^{-1} in case of the *Synechocystis* Δ*flv1A* mutant), with a multiple turnover (MT) pulse after 200 ms to fully reduce the Fed pool was applied. Secondly, a four second dark period was applied. Thirdly, 10 s of far-red illumination (intensity setting 20), with a MT pulse administered at the end of the illumination period to fully oxidize P700, was applied. The P700 and Fed signals were deconvoluted using *Anabaena* model spectra. The signals were then normalized to the maximal redox changes and the data was smoothed and baseline corrected. The size of the photo reducible Fed pool was calculated during actinic light illumination from about 100 datapoints during the maximal reduction phase.

Measurement of the electrochromic shift (ECS). For measurement of the ECS, 500-480 nm absorbance differences were measured (Viola et al., 2019) via a Joliot-type spectrophotometer (JTS-10) (BioLogic, Seyssinet-Pariset, France). Cells were cultivated under LC conditions, harvested and resuspended in fresh Z8x medium to a Chl a concentration of 7.5 µg mL^{-1} followed by five minutes of dark-adaption. First, cells were subjected to illumination with 500 µmol photons m^{-2} s^{-1} for two minutes with 600 ms dark periods at specific timepoints. The dark interval relaxation kinetics (DIRKs) of the ECS were used to determine the magnitude of the *pmf* as the

light induced change in the ECS signal. The conductivity of the thylakoid membrane (gH^+) was determined as the inverse of the time constant of a first order fit to DIRKs kinetics, and the thylakoid proton flux (vH^+) as the product of *pmf* and gH^+.

Determination of fluorescence emission spectra at 77 K and the transient post-illumination fluorescence (F_0 rise). 77 K spectra were measured via a QE Pro-FL spectrofluorometer (Ocean Optics). Cells were grown under diazotrophic conditions in LC for four days and were then harvested and resuspended in fresh Z8x medium. Cells were adjusted to 5 µg mL^{-1} Chl *a* and rapidly frozen in liquid N_2 after dark adaptation for 15 min. The excitation wavelength was 580 nm and normalization of the fluorescence spectra was done relative to the PSI peak at 730 nm. Measurements conducted for nine minutes under red actinic light at 50 µmol photons m^{-2} s^{-1} were used to access the F_0 rise for nine seconds after termination of the actinic light. Normalization of traces was done in relation to the steady-state-level fluorescence (F_s), to make comparison of kinetics easier.

3.3 Transcript analysis

RNA-isolation. Cells were grown for four days with NH_4^+ as the sole N source in the medium. Harvesting of cells was done via filtration using Millipore HATF nitrocellulose membranes (0.45 µm) and cells were resuspended in NO_3^- containing growth medium and grown for one hour or 12 h. For each timepoint (before shifting the cells to the new medium and one hour and 12 h after the shift), cells were resuspended in RNA resuspension buffer (Walter et al., 2016), centrifuged for three minutes at 4 °C and then snap frozen in liquid N_2. The hot-phenol method was employed to isolate total RNA (Walter et al., 2016). However, incubation in phenol:chloroform:iso-amyl alcohol was performed at 65 °C instead of 95 °C. The samples were then resuspended in 25 µL of Milli-Q H_2O. To remove genomic DNA, the invitrogen kit was used. The RNA concentration was measured using a DS-11+ spectrophotometer (DeNovix).

Reverse transcription quantitative PCR (RT-qPCR). All steps during total RNA isolation, reverse transcription and qPCR analysis were performed as descried previously (Ermakova et al., 2013). For normalization, the *rnpB* gene was used as reference. Primer pairs can be found in Paper I.

RNA sequencing (RNA-seq). From RNA samples isolated previously, 3 µg were sent to BGI (China) for sequencing. The RNA quality check encompassed agarose gel electrophoresis, as well as checking of the RNA integrity number (RIN) values after rRNA depletion. RIN values were acceptable (7.2-8.2). RNA was sequenced

using DNBseq with a read length of PE 100 bp. For each time point and strain, three biological replicates were measured and reliability of data was confirmed via principal component analysis (PCA). Data analysis was conducted using the Chipster software via the following steps: 1. FastX for initial trimming 2. TopHat2 for alignment with the genome of *Anabaena* (downloaded from EnsemblBacteria (bacteria.ensembl.org), nostoc_sp_pcc_7120_fachb_418_gca_000009705, version ASM970v1_, current ENSEMBL release, October 2023). 3. HTseq for counting aligned reads per gene 4. DeSeq2 for differential expression analysis ($log_2FC \geqq I1I$, $p < 0.05$). Then, the R-package "clusterProfiler" was used for enrichment analysis.

3.4 Metabolic Analysis

Determination of N uptake and intracellular C and N content. Determination of NO_3^- concentrations in the growth media was conducted spectrophotometrically as described previously (Rice et al., 2012). Samples were prepared by filtration. Intracellular C/N rations were determined as follows: Cells were harvested after 48 h of growth in medium containing NO_3^- as the only N source. 10 mg of biomass were lyophilized, and total C and N analysis was conducted via a FLASH 2000 Organic Elemental Analyzer (Thermo Scientific).

Metabolite extraction and quantification. Cells were grown for four days with NH_4^+ as the sole N source in the medium. Harvesting of cells was via filtration using Millipore HATF nitrocellulose membranes (0.45 µm) and cells were resuspended in NO_3^- containing growth medium and grown for one or 12 more hours. For each timepoint (before shifting the cells to the new medium and one hour and 12 h after the shift), cells were again harvested via rapid filtration and filters were immediately frozen in liquid N_2. Cells were then resuspended in PBS buffer, pelleted and stored at –80 °C. The following steps were performed by the Institute for Molecular Medicine Finland, Helsinki. Extraction was done with acetonitrile:methanol:H_2O; 40:40:20 cold extraction solvent. High pressure liquid chromatography (HPLC) analysis was done with a Thermo Vanquish UHPLC coupled with a Q-Exactive Orbitrap quadrupole mass spectrometer equipped with a heated electrospray ionization (H-ESI) source probe (Thermo Fischer Scientific). Chromatographic separation of metabolites via a SeQuant ZIC-pHILIC (2.1 × 100 mm, 5 µm particle) column (Merck), which was maintained at +40 °C. Scanning in mass range of 55 to 825 m/z. Gradient elution was carried out with acetonitrile and 20 mM ammonium hydrogen carbonate in H_2O, adjusted to pH 9.4, as mobile phases. TraceFinder 4.1 software (Thermo Fischer Scientific) was used for data analysis.

3.5 Protein Analysis

Protein extraction and immunoblotting. Total protein extraction was performed as described previously (P. Zhang et al., 2009). Gel electrophoresis, based on equal protein content, as well as subsequent immunoblotting was also performed as described previously (Mustila et al., 2016). Flv3A antibodies were ordered from Agrisera, Vännäs, Sweden, NdhK and NifH antibodies were ordered from Agrisera and HupL antibodies were kindly provided by P. Tamagnini.

3.6 Nitrogenase activity

Nitrogenase activity assay. To determine nitrogenase activity, an acetylene reduction assay was conducted as described previously (Leino et al., 2014). Cells were placed in air tight vials, flushed with Ar and supplemented with 10 % acetylene in the headspace. The cells were illuminated for 20 h at 30 °C with 50 µmol photons m^{-2} s^{-1} while shaking at 120 rpm. Then, 20 µl of sample were taken to analyse ethylene content in the headspace via a gas chromatograph with a Carboxen®-1010 PLOT Capillary Column and flame ionization detector (FID). Enzymatic activity was calculated via the peak area and normalized to the total protein content.

3.7 Determination of H_2 production and D_2 uptake

Determination of H_2 production and D_2 uptake. Experimental cultures were harvested after four days and resuspended in fresh Z8x. Chl *a* concentrations of 3-4 µg mL^{-1} were adjusted. The cultures were sparged with N_2 or Ar for 30 min in the dark to generate anaerobic conditions. Then, cultures were incubated in an N_2 or Ar atmosphere for two more hours in the dark at 25 °C. Then, the H_2 concentration was measured for six minutes under actinic light (800 µmol photons m^{-2} s^{-1}) using a Clark type Pt-silver/silver-chloride electrode chamber (DW1/AD; Hansatech, King's Lynn, UK) connected to a homemade polarographic box. H_2 production rates were calculated via linear regression.

3.8 Microscopy

Determination of heterocyst frequency. Heterocysts were stained using Alcian Blue, which selectively stains the polysaccharide layer of the heterocyst envelope as previously described (McKINNEY, 1953). Cell suspensions were mixed in a ratio of 1:8 with 0.5 % Alcian Blue stain prepared in 50 % ethanol-H_2O. Visualization was achieved via a Wetzlar light microscope (Leica, Germany). Micrographs with a magnification of x 400 were taken via a mounted camera from Leica. The Leica

Application Suite (Leica Microsystems) was used to process the images. Per sample, 1000–2000 cells were counted. Heterocyst frequencies were calculated as a percentage of total cells counted.

4 Results

4.1 The special role of vegetative cell-specific Flv3A in O_2 photoreduction and H_2 photoproduction in *Anabaena*

4.1.1 Deletion of *flv1A* and *flv3A* affect the PETC differently under LC, possibly due to *flv2* and *flv4* expression

To characterize the *Anabaena* Δ*flv1A* and Δ*flv3A* mutants, as well as the Δ*flv1A/3A* double mutant they were compared to the WT in regards to FDP gene transcription levels, growth and heterocyst formation.

Intriguingly, the Δ*flv3A* mutant exhibited an elevated level of *flv1A* transcripts under LC and growth light conditions (Paper I; Fig. 1 c). This is in contrast to *Synechocystis*, where Flv1 and Flv3 are co-expressed (Jackson et al., 2023; Mustila et al., 2016).

While upregulation of *flv1A* can't rescue the Δ*flv3A* phenotype, clearly the Δ*flv3A* phenotype is not caused by the downregulation of other FDPs.

Under similar growth conditions (diazotrophic conditions, LC, 4 d, 50 µmol photons m^{-2} s^{-1}), neither single mutant showed a growth phenotype compared to the WT (Paper I; Table I). Chl *a*, total protein or sugar content were also comparable across all strains (Paper I; Table I). Moreover, no difference in heterocyst frequency (Paper I; Table I) or morphology (Paper I; Fig. S5) was found.

Thus, deletion of *flv1A* or *flv3A* under continuous illumination alone had no effect on diazotrophic growth (Paper I; Table 1, Fig. S4 b).

Next, photosynthetic performances of the FDP mutants were investigated using a range of spectroscopic analysis. In LC, Chl *a* fluorescence kinetics during dark-to-light-transitions differed between the two mutants. In case of Δ*flv3A*, fluorescence rapidly increased upon illumination, then gradually quenched but stabilized at a higher F_s than in the WT or Δ*flv1A* (Paper I; Fig. 1 a). Fluorescence in the Δ*flv1A* mutant increased only moderately and then decayed gradually, eventually reaching WT F_s levels. In contrast, under HC conditions, the fluorescence increase during the dark-to-light transition was similar between the mutants, eventually decaying to WT levels (Paper I; Fig. 1 b). The more pronounced Chl *a* fluorescence phenotype

observed in LC may be related to presence of *flv2* and *flv4* only under LC (Paper I; Fig. 1 c) as discussed later.

A more pronounced state 2 was observed in the Δ*flv1A* and Δ*flv3A* mutants, compared to the WT, as indicated by reduced PSII and PBS emission peaks relative to the PSI peak in the 77 K fluorescence emission spectra after dark adaptation (Paper I; Fig. S6 d). This was further supported by a significantly lower maximum fluorescence in the dark (Fm^D) in the mutants under LC conditions, with a similar trend observed under HC (Paper I, Fig. 1 a, b).

Additionally, both the Δ*flv1A* and the Δ*flv3A* mutant exhibited an enhanced post-illumination F_0 rise under both LC and HC conditions (Paper I; Fig. S 6 a, b). However, the protein abundance of NdhK, a core subunit of the NDH-1 complex, was found to be comparable across all strains (Paper I; Fig. S6 c).

An enhanced post-illumination F_0 rise is indicative of a reduction of the PQ pool in darkness, a process mediated by NDH-1 (Mi et al., 1995). However, in this case, the enhanced F_0 rise cannot be attributed to higher NDH-1 protein levels.

In the WT, Y(II) slightly decreased and remained stable over the illumination period under both LC and HC. Under LC, Y(II) decreases to 70 % of the WT level in the Δ*flv1A* mutant and to only 37 % of the WT level in the Δ*flv3A* mutant (Paper I, Fig. 1a). In contrast, in HC, both mutant strains showed a similar decrease, with Y(II) declining to 42 % and 37% of WT levels in the Δ*flv1A* and Δ*flv3A* mutants, respectively. Despite this, the maximum quantum yield of PSII (variable fluorescence/maximal fluorescence F_v/F_m), did not differ significantly between the WT and the mutants.

Both mutants have significantly lower rates of initial Fed reduction upon illumination as well as significantly delayed reoxidation of Fed. The Δ*flv3A* mutant displayed a more pronounced delay in Fed reoxidation (Paper I, Fig. 2). To determine whether these effects were due to differences in the ratio of the sizes of the reducible Fed pool and the oxidizable P700 pool, maximal near infrared absorbance changes associated with Fed reduction and P700 oxidation were measured. These analyses confirmed that the pool sizes were comparable among the WT and mutant strains, ruling out pool size as a factor contributing to altered e^- transport around PSI (Paper I; Fig. S 9 c).

4.1.2 Flv3A performs moderate O_2 photoreduction, independent from Flv1A, but only in the presence of Flv2 and Flv4

To distinguish O_2 reduction under light and photosynthetic O_2 production, the WT, Δ*flv1A*, Δ*flv3A* and the Δ*flv1A*/*3A* strains were investigated using MIMS and $^{18}O_2$ isotope. In the WT, under both LC and HC conditions, O_2 uptake followed a triphasic

kinetic of O_2 photoreduction (Burlacot et al., 2020; Santana-Sanchez et al., 2019; Saroussi et al., 2019). However, O_2 photoreduction were significantly impaired in all mutants (both maximal and steady state) under both LC and HC. In particular, the Δ*flv3A* mutant was strongly impaired in LC, reaching only 28 % of the WT maximal rate at the onset of light. The Δ*flv1A* mutant in contrast displayed an intermediate phenotype, reaching a maximum of 52 % of the O_2 photoreduction rate of the WT level in LC. In the *Δflv1A/3A* double mutant O_2 photoreduction under LC was more strongly inhibited than in either of the single mutants. Under HC, O_2 photoreduction in all mutants was completely abolished (Paper I, Fig. 3).

A possible alternative source of residual light induced O_2 photoreduction in the Δ*flv1A* mutant under LC, aside from FDP activity, could be the activity of the *Anabaena* PTOX homologue (McDonald et al., 2003). Interestingly, transcript levels of *ptox* were significantly elevated in the Δ*flv3A* mutant, under LC (Paper I, Fig S12 d). To test this possibility, O_2 levels were measured in the presence of *n*-propyl gallate (nPG), a PTOX inhibitor (Kuntz, 2004). O_2 photoreduction remained largely unaffected by nPG, suggesting that the process is independent of PTOX activity (Paper I, Fig S12 a-c).

4.1.3 *Flv1A* and *flv3A* deletion affects O_2 evolution, CO_2 fixation and *pmf* generation

To further characterize real-time gas-exchange properties of the mutants as well as the impact on *pmf* generation, MIMS and ECS analysis were employed.

Under LC, O_2 evolution upon illumination was significantly delayed only in the Δ*flv1A* and the Δ*flv1A/3A* double mutant compared to the WT (Paper I; Fig. 3a, Fig. S13 d). In contrast, under HC, O_2 evolution upon illumination was delayed significantly in a similar manner in all mutant strains (Paper I; Fig S13 e).

Under LC, the steady state CO_2 fixation rates of single and double mutants were lower than in the WT (statistically significant for the Δ*flv3A* mutant) (Paper I; Fig. 4 a). The CCM coefficient was also lower in single and double mutants than in the WT (statistically significant for the Δ*flv1A/3A* double mutant) (Paper I, Fig. 4 b).
To determine how *pmf* generation is affected in the Δ*flv1A* and Δ*flv3A* mutants, the DIRKs of the ECS signal during transitions from dark to high irradiance in cells grown under LC were investigated. The Δ*flv1A* and Δ*flv3A* mutants are significantly impaired in generating *pmf*, when transitioning to higher irradiance. The reason for this was a diminished *v*H+ (calculated as *pmf* x gH^+), which was only partially compensated by a lower gH^+, largely dependent on ATP synthase activity (Paper I, Fig 5, Fig. S3).

4.1.4 The lack of Flv3A results in a strong downregulation of the heterocyst-specific *hupL* gene, leading to enhanced H_2 photoreduction

The results described above indicate that Flv1A and Flv3A in vegetative cells have different impacts on bioenergetics of LC grown filaments. Next, to investigate impacts on heterocyst metabolism, nitrogenase activity as well as H_2 formation and turnover were investigated in *Anabaena* WT as well as the *Δflv1A* and *Δflv3A* mutants.

Under both HC and LC, the *Δflv3A* and the *Δflv1A*/*Δflv3A* double mutants displayed increased H_2 production in the dark as well as elevated light induced H_2 production, as detected by MIMS (Paper I; Fig. 3).

H_2 production was also measured in microoxic cultures (N_2 or Ar atmosphere) with a Clark type electrode. The *Δflv3A* mutant had a significantly higher light-induced net H_2 yield and the H_2 production rate compared to the WT was increased threefold under a N_2 atmosphere. The specific H_2 photoproduction rate of the WT under an Ar-atmosphere was seven times higher than under N_2. For the *Δflv3A* mutant, this rate was 10 times higher (Paper I; Fig. 6 d). This may indicate that H_2 production is nitrogenase-dependent, since nitrogenase reduces protons to H_2 if no N_2 is available (Skizim et al., 2012).

Moreover, to assess if Hox contributes to H_2 production, the *hoxH* transcript levels were examined. Both the *Δflv1A* and the *Δflv3A* mutant showed a drastic reduction in *hoxH* transcript abundance relative to WT (Paper I; Fig. S7 b). This could mean, that Hox has a negligible contribution to H_2 production in the *Δflv3A* mutant. In line with this, He et al. (2025) found, that long-term H_2 photoproduction in the Δ*flv3A* mutant is strongly dependent on nitrogenase activity and independent of Hox hydrogenase.

Under LC conditions, only the *Δflv3A* mutant showed a significant decrease in nitrogenase activity in relation to the WT (Paper I; Fig. 6 a). This reduction was accompanied by lower nitrogenase content, as indicated by decreased amount of NifH protein (Paper I; Fig. 6 c), despite unchanged *nifH* transcript amount. In contrast, the *Δflv1A*/*Δflv3A* double mutant exhibited significantly higher *nifH* transcript levels (Paper I, Fig. 6 b). This aligns with low nitrogenase activity found previously in Δ*hupL* mutants which still had significantly increased rates of H_2 production (Happe et al., 2000; Leino et al., 2014).
Thus, increased levels of nitrogenase or increased nitrogenase activity were likely not responsible for increased H_2 production in the *Δflv3A* mutant and thus perhaps also not in the *Δflv1A*/*Δflv3A* double mutant (Fig. 6 a-c, S7 d).

Despite lower nitrogenase activity in Δ*flv3A*, increased transcript levels of the heterocyst specific Fed encoding gene (*fdxH*), which functions as e^- donor to

nitrogenase (Magnuson, 2019) was detected in Δ*flv3A* and Δ*flv1A*/Δ*flv*3A (Paper I, Fig. S7 c).

Interestingly, the enhanced net H_2 yield in the *Δflv3A* mutant (Paper I; Fig. 6d) is comparable to that of the *ΔhupL* mutant (Paper I, Fig. S14). Uptake of D_2 was traced in the WT, the *Δflv1A* and the *Δflv3A* mutants. The *Δflv3A* mutant showed significantly lower D_2 uptake than the other two strains (Paper I, Fig. 6 e). The mature form of the *hupL* transcript in the *Δflv1A* and the *Δflv3A* mutants as well as in the *Δflv1A/ Δflv3A* double mutant was significantly downregulated. The effect was stronger in the *Δflv3A* mutant compared to the *Δflv1A* mutant and in the *Δflv1A/ Δflv3A* double mutant compared to the single mutants (Paper I; Fig. 6 f). Moreover, HupL protein was undetectable by immunoblotting in both the Δ*flv3A* and the Δ*flv1A*/Δ*flv3A* double mutant (Paper I; Fig. 6 c). Transcriptional and translational HupL downregulation is similar to the *Anabaena* Δ*hupL* mutant (Paper I, Figs. 6 c, S7 d, S14).

Thus, increased nitrogenase mediated H_2 production in the *Δflv3A* mutant (Paper I, Fig. 6d) is probably due to impaired Hup gene expression.

4.2 Deletion of *pacR* affects photosynthesis and N metabolism

4.2.1 The PacR phenotype becomes apparent under different N sources

To characterize the Δ*pacR* mutant, we investigated growth and Chl-content as well as heterocyst formation, N-uptake and -content in different N-sources. The Δ*pacR* mutant exhibited significantly slower growth in medium containing either NO_3^- or NH_4^+ as the sole N source, reaching only around 80 or 70 %, respectively, of the CS growth measured by OD_{750} after 48 h (Paper II, Fig. 1 A).

The Chl/OD_{750} ratio was reduced by around 20 % in NO_3^- containing medium after 48 h in the Δ*pacR* mutant compared to the CS (Paper II, Fig. 1 B). While almost no heterocyst were observed in the CS after 48 h in NO_3^- containing medium, heterocyst frequency of about 7 % was found in the Δ*pacR* mutant (Paper II; Fig. 2 B, Table S1), resembling *Anabaena* WT under diazotrophic conditions (Perin et al., 2021). As this phenotype was not apparent in NH_4^+ containing medium, the mutant was further investigated during the transition from NH_4^+ to NO_3^- containing medium.

Impaired NO_3^- uptake in the Δ*pacR* mutant became evident after 48 h, with 1.5 ± 0.2 times more residual NO_3^-/OD_{750} left in the growth medium of the mutant (Paper II, Fig. 2 C). This impaired uptake was evident during a total cultivation time of 120 h (Paper II, Fig. S3). In accordance with this, the C/N ratio in the Δ*pacR* mutant after 48 h of growth in NO_3^- containing medium was increased, with around 14 %

reduction in total N content (Paper II; Fig. 2 D, Table S2), suggesting N deprivation in the mutant.

4.2.2 The Δ*pacR* mutant displays impaired PSI activity and a smaller Fed pool as well as impaired O_2 photoreduction

Next, the photosynthetic phenotype of the Δ*pacR* mutant was investigated including performance of the photosystems, redox properties and gas-exchange.

After culturing for 48 h in NO_3^- containing medium, the effective yield of PSI, Y(I), was smaller in the mutant than in the CS, while the acceptor side limitation of PSI, Y(NA), was larger (Paper II, Fig. 3 A, B). Concurrently measurements of the redox state of photosynthetic components revealed markedly reduced PSI reoxidation in the mutant. These measurements also revealed in the mutant a slight but significant decrease in the size of the pool of photo reducible Fed compared to the CS, with no observable changes in the redox kinetics of Fed (Paper II, Fig. S5).

Using MIMS, light-induced O_2 uptake, which is primarily attributed to FDPs (Ermakova et al, 2014), was measured under the same conditions as above. Upon illumination, the CS reached a maximum O_2 uptake rate of around 40 μmol mg^{-1} Chl *a* h^{-1}, with a plateau of around 23 μmol mg^{-1} Chl *a* h^{-1}. In contrast, the Δ*pacR* mutant showed a significantly lower O_2 photoreduction, with a maximum of only around 13 mg^{-1} Chl a h^{-1} and a plateau level of around 7 μmol mg^{-1} Chl *a* h^{-1}. Notably, the gross photosynthetic O_2 evolution was comparable between the CS and the Δ*pacR* mutant (Paper II, Fig. 3 C, D, Table S3). These results indicate impaired O_2 photoreduction in the Δ*pacR* mutant.

4.2.3 The Δ*pacR* mutant has a distinct metabolic profile

To understand possible metabolic triggers of heterocyst formation in the Δ*pacR* mutant after the shift from NH_4^+ to NO_3^- as the sole N source in the medium, we monitored several key metabolites of the TCA, GS/GOGAT and OAC cycles. Metabolite levels were measured directly before the shift to NO_3^- containing medium, as well as one hour and 12 h after the shift. Deviations between strains and observed standard deviations should be interpreted in the context of potential metabolite turnover during sample harvesting – albeit this effect was likely minimized by rapid harvesting inside the growth chamber followed by immediate freezing in liquid N_2.

Differences in metabolite levels became more apparent with longer exposure to NO_3^-, with metabolite levels generally decreasing in the mutant in relation to the CS, with the exception of Ala, which increased significantly in the mutant after 12 h. Glu

levels were consistently lower in the Δ*pacR* mutant at all timepoints (statistically significant only after the shift), with the same trend (albeit not significant) for Gln (Paper II; Fig. S6).

The levels of 2-OG, the primary signalling metabolite for heterocyst-formation (Laurent et al., 2005; J. H. Li et al., 2003; M. I. Muro-Pastor et al., 2001; C. C. Zhang et al., 2018), increased in both strains after the shift, as expected during N step down conditions (C. C. Zhang et al., 2018). However, this increase was only significant in the CS and no significant differences were found between the strains in either 2-OG levels or 2-OG/Glu ratios (Paper II, Fig. S6, S7, S8).

4.2.4 The Δ*pacR* mutant shows global deregulation of transcription

To elucidate possible mechanisms responsible for triggering the PacR deletion-mutant phenotype, a transcriptomic analysis was conducted.

RNA-seq analysis was performed directly before, and at one and 12 h after the shift from NH_4^+ to NO_3^- as the sole N source in the medium. Before the shift, 705 genes were upregulated and 774 genes downregulated, whereas 639 genes were upregulated and 707 genes downregulated one hour after the shift, and after 12 h 1344 genes were upregulated and 1034 genes downregulated in the Δ*pacR* mutant relative to the CS. Altogether, at any of the measured timepoints, up to about 38 % of the transcriptome of *Anabaena* (RefSeq: GCF_000009705.1) were found to be differentially expressed in the Δ*pacR* mutant (GEO accession number: GSE280386).

Differentially expressed genes were found in diverse categories, e.g. global transcriptional regulators, N uptake and heterocyst formation, the GS/GOGAT cycle, the OAC and cyanophycin synthesis, C_i uptake as well as the components of photosynthetic machinery (Paper II, Fig. 5). Enrichment analysis confirmed the elevation of N transporter genes one hour after the shift. After 12 h, photosynthetic antenna proteins were enriched (Paper II; Table S10). Thus, genes encoding components of N metabolism and photosynthesis were investigated in more detail. Additionally, since PacR is a known regulator of C metabolism (Picossi et al. 2015), genes of this category were also analysed. In the following, differential expression of genes is categorized as either slight (log_2FC = 1–2), intermediate (log_2FC = 2–4) or high (log_2FC >4).

Transcriptional regulators. As expected from previous reports (Picossi et al., 2015) *pacR* transcription levels in the CS remained independent of the N source (Paper II, Tables S4-6). Strikingly, *ntcA* transcript levels were slightly, but significantly upregulated at t=12 h in the Δ*pacR* mutant (Paper II, Table S 6). Transcripts of *furA* were slightly higher than in the CS in the mutant one hour after the shift, likely due to the absence of a transient downregulation observed in the CS

(Paper II, Table S 5). Transcripts of *cmpR* however, were not differentially regulated between the CS and the Δ*pacR* mutant (Paper II, Tables S4-6).

Nitrogen metabolism. The *nirA* operon (*nirA-nrtABCD-narB*), which codes for NO_3^- uptake machinery components (Herrero et al., 2001; B. Li et al., 2024; Seth et al., 2022), was found to be highly upregulated in the CS at one hour following the shift to NO_3^- (Paper II, Table S7). Strikingly, there was a delay in this upregulation in the Δ*pacR* mutant, where slightly, but significantly lower transcript levels were found at the same timepoint in relation to the CS (Paper II, Tables S5, 7, 8). A notable gene found to be constitutively upregulated in the Δ*pacR* mutant and involved in N metabolism was *mobA* (Paper II; Tables S4-6), who is a known direct target of PacR (Picossi et al., 2015) and whoes gene product is involved in molybdenum cofactor biosynthesis (Puerta-Fernández & Vioque, 2011). Moreover, genes associated with the GS/GOGAT cycle were also found to be deregulated in the mutant. The Glutaminase 1 encoding gene (*glsA1*) (Zhou et al., 2008) was slightly and constitutively upregulated in the Δ*pacR* mutant (Paper II, Tables S4-6). Similarly, *glnA* (the glutamine synthetase encoding gene) (Herrero & Flores, 2019) was slightly upregulated in the Δ*pacR* mutant at t=1 h compared to t= 0 h, with both strains exhibiting upregulation at 12 h (Paper II; Tables S7, 8). The gene for diaminobutyrate-pyruvate transaminase (*dat, all0396*) also possesses a PacR-regulated promoter (Picossi et al., 2015), and this gene was indeed found to be constitutively downregulated in the Δ*pacR* mutant (Paper II; Tables S4-6). The transcription of the gene encoding leucine dehydrogenase *(ldh*) was downregulated in the CS after the shift, but this did not take place in the mutant (Paper II; Tables S7, 8). Moreover, alanine dehydrogenase (ADH) gene (*ald*) transcript levels were slightly higher in Δ*pacR* than in the CS at t=12 h (Paper II, Table S6). Urease accessory protein encoding gene (*ureG*) transcription was constitutively upregulated at an intermediate level in the Δ*pacR* mutant (Paper II, Tables S4-6). Moreover, the cyanophycinase encoding gene *cphB1* was found to be slightly downregulated in the mutant before the shift (Paper II, Table S4).

Heterocyst formation. 12 h after N stepdown, a large number of heterocyst formation genes were upregulated in the Δ*pacR* mutant compared to both the CS and the pre-shift condition. For example, the expression of genes related to the formation of the heterocyst envelope Hep and Hgl layers, nitrogenase, the heterocyst-specific Fed (*fdxB*) (Kourpa et al., 2019), Hup, as well as the heterocyst-specific FDPs (*flv1B* and *flv3B*), were upregulated (Paper II, Tables S6, 8).

Carbon metabolism. Strikingly, two C_i transporters were downregulated in the Δ*pacR* mutant. Firstly, *sbtA*, encoding the putative SbtA C_i transporter orthologue, is

constitutively downregulated in the mutant and did not exhibit the transient upregulation one hour after the shift as found in the CS (Paper II, Tables S4-8). The HCO_3^- transporter encoding gene, *cmpB*, also lacked the induction seen after one hour in the CS (Paper II, Tables S5, 7, 8). Also, the transcription of the sucrose synthase encoding gene (*susB*) was only intermediately downregulated in the mutant after the shift, whereas it was highly downregulated in the CS (Paper II, Tables S7, 8).

Photosynthesis and respiration. Genes related to photosynthesis and respiration were frequently differentially expressed in the Δ*pacR* mutant over the course of the experiment. The PSII D1 protein coding gene (*psbA1*) was slightly upregulated in the mutant compared to the CS at t= 1 h (Paper II, Table S5). In contrast, *psbA3*, which codes for the high light inducible form of D1 and increases D1 availability (Sander et al., 2010; Summerfield et al., 2008), was less upregulated in the mutant than in the CS at t= 1 h (Paper II; Table S5). Intriguingly, the promoter of *psbA3* is directly bound by PacR as demonstrated by Picossi et al., 2015. Additional genes coding for the CP43 homologues IsiA2 and IsiA3, which are antennae complexes associating with PSI under Fe-deficiency and HL conditions (Havaux et al., 2005; Nagao et al., 2021), were only upregulated in the mutant after 12 h (Paper II, Fig. S6, 8).

The *pec* operon of *Anabaena* consists of five genes (*pecA*, *pecB*, *pecC*, *pecE*, *pecF*). Before the shift, *pecE* and *pecF* were expressed at slightly lower levels in the Δ*pacR* mutant compared to the CS (Paper II, Tables S4). One hour after the shift all genes of the pec operon displayed equally reduced expression levels in both strains (Paper II, Tables S7, 8). After 12 h, a slightly to intermediately lower expression of the entire *pec* operon in the mutant compared to the CS became apparent (probably due to a missing upregulation as can be deducted from the transcripts per kilobase million (TPM)-values) (Paper II, Tables S6-8, Appendix S4).

The genes *all4940* and *alr4783*, which are associated with the OCP, were transcribed at slightly lower levels in the Δ*pacR* mutant compared to the CS at t = 0 h (Paper II, Tables S4). In NO_3^- containing medium, both of these genes were significantly downregulated irrespective of the genotype in relation to before the shift (except for *all4940* 12 h after the shift in the mutant) (Paper II; Tables S7, 8). Respiratory genes *coxA2* and *coxC2* as well as *coxA3* (coding for the ARTOs Cox2 and Cox3 (Stebegg R, 2011)) were intermediately to highly upregulated in the Δ*pacR* mutant compared to the CS at t = 12 h (Paper II; Table S6). Moreover, *petF,* encoding vegetative cell-specific Fed-1, was constitutively downregulated in the Δ*pacR* mutant (Paper II; Tables S4-6). This may be explained by the fact that the promoter of *petF* is directly bound by PacR (Picossi et al., 2015). One hour after the shift, *flv2* as well as *flv4* transcripts were downregulated in the mutant relative to the CS (Paper II, Table S5), whereas transcripts of *flv1A* and *flv3A* were not differentially expressed between studied strains.

5 Discussion

The crosstalk and regulatory networks between vegetative cells and heterocysts are not well elucidated in *Anabaena.* In this work, I investigate the role of FDPs in *Anabaena*, as photoprotective e^- sinks and elements of the crosstalk between vegetative cells and heterocysts. On a more global scale, I also investigated the role of the TF PacR, which has been previously shown to regulate C metabolism, photosynthesis and FDPs directly (Picossi et al., 2015).

5.1 Flavodiiron proteins have distinct roles in *Anabaena* and are part of the vegetative cell-heterocyst crosstalk

5.1.1 Deletion of *flv1A* and *flv3A* causes overreduction of the PETC and reduced photosynthetic efficiency with possible implications for C_i fixation

Both Flv1A as well as Flv3A were found to be indispensable for survival under severe fluctuating light, under different N and C_i conditions in *Anabaena* (Paper I, Fig. S4), which is in line with previous results in *Anabaena* and *Synechocystis* sp. PCC 6803 (Allahverdiyeva et al., 2013).

The functional redundancy and coordination between Flv1/3 and NDH-1 has been suggested to ensure efficient oxidation of PSI in *Synechocystis* sp. PCC 6803 during changes in light or C_i availability (Nikkanen et al., 2020) and in the moss *Physcomitrella patens* (Storti, Puggioni, et al., 2020). Cooperation of FDPs and NDH-1 protects the PETC especially during shifts to LC/HL, contributing to PSI oxidation, *pmf* generation via the PETC mediated H^+ pumping, and expression of low C_i inducible CCM genes (Nikkanen et al., 2020). A similar situation is implied in *Anabaena* Δ*flv1A* and Δ*flv3A* mutants. Here, enhanced NDH-1 activity in the dark (Paper I, Fig. S6 a, b) may be a consequence of FDP gene deletion, leading to a stronger reduction of the PQ pool in the dark (Paper I, Fig. 1 a, Table 1, Fig. S6 d). Also, after illumination, the PETC is over-reduced due to impaired Fed reoxidation, most likely caused by the deletion of FDPs, which are direct recipients of e^- from

Fed (Nikkanen et al., 2020, 2025; Sétif et al., 2020). Interestingly, both in *Anabaena* (Paper I, Fig. 2 a-d) as well as *Synechocystis* sp. PCC 6803 (Nikkanen et al., 2020), it is the deletion of the Flv3(A) coding gene, which has the most marked impact on Fed reoxidation.

Delay in P700 reoxidation upon illumination is a typical phenotype in FDP deletion mutants (Ilik et al. 2017, Elanskaya et al., 2021) and was also found in this work (Paper I, Fig. 2 a-c). Additionally, impairment of *pmf* generation was found in the mutants (Paper I, Fig. 5) which is also similar to the phenotype found in *Synechocystis* sp. PCC 6803 (Nikkanen et al., 2020), *P. patens* (Gerotto et al., 2016) and *C. reinhardtii* (Chaux et al., 2017). As determined by Nikkanen et al., 2020, NDH-1 activity, which facilitates CET, has only a minor effect on P700 redox kinetics and *pmf* generation. Instead, both are significantly affected by FDPs. Impairment of *pmf* is probably mostly an indirect consequence of FDP deletion via the diminished PSII yield (Paper I, Fig. 1 a, b) and thus diminished charge separation and H^+ translocation via H_2O oxidation at PSII and a less active Q cycle. Therefore, possibly also in *Anabaena*, P700 reduction and *pmf* generation are mainly dependent on a strong downstream e^- sink, the FDPs with only minor contribution from NDH-1. Interestingly, the Δ*flv1A* and Δ*flv3A* single and the Δ*flv1A*/Δ*flv3A* double mutants have a diminished CO_2 uptake capacity (Paper I, Fig. 4a, b, S13b, c).

In algae, CCM induction is dependent on *pmf* generation by FDPs and the CET (Burlacot et al., 2022). In *Synechocystis*, the expression of CCM protein coding genes show, to some extent, coregulation with the expression of FDP coding genes (Burnap et al., 2015; Mustila et al., 2016; Nikkanen et al., 2020), possible due to the FDPs (and NDH-$1_{1,2}$) functioning as a safety valve in case the CBB doesn't consume enough reductants, e.g. under LC (Nikkanen et al., 2020). Thus, it could also be speculated, that in this work FDP deletion leads to CCM gene downregulation accounting for CCM impairment (Paper I, Fig. 4) and that also in cyanobacteria, CCM induction is dependent on FDP activity.

As discussed below (see chapter 5.2.3.), the global transcription factor PacR may be involved in coordinating e^--sink capacity provided by FDPs and the CBB cycle operating downstream of PSI. Thus, PacR could be implicated in the CCM downregulation observed in the FDP deletion mutants.

5.1.2 Flv3A has a special role in *Anabaena* and may be engaged in a crosstalk with Flv2 and Flv4

Anabaena Δ*flv1A* and Δ*flv3A* mutants exhibited impairment of O_2 photoreduction, with the Δ*flv3A* mutant having a more pronounced phenotype compared to the Δ*flv1A* mutant (Paper I, Fig. 3 a). This implies that in *Anabaena* Flv3A is able to maintain O_2 photoreduction without Flv1A. Moreover, since steady-state O_2

photoreduction was nearly eliminated in the Δ*flv1A/*Δ*flv3A* double mutant in LC (Paper I, Fig. 3 a) and in the Δ*flv1A* mutant only under HC conditions, when *flv2* and *flv4* were not expressed (Paper I, Fig. 1 c, 3 b), this may suggest functional Flv3A/Flv2-4 oligomerization, and/or Flv3A/Flv3A homo-oligomer and Flv2/Flv4 homo- or hetero-oligomers cooperating in order to perform the Mehler-like reaction. Moreover, it may indicate Flv1A being less efficient or unable to operate as a homo-oligomer and/or cooperate with Flv2 and/or Flv4. Potential cooperation or redundancy of the FDPs is also indicated by the fact that the deletion of *flv1A* or *flv3A* and particularly concomitant deletion of *flv1A* and *flv3A* in the double-mutant, caused higher expression of *flv2* and *flv4* in LC (Paper I; Fig. 1 c). The situation in *Anabaena* differs from *Synechocystis*, where only the Flv1/Flv3 homo-oligomer can perform the Mehler-like reaction (Paper I; Fig. S10) (Mustila 2016).

Previously, Flv3 has been found to be more abundant that Flv1 on both transcript and protein levels in *Synechocystis* sp. PCC 6803 (Jackson et al., 2023; P. Zhang et al., 2009) and the same can be speculated for *Anabaena* (Ermakova et al., 2013). Flv3 homo-oligomers occur in *Synechocystis* sp. PCC 6803, but they are not involved in the Mehler-like reaction (Mustila et al., 2016). It has previously been speculated that the C-terminal domain of FDPs may be involved in unknown physiological functions of FDP homo-oligomers (Nikkanen et al., 2025).

Nikkanen et al., 2025, observed an interaction of Flv3 in *Synechocystis* sp. PCC 6803 with FNR, which was localized at the thylakoid membrane. However, FNR was not found to be an e^- donor for the Flv1/3 Mehler-like reaction and FNR may thus interact with Flv3 homo-oligomers to perform an unknown function possibly related to thylakoids or the phycobilisomes (which bind FNR) (Liu et al., 2019).

Moreover, in *Synechocytsis*, Flv3 also appears to play a more important role in stress acclimation (Mustila et al., 2016). A possible photoprotective role of the Flv3 homo-oligomers has been suggested (Mustila et al., 2016). It is possible that Flv3A of *Anabaena* has similar additional functions as speculated in *Synechocystis*. Moreover, a role of Flv3A homo-oligomers in reducing NO may be proposed, e.g. similar to FDPs of *C. reinhardtii* (Burlacot et al., 2020). This may serve photoprotective (Solymosi et al., 2022) or regulatory functions (Astier et al., 2021; N. Gupta et al., 2025).

5.1.3 *HupL* is downregulated in the *flv3A* deletion mutant causing increased H_2 production

The Δ*flv3A* mutant and the Δ*flv1A*/Δ*flv3A* double mutant demonstrated increased nitrogenase-mediated H_2 production (Paper I; Fig. 3 a, Fig. 6 d, S7 a) due to significant downregulation of *hupL* transcription and translation (Paper I, Fig. 6 c, f). Since Hup oxidizes H_2, this downregulation hindered H_2 recycling (Paper I; Fig.

6 e) (Tamagnini et al., 2007), resulting in the release of H_2 in the Δ*flv3A* mutant (Paper I, Fig. 6 d), similar to the Δ*hupL* mutant (Paper I, Fig. S 14). This is confirmed by previous results, which indicate that the most effective way to enhance H_2 photoproduction in various *Anabaena* sp. strains is inactivation of Hup on a genetic level (M. He et al., 2025).

A possible explanation for *hupL* downregulation in the Δ*flv3A* mutant is, that both the *flv3A* and heterocyst specific *hupL* genes have FurA binding sites (González et al., 2014). Deletion of a competing binding site may alter the expression pattern mediated by FurA, thereby also interfering with the regulatory network that coordinates the distribution of Fe between photoprotection and the N_2 and H_2 metabolism. Importantly, this proposed mechanism is speculative, as direct evidence for changes in iron homeostasis or FurA activity is currently lacking.

An alternative explanation may be that the deletion of the e^- sink Flv3A is compensated for by decreasing e^- recycling activity from Hup, using H_2 as an alternative e^- sink for the entire filament. A re-direction of excess electrons to H_2 may also explain increased transcript levels corresponding to the heterocyst specific Fed, which functions as e^- donor to nitrogenase (Magnuson, 2019) in Δ*flv3A* and Δ*flv1A*/Δ*flv*3A (Paper I, Fig. S7 c).

5.2 The C metabolism and photosynthetic regulator PacR also plays a significant role in regulating N metabolism

Heterocyst differentiation in the Δ*pacR* mutant resembles *Anabaena* WT under diazotrophic conditions (Kumar et al., 2010), when the primary N source was changed from NH_4^+ to NO_3^- under 1 % CO_2 (Paper II, Fig. 2 A, B). This phenotype is closely parallel to that reported in a recent study by G. M. Lin et al., 2025, for an independent *Anabaena* Δ*pacR* mutant under similar conditions. Since heterocyst deregulation occurred only after the shift from NH_4^+ to NO_3^- (Paper II, Table S1) and the upregulation of heterocyst differentiation genes occurred in an expected timeframe for heterocyst formation being triggered due to the shift (Paper II, Fig. 5, Suppl. Tables S4-S8) (Flores, Picossi, et al., 2019), it can be concluded, that deletion of the PacR encoding gene did not directly trigger heterocyst formation. This could have been argued to be the case e.g. due to the possible deregulation of the direct targets of PacR, *patS,* and *hetN* (G. M. Lin et al., 2025; Picossi et al., 2015) which are likely repressed by PacR when NO_3^- is available (G. M. Lin et al., 2025). Moreover, it has previously been found that deletion of *patS*, an inhibitor of heterocyst formation, leads to heterocyst formation despite the presence of NO_3^- (Yoon & Golden, 1998, 2001), making a possible upregulation of *patS* due to PacR deletion even less likely the cause of the heterocyst deregulation phenotype.

Moreover, despite rising 2-OG levels being considered the main trigger for heterocyst formation in *Anabaena* (Laurent et al., 2005; J. H. Li et al., 2003), such a rise was not observed in this study (Paper II, Fig. S6 C, S7). Similarly, no changes were observed in the ratio of 2-OG to Glu (Paper II, Fig. S8), despite a typically inverse correlation between 2-OG and free Glu (Perin et al., 2021). However, we can not exclude the possibility of increased 2-OG levels in the mutant, as single-time-point-sampling may fail to capture a transient rise. Nevertheless, as the most prominent triggers for heterocyst formation were not detected in the mutant, we focused on possible secondary effects after the shift to another N source, which is likely to perturb the C/N balance (C. C. Zhang et al., 2018). Indeed, the C/N ratio was significantly increased in the Δ*pacR* mutant 48 h after the shift (Paper II, Fig. 2 D), indicating internal N shortage. A previous study has shown that *Anabaena* becomes prone to heterocyst differentiation in NO_3^- containing medium when CO_2 levels rise, since this depresses both NO_3^- uptake rate and NO_3^- reduction enzyme activity. The CCM may compete with NO_3^- assimilation for energy and electrons and the CCM appears to be favoured (Kang et al., 2005), making NO_3^- only a weak inhibitor of heterocyst differentiation in contrast to NH_4^+ (J. H. Li et al., 2003). This may lead to a high intracellular C/N ratio and relative N limitation thus triggering heterocyst formation. However, a high CO_2 level did not suffice to trigger heterocyst differentiation in the CS strain (Paper II, Fig. 2 A, B). In contrast, in the Δ*pacR* mutant, this shift to conditions that are more prone to lead to intracellular N limitation was clearly sufficient to trigger heterocyst differentiation.

5.2.1 Deregulation of central N assimilation pathways in the Δ*pacR* mutant

Prolonged impairment of NO_3^- uptake appeared to be a central factor in the internal N shortage of the Δ*pacR* mutant (Paper II, Fig. S3) and may be partially explained by delayed upregulation of the *nir* operon (Paper II, Fig. 5, Suppl. Tables 4-8). G. M. Lin et al., 2025, also observed impairment of NO_3^- uptake in the Δ*pacR* mutant after the shift from NH_4^+ to NO_3^- as the N source. Despite the concurrent upregulation of two positive regulators, *ntcA* and *ntcB*, they reported decreased expression of the *nir* operon. They were able to confirm direct binding of PacR to the promoters of both *nirA* and *ntcB* as well as *ntcA*. Thus, PacR may maintain NO_3^- homeostasis by directly activating *nir* expression and at the same time inhibiting expression of *nir* activating genes, *ntcA* and *ntcB* (G. M. Lin et al., 2025). This strongly suggests that decreased NO_3^- uptake described in Paper II was indeed due to deletion of the PacR encoding gene. Thus, PacR appears to directly regulate NO_3^- import, possibly coordinating the expression of the *nir* operon with changing levels

of external NO_3^-. Several studies have indeed concluded that their observation of heterocyst formation in NO_3^- containing medium was due to impaired NO_3^- uptake (Frias et al., 2000; Frías et al., 2003; Puerta-Fernández & Vioque, 2011; Y. Zhang et al., 2007).

In addition to impaired NO_3^- uptake, availability of N to the central metabolism was further reduced by depletion of the GS/GOGAT cycle in the Δ*pacR* mutant. After the shift to NO_3^-, a large decrease in Gln levels was observed only in the Δ*pacR* mutant (Paper II, Figs. 4, S6, S7), which is typical for *Anabaena* WT after a shift to diazotrophic conditions (Perin et al., 2021). A possible cause may be the constitutive upregulation of *glsA1* in the Δ*pacR* mutant (Paper II, Fig. 5, Suppl. Tables 4-6). GlsA1 is mainly responsible for Gln deamination, forming Glu and NH_4^+, and *glsA1* is normally transiently downregulated under N limiting conditions (Zhou et al., 2008). Elevated GlsA1 activity may interfere with the activity of GS, which is a key regulator enzyme of the GS/GOGAT cycle (see chapter 1.5.2.). The *glnA* gene is typically expressed at higher levels under diazotrophic conditions via NtcA mediated regulation (Flores, Picossi, et al., 2019; Frías et al., 1994; Tumer et al., 1983; Wei et al., 1994). Notably, inhibition of GS with the specific inhibitor MSX has been shown to counteract the suppressive effects of N on N-fixation and heterocyst formation in *Anabaena* sp. (A. K. Mishra, 2003; Ramos et al., 1985; Stewart & Rowell, 1975). Thus, the assimilation of NH_4^+ via GS appears to be a requirement for N control to take effect (Flores & Herrero, 1994; A. K. Mishra, 2003). This is supported by GS impaired *Anabaena variabilis* strains, which also show impaired N control (Kerby et al., 1986; Spiller et al., 1986). Thus, GS mediated N control may be perturbed in the Δ*pacR* mutant. The upregulation of *glnA* in the Δ*pacR* mutant one hour after the shift (Paper II, Fig. 5, Suppl. Tables 7, 8), may thus serve as an adaptive mechanism presumably to increase GS abundance and counteract the putative leakage of NH_4^+ out of the GOGAT cycle and restore N control. However, it should be noted, that GS activity is also regulated post-translationally, e.g. via the IF7A (see chapter 1.5.2.) which was not differentially expressed in the Δ*pacR* mutant compared to the CS (Paper II, Appx. S1).

The observed impairment of NO_3^- uptake and reduced GS/GOGAT activity in the ΔpacR mutant may also be linked to the general reduction in photosynthetic efficiency. This impairment is directly connected to deletion of the PacR encoding gene. Strikingly, PacR directly regulates flavodiiron proteins, which are essential for photoprotection under fluctuating light and were found to be downregulated and less active also in this work. Moreover, the photoprotective gene *psbA3* (Sander et al., 2010; Summerfield et al., 2008) was downregulated in the mutant and its promotor is directly bound by PacR (Paper II, Fig. 3 A, B, 5, Tables S5, S8, S7) (Picossi et al., 2015). Moreover, *petF*, encoding the vegetative cell specific Fed-1 (Alam et al., 1986; Pernil & Schleiff, 2019) was constitutively downregulated in the mutant

(Paper II, Fig. 5, Suppl. Tables 4-6), probably reflecting the direct transcriptional control of PacR over *petF* (Picossi et al., 2015). Correspondingly, the size of the photoreducible Fed pool was slightly, but statistically significantly, decreased in the Δ*pacR* mutant (Paper II, Figs. S5 A, B), which suggests impaired e^- flux from photosynthesis to N fixation. Since both NR and NiR use PSI-reduced Fed-1 as an e^- donor (See chapter 1.4.2.) decrease in both photosynthetic efficiency and Fed-1 levels are expected to impact NO_3^- uptake and reduction.

The observed impairment of GS/GOGAT activity may also be due to the shortage of photosynthetic reduced Fed, as it is the only e^- donor of GOGAT in *Anabaena* (See chapter 1.4.3.). Since Gln is a central precursor for protein synthesis, including the phyobilisome, the GS/GOGAT cycle impairment may be connected to the observed defects in both growth (Paper II, Fig. 1 A) and photosynthetic performance (Paper II, Fig. 3 A, B), creating a negative feedback loop between N metabolism and photosynthesis.

5.2.2 A network of global TFs regulates C and N metabolism and photosynthesis

In *Anabaena*, PacR, NtcA and FurA all play a significant role in coordinating C/N balance, regulating heterocyst formation and modulating photosynthesis, and their regulons exhibit a significant overlap (González et al., 2013; Guío et al., 2020, 2025; Picossi et al., 2015). Possibly this is including the regulation of vegetative cell-specific flavodiiron proteins by FurA (Flv3A) (González et al., 2014) as well as by PacR (Flv1A, Flv2 and Flv4) (Paper II, Fig. 5) (Picossi et al., 2015), with targets indicated in brackets.

Importantly, PacR may directly inhibit *ntcA* expression (G. M. Lin et al., 2025). G. M. Lin et al., 2025, further found, that PacR and NtcA coregulate the expression of the *nir* operon and absence of PacR leads to a clear delay in NO_3^- uptake. Thus, our results, as discussed above, are in line with G. M. Lin et al., 2025, and it may also be concluded, that PacR and NtcA together adapt the cellular metabolism to nutrient availability and the cells metabolic status.

Misregulation of *furA* in the Δ*pacR* mutant (Paper II, Fig. 5, Suppl. Table 5) may also impact flavodiiron protein regulation and be related to heterocyst formation, which requires temporary upregulation of *furA* at the beginning of the differentiation process (González et al., 2013, 2014; Guío et al., 2020). However, due to the central role of FurA (González et al., 2014), broader consequences are possible: In *Anabaena*, FurA is the master sensor and regulator of Fe and redox metabolism as well as stress (González et al., 2012, 2014) and may connect Fe homeostasis and heterocyst differentiation by modulating NtcA activity (Guío et al., 2020). Furthermore, in *Anabaena*, NtcA can regulate *furA* as well as other Fe acquisition

related genes (López-Gomollón et al., 2007; Picossi et al., 2014). Also taking into account that promoters often contain bindings sites for multiple TFs, the absence of PacR may alter the activity of NtcA and FurA as well as the crosstalk between Fe and N metabolism mediated by them.

Furthermore, both NtcA and FurA interact with 2-OG (Flores, Picossi, et al., 2019; Guío et al., 2020). However, the type of the RbcR effector molecule in unicellular cyanobacteria remains unknown (Kurkela & Tyystjärvi, 2024), and to my best knowledge no effector molecule has been identified for PacR in *Anabaena*. Still, PacR is an LTTR TFs, which in general can function as sensors for metabolic states as they can alter gene expression by binding small effector molecules (Bolay et al., 2022; Maddocks & Oyston, 2008). In LTTRs, the DNA-binding domain is connected to a sensor domain which binds these effector molecules. This alters gene expression patterns according to the metabolic state (Maddocks & Oyston, 2008; Schell, 1993). Thus, since PacR clearly acts in concert with NtcA and FurA, it is possible that PacR is also a 2-OG sensor (Illustrated in Fig. 6).

The *dat* gene, whose expression is regulated by Fe availability (Stevanovic et al., 2012), and also directly regulated by PacR (Picossi et al., 2015) was indeed found to be constitutively downregulated in the Δ*pacR* mutant (Paper II, Fig 5, Suppl. Tables 4-6). The *dat* gene product, diaminobutyrate-transaminase, may influence N flux between 2-OG and Glu, thus potentially influencing the GS/GOGAT cycle as well as connecting the GS/GOGAT cycle with the OAC, as one of the intermediates of the reaction, L-aspartate-4-semialdehyde, is connected to Asp metabolism (Mantas et al., 2021; L. Su et al., 2024). Moreover, the *ldh* gene exhibited constitutively low expression in the Δ*pacR* mutant, while it was highly expressed in the CS before the N stepdown and downregulated thereafter (Paper II, Fig. 5, Suppl. Tables. 4-8). It could be speculated, that regulation of transaminases by PacR could help cells to buffer short term fluctuations in N availability, preventing premature induction of heterocyst formation in response to only short-term fluctuations in N availability.

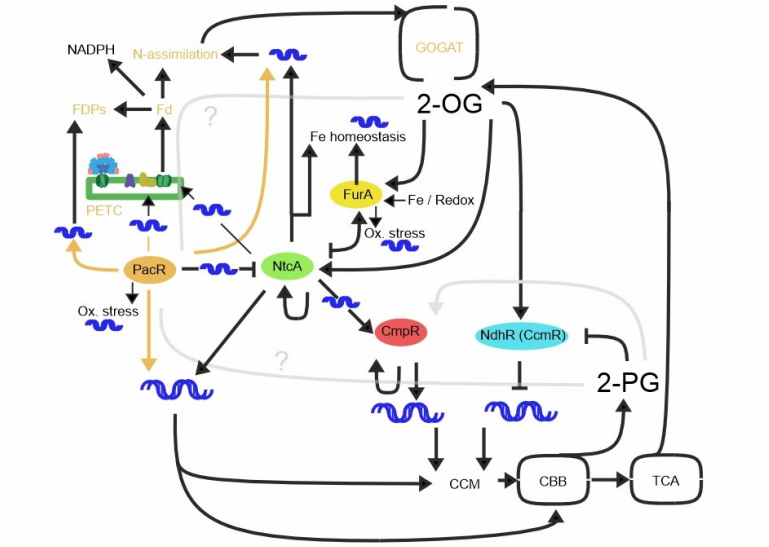

Figure 6. Signal transducing network of the C/N balance in *Anabaena*. The C/N balance is regulated by a number of global transcription factors, which also adapt the cellular metabolism to any shifts in this balance. NtcA is one of the most important translational regulators of N metabolism, including heterocyst formation related genes. Moreover, it regulates C metabolism, photosynthesis and Fe acquisition related genes (Picossi et al., 2014). NtcA is positively autoregulated (J. H. Li et al., 2003) and binds 2-OG directly (Flores, Picossi, et al., 2019). PacR is a global TF, which balances C metabolism and photosynthesis (including FDPs) (Picossi et al., 2015). PacR may also directly inhibit *ntcA* expression (G. M. Lin et al., 2025) and some N metabolism related genes (Paper II, Fig. 5). Under N limitation, the NtcA/2-OG complex activates transcription of genes involved in the uptake and assimilation of N, while the NdhR/2-OG complex represses CCM related genes. Under C_i limitation the apo form of NtcA has a low DNA-binding affinity, leading to a decrease in N uptake and assimilation, while NdhR/2-PG complex can't act as a repressor, so that CCM genes are expressed (C. C. Zhang et al., 2018). FurA senses Fe availability and the redox state of the cell and *furA* is upregulated by NtcA upon N deprivation ilistn *Anabaena* (Guío et al., 2020). In turn, FurA negatively regulates *ntcA* depending on 2-OG binding, co-regulating heterocyst differentiation (Guío et al., 2020). FurA also regulates *flv3A* and *hupL* (González et al., 2014). CmpR may have 2-PG as a positive effector (C. C. Zhang et al., 2018) and activates the *cmp* operon and positively auto-regulates its own gene expression in response to C_i limitation (López-Igual et al., 2012; C. C. Zhang et al., 2018). Expression of *cmpR* under low C_i is boosted when N is absent via co-regulation of its expression by NtcA (López-Igual et al., 2012). Marked in orange are all processes for which a significant effect of PacR deletion was shown in this work.

5.2.3 FDPs and PacR influence C/N balancing and heterocyst metabolism

Having established PacR as a central TF in C and N metabolism as well as photosynthesis, it is intriguing to investigate the connection between PacRs and FDPs, which are not only central to photosynthetic performance, especially under fluctuating light, but may also influence C/N metabolism.

So far, PacR-mediated regulation has only been demonstrated for flv1A (Picossi et al., 2015), *flv2* (Paper II, Fig. 5) and *flv4* (Paper II, Fig. 5) (Picossi et al., 2015). Since *flv3A* and *flv1A* are not organized in an operon in *Anabaena* and transcribed independently (Ermakova et al., 2013), it is not clear if PacR also regulates *flv3A* transcription. However, FurA may regulate *flv3A* (González et al., 2014) and since *furA* is also being differentially expressed in the mutant, FDP expression could also be indirectly affected though FurA in the PacR deletion mutant.

Notably, one hour after the shift to NO_3^- containing medium, lower expression levels of *flv2* and *flv4* became evident in the mutant (Paper II, Fig. 5, Suppl. Tables 4, 5, 7). This may reflect the initiation of heterocyst differentiation, as under diazotrophic conditions expression of *flv1A* and *flv3A* is typically downregulated by approximately 50 %, with *flv2* and *flv4* following a similar trend (Ermakova et al., 2013). However, in the Δ*pacR* mutant, *flv1A* and *flv3A* downregulation was not observed (Paper II, Appendix 1), indicating that instead, FDP upregulation could also play a role in triggering heterocyst formation. PacR may normally induce FDP gene expression in response to shifting e^- sink demand, such as after N stepdown, to prevent overreduction of the PETC. This resembles FDP responses to fluctuating light (Paper II) or C_i deprivation (Ermakova et al., 2013), where they help alleviate excess excitation pressure. As discussed above, CCM induction was speculated to dependent on FDP activity (see chapter 5.1.1.). Since both processes are deregulated in the PacR mutant, it is conceivable that PacR may also play a role in balancing the e^- sinks provided by FDPs and the CBB cycle.

If deletion of *pacR* causes *flv* downregulation, this could lead to the 2-PG pathway compensating as an e^- sink, which may lead to higher 2-OG levels in relation to 2-PG, possibly triggering heterocyst formation as illustrated in the following: In cyanobacteria, there is evidence for cooperative interaction between FDP-mediated O_2 photoreduction and the photorespiratory 2-PG pathway (Allahverdiyeva et al., 2011; Hackenberg et al., 2009; Mustila et al., 2016). The 2-PG pathway generates CO_2 and NH_3 as byproducts, and their reassimilation requires substantial amounts of NADPH (and thus Redox-equivalents) and ATP. Moreover, this pathway transforms Glu into 2-OG (Bauwe et al., 2010). In *Synechocystis* sp. PCC 6803, photorespiration has been shown to serve as an auxiliary sink for excess reductants, functioning alongside FDPs (Allahverdiyeva et al., 2011; Hackenberg et al., 2009). Next to *flv* genes, PacR may regulate 2-PG pathway genes (such as *alr1004* and *alr2873*) (Picossi et al., 2015), which are possibly linked to photorespiration (Eisenhut et al., 2008). It is thus conceivable, that PacR coordinates both these pathways to maintain redox homeostasis and control intracellular NH_4^+ levels as well as the 2-OG/2-PG ratio. PacR deletion and the subsequent downregulation of *flv* genes may increase activity of the 2-PG pathway to compensate lost e^- sink capacity. Increased photorespiration may lead to further

depletion of the GOGAT-cycle and loss of NH_4^+ from the central metabolism. Moreover, depletion of 2-PG could take place, which would suppress the CCM. Indeed, transient downregulation of *sbtA* in the Δ*pacR* mutant (Paper II, Fig. 5; Suppl. Tables 4–7) may reflect such a metabolic shift. Since 2-OG (the N starvation signal) and 2-PG (the C starvation signal) levels are inversely correlated (C. C. Zhang et al., 2018), a possible decrease in 2-PG levels in relation to 2-OG levels in the Δ*pacR* mutant may thus be the signal triggering heterocyst formation.

6 Outlook

In the last decade, interest in the use of heterocystous cyanobacteria for biotechnological applications has increased (Allahverdiyeva et al., 2021; Deora et al., 2025; M. He et al., 2025; Magnuson, 2019; Wegelius et al., 2018). They provide the possibility of combining photosynthetic with anaerobic metabolism in one production platform. Important factors that need to be considered are the C source, which needs to be imported from vegetative cells, and how ATP and reductant usage can be optimized in heterocysts (Magnuson, 2019).

Two main resources provided by the heterocyst are fixed N_2 and H_2. N_2 fixation via heterocystous bacteria may provide a sustainable alterative to industrial production of NH_3 via the Haber-Bosch process, which is energy and resource intensive (Volgusheva et al., 2019). Considering that H_2 gas is an important alternative energy carrier, research into photosynthetic H_2 production has increased rapidly this century. Most hydrogenases are sensitive to O_2, therefore H_2 production in unicellular cyanobacteria can be achieved in the dark or by strict control of photosynthesis. Heterocystous cyanobacteria, however, can produce H_2 under normal growth conditions. Therefore, several attempts have been made to increase nitrogenase-based H_2 production, despite the inherently poor energy efficiency of nitrogenase (Magnuson, 2019; Roumezi et al., 2020). One possible alternative is the deletion of *hupL*, which encodes the uptake hydrogenase large subunit in heterocysts, which has been attempted before in *Anabaena* sp. (M. He et al., 2025; Kosourov et al., 2014; Lindberg et al., 2002; Masukawa et al., 2002). A major limitation when using heterocysts as cell factories is the limited availability of reductants and C sources. This may be addressed by increasing CO_2 levels, increasing the rate of CO_2 fixation via the CBB or by increasing sugar breakdown in the heterocyst. Another strategy may be to limit e^- flow to nitrogenase, which may favour other production pathways (Magnuson, 2019). It has e.g. been previously shown, that a modified uptake hydrogenase expressed in the heterocysts of *N. punctiforme* produced H_2 after a decline in nitrogenase activity (Raleiras et al., 2016). Moreover, heterologous expression of [Fe-Fe] hydrogenases from anaerobic organisms, which have higher H_2 production activities, in the heterocyst of *Anabaena* have shown potential (Avilan et al., 2018; Gärtner et al., 2012).

Recently, immobilization of isolated heterocysts in polymer matrices is starting to be used to prolong bioproduction times. Improved stability and H_2 photoproduction have been demonstrated in photosynthetic cyanobacteria and microalgae immobilized in thin films as opposed to suspension cultures. Production periods of several months were obtained (Kosourov et al., 2014; Leino et al., 2012; Murukesan et al., 2019; Volgusheva et al., 2019). Thin layer immobilization of cyanobacterial heterocysts could provide a long-lived biocatalyst producing NH_3, an important bioindustrial compound used as a fertilizer or fuel, and H_2, which is an environmentally friendly, clean energy source. A proof of concept for such a production platform was already provided and depending on addition of H_2 or N_2 as substate for nitrogenase, this production platform can switch between H_2 and NH_3 production (Volgusheva et al., 2019). Moreover, the immobilized *Anabaena* Δ*hupL* mutant was previously shown to be suitable for long term H_2 production (Leino et al., 2012). Beyond N_2 and H_2 production, the anaerobic heterocyst metabolism has been investigated. For example, ethanol production in the heterocysts of a modified *Anabaena* stain has been previously demonstrated, leading to increased ethanol production alongside N (Ehira et al., 2018). Moreover, parallel usage of oxygenic photosynthesis in vegetative cells may also be possible.

In unicellular cyanobacteria, it is already being investigated how to redirect e^- to reductive biotransformations by deleting FDPs as competitive e^- sinks (Assil-Companioni et al., 2020; Hubáček et al., 2024). While retained in cyanobacteria, algae, and gymnosperms, FDPs were lost during angiosperm evolution (Jokel et al., 2018), likely due to the emergence of compensatory photoprotective mechanisms (Allahverdiyeva, Suorsa, et al., 2015). Nevertheless, numerous studies have demonstrated that angiosperms remain susceptible to PSI photoinhibition under fluctuating light, which can substantially limit CO_2 assimilation and growth (Huang et al., 2019; Kono et al., 2014; Sun et al., 2023; Yamamoto & Shikanai, 2019; Yang et al., 2024). Heterologous expression of FDPs from cyanobacteria or *Physcomitrium patens* in angiosperms improves photosynthetic performance and biomass accumulation (Basso et al., 2022; Gómez et al., 2018; Rizzetto et al., 2025; Wada et al., 2018; Yamamoto et al., 2016; Yamamoto & Shikanai, 2019). To date, however, FDPs from heterocystous cyanobacteria such as *Anabaena* have not been tested in angiosperms, leaving open the question of whether their distinct regulatory or kinetic properties could confer additional benefits in crop species.

This thesis further highlights the role of global transcriptional regulation in balancing electron sinks and metabolic demands. The identification of PacR as a regulator linking FDP expression, carbon metabolism, photosynthesis, and heterocyst development suggests that redox-dependent transcriptional control may

be central to coordinating photosynthetic electron flow with cellular metabolic capacity. Understanding how PacR integrates photosynthetic signals with nitrogen and carbon metabolism remains an important objective for future research.

Acknowledgements

I would like to thank with sincere gratitude all who have supported me during my PhD journey.

My studies would not have been possible without the University of Turku offering me a funded position in the Doctoral Program in Technology and Prof. Yagut Allahverdiyeva providing the matching funding. I would also like to thank the Finnish Foundation for Technology Promotion and the Swedish Academy of Engineering Sciences in Finland (STV) for providing me with supportive grants.

My sincere thanks go out to my pre-examiners, **Prof. Amel Latifi** and **Prof. Giorgio Perin** in reviewing and improving my thesis. A special thanks to **Dr. Szilvia Tóth** for accepting my invitation to be my opponent during my doctoral disputation. I would also like to thank the members of my advisory committee, **Prof. Yagut Allahverdiyeva**, **Dr. Tuomas Huokko**, **Dr. Lauri Nikkanen** and **Dr. Taina Tyystjärvi** for their support and valuable comments.

I am immensely grateful to **Prof. Yagut Allahverdiyeva** for welcoming me into the Photomicrobes group as a Doctoral Researcher directly after completing my Master's Thesis. Many thanks for supervising my work and your invaluable feedback, your guidance and patience during these four years and especially for giving me the space and time to develop my own ideas and grow as a professional and as an individual.

To **Dr. Tuomas Huokko** – You have guided me through planning my first independent experiments, writing my first paper and writing my first thesis – many Firsts that come with questions, setbacks and challenges. I will always be grateful for your constant support and kindness as my supervisor, which have truly carried me through the PhD process.

Dr. Lauri Nikkanen, I truly appreciate the sharing of your deep insight and our brain-storming sessions, especially when I was stuck on a particular question or challenge in my project. Your guidance in developing my scientific hypothesis have truly helped me to lift my research to a new level.

I am also very thankful towards all my coauthors of the original publications, without your vital contributions this work would not have been possible. Many thanks to Prof. Yagut Allahverdiyeva, Dr. Tuomas Huokko and Dr. Lauri Nikkanen

for carefully checking the language and readability and the content of my paper and my thesis. Many thanks to **Prof. emer. Eevi Rintamäki** for her support in organizing my doctoral thesis.

My deep gratitude goes towards all members of the Photomicrobes group and everyone I have encountered at the Molecular Plant Biology Lab. I have enjoyed our weekly scientific discussions and working alongside you. I deeply appreciate your support with everyday tasks and your companionship during chats and lunches.

Dr. Anita Santana-Sánchez, thank you for coaching me and teaching me at the beginning of my thesis and enabling me to contribute to your paper – I truly learned much from you and am grateful that you trusted me with continuing your projects.

A heartfelt thank you also to **Dr. Michal Hubáček**, you have guided me from the very beginning in organizing my move to Turku, as well as later in the lab. I enjoyed our talks about our projects and career prospects – with your willingness to lend a helping hand and an open ear wherever needed you have truly been the heart of our PhD community.

For your support during planning and conducting my experiments, I would also like to warmly thank **Dr. Gábor Tóth** – I could always rely on you to help me think through everyday challenges in the lab.

For their help and guidance in my laboratory work I would like to sincerely thank also **Dr. Vilja Siitonen**, **Dr. Henna Mustila** and **Dr. Juha Kurkela**.

My thanks goes out to Keyla Crosbie for sharing my concern on the usage of vegan antibodies – I am grateful to have found someone to collaborate with on a topic close to my heart.

For enlightening and fun coffee-break conversations I would like to thank all fellow PhD students I had the pleasure to work alongside over the years – Anita, Gábor, Michal, Emren, Radin, Keyla, Joao, Khadijatul, Eba, Elia, Samuele, Han and Filippo.

I would like to warmly thank our technical staff, Dr. Mika Keränen, Eveliina Pakula and Anniina Lepistö for their constant help and support in everyday lab tasks – thank you for your patience and giving a helping hand and advice whenever needed.

Since joining the Team of the Young Algaeneers Symposium in 2023, they have become a supportive community. My deep gratitude goes towards the EABA team, Carlos Unamunzaga, Vítor Verdelho, Dr. Jean-Paul Cadoret, Lisandra Meinerz and Christie de Vrij for their wealth of advice and patience. Special thanks to Daniel Figueiredo who guided me from the start and helped me to expand my communication, networking and team-leading skills and trusted me with chairing the 2026 edition of YAS. A big thank you also to Dr. Arianna Rizzo and Dr. Sheyma

Khemiri for guiding me and supporting me during my YAS journey. I am grateful to have met many more amazing and supportive people on the team over the years - Oscar, Rafael, Anna, Gloria, Ben, Inge, Áureo, Luca – it has been a lot of fun working with you!

Turku, June 2026

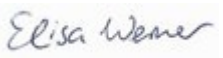

Elisa Werner

List of References

Adir, N., Bar-Zvi, S., & Harris, D. (2020). The amazing phycobilisome. Biochimica et Biophysica Acta (BBA) - Bioenergetics, 1861(4), 148047.

Aichi, M., Takatani, N., & Omata, T. (2001). Role of NtcB in activation of nitrate assimilation genes in the cyanobacterium Synechocystis sp. strain PCC 6803. Journal of Bacteriology, 183(20).

Alam, J., Whitaker, R. A., Krogmann, D. W., & Curtis, S. E. (1986). Isolation and sequence of the gene for ferredoxin I from the cyanobacterium Anabaena sp. strain PCC 7120. Journal of Bacteriology, 168(3), 1265–1271.

Alboresi, A., Storti, M., Cendron, L., & Morosinotto, T. (2019). Role and regulation of class-C flavodiiron proteins in photosynthetic organisms. The Biochemical Journal, 476(17), 2487–2498.

Albracht, S. P. J. (1994). Nickel hydrogenases: in search of the active site. Biochimica et Biophysica Acta (BBA) - Bioenergetics, 1188(3), 167–204.

Allaf, M. M., & Peerhossaini, H. (2022). Cyanobacteria: Model Microorganisms and Beyond. Microorganisms, 10(4), 696.

Allahverdiyeva, Y., Aro, E. M., van Bavel, … M., Skomedal, H., ...Skjermo, J. (2021). NordAqua, a Nordic Center of Excellence to develop an algae-based photosynthetic production platform. Physiologia Plantarum, 173(2), 507–513.

Allahverdiyeva, Y., Ermakova, M., Eisenhut, M., Zhang, P., Richaud, P., Hagemann, M., Cournac, L., & Aro, E. M. (2011). Interplay between flavodiiron proteins and photorespiration in Synechocystis sp. PCC 6803. Journal of Biological Chemistry, 286(27), 24007–24014.

Allahverdiyeva, Y., Isojärvi, J., Zhang, P., & Aro, E. M. (2015). Cyanobacterial oxygenic photosynthesis is protected by flavodiiron proteins. In Life (Vol. 5, Number 1).

Allahverdiyeva, Y., Mustila, H., Ermakova, M., Bersanini, L., Richaud, P., …Aro, E. M. (2013). Flavodiiron proteins Flv1 and Flv3 enable cyanobacterial growth and photosynthesis under fluctuating light. Proceedings of the National Academy of Sciences of the United States of America, 110(10).

Allahverdiyeva, Y., Suorsa, M., Tikkanen, M., & Aro, E. M. (2015). Photoprotection of photosystems in fluctuating light intensities. Journal of Experimental Botany, 66(9), 2427–2436.

Alleman, A. B., & Peters, J. W. (2023). Mechanisms for Generating Low Potential Electrons across the Metabolic Diversity of Nitrogen-Fixing Bacteria. In Applied and environmental microbiology (Vol. 89, Number 5).

Appel, J., Phunpruch, S., Steinmüller, K., & Schulz, R. (2000). The bidirectional hydrogenase of Synechocystis sp. PCC 6803 works as an electron valve during photosynthesis. Archives of Microbiology, 173(5–6), 333–338.

Armbruster, U., Correa Galvis, V., Kunz, H. H., & Strand, D. D. (2017). The regulation of the chloroplast proton motive force plays a key role for photosynthesis in fluctuating light. In Current Opinion in Plant Biology (Vol. 37).

Artz, J. H., Tokmina-Lukaszewska, M., Mulder, D. W., Lubner, C. E., … King, P. W. (2020). The structure and reactivity of the HoxEFU complex from the cyanobacterium Synechocystis sp. PCC 6803. Journal of Biological Chemistry, 295(28), 9445–9454.

Assil-Companioni, L., Büchsenschütz, H. C., Solymosi, D., …Kourist, R. (2020). Engineering of NADPH Supply Boosts Photosynthesis-Driven Biotransformations. ACS Catalysis, 10(20).

Astier, J., Rossi, J., Chatelain, P., Klinguer, A., Besson-Bard, A., ...Wendehenne, D. (2021). Nitric oxide production and signalling in algae. Journal of Experimental Botany, 72(3), 781–792.

Avilan, L., Roumezi, B., Risoul, V., Bernard, C. S., Kpebe, A., …Latifi, A. (2018). Phototrophic hydrogen production from a clostridial [FeFe] hydrogenase expressed in the heterocysts of the cyanobacterium Nostoc PCC 7120. Applied Microbiology and Biotechnology 2018 102:13, 102(13), 5775–5783.

Badger, M. R., & Price, G. D. (2003). CO2 concentrating mechanisms in cyanobacteria: Molecular components, their diversity and evolution. In Journal of Experimental Botany (Vol. 54, Number 383).

Badger, M. R., Price, G. D., Long, B. M., & Woodger, F. J. (2006). The environmental plasticity and ecological genomics of the cyanobacterial CO2 concentrating mechanism. Journal of Experimental Botany, 57(2 SPEC. ISS.).

Bandyopadhyay, A., Ye, Z., Benedikty, Z., Trtilek, M., & Pakrasi, H. B. (2021). Antenna Modification Leads to Enhanced Nitrogenase Activity in a High Light-Tolerant Cyanobacterium. MBio, 12(6).

Baniulis, D., Yamashita, E., Zhang, H., Hasan, S. S., & Cramer, W. A. (2008). Structure–Function of the Cytochrome b6f Complex†. Photochemistry and Photobiology, 84(6), 1349–1358.

Basso, L., Sakoda, K., Kobayashi, R., Yamori, W., & Shikanai, T. (2022). Flavodiiron proteins enhance the rate of CO2 assimilation in Arabidopsis under fluctuating light intensity. Plant Physiology, 189(1), 375–387.

Bauwe, H., Hagemann, M., & Fernie, A. R. (2010). Photorespiration: players, partners and origin. In Trends in Plant Science (Vol. 15, Number 6).

Beraldo, C., Traverso, E., Boschin, M., Cendron, L., Morosinotto, T., & Alboresi, A. (2024). Physcomitrium patens flavodiiron proteins form heterotetrametric complexes. Journal of Biological Chemistry, 300, 107643.

Böhme, H. (1998). Regulation of nitrogen fixation in heterocyst-forming cyanobacteria. Trends in Plant Science, 3(9), 346–351.

Bolay, P., Schlüter, S., Grimm, S., Riediger, M., Hess, W. R., & Klähn, S. (2022). The transcriptional regulator RbcR controls ribulose-1,5-bisphosphate carboxylase/oxygenase (RuBisCO) genes in the cyanobacterium Synechocystis sp. PCC 6803. New Phytologist, 235(2).

Bothe, H., Schmitz, O., Yates, M. G., & Newton, W. E. (2010). Nitrogen Fixation and Hydrogen Metabolism in Cyanobacteria. Microbiology and Molecular Biology Reviews, 74(4), 529–551.

Burgess, B. K., & Lowe, D. J. (1996). Mechanism of Molybdenum Nitrogenase. Chemical Reviews, 96(7), 2983–3011.

Burgstaller, H., Wang, Y., Caliebe, J., Hueren, V., Appel, J., ...Gutekunst, K. (2022). Synechocystis sp. PCC 6803 Requires the Bidirectional Hydrogenase to Metabolize Glucose and Arginine Under Oxic Conditions. Frontiers in Microbiology, 13, 896190.

Burlacot, A., Dao, O., Auroy, P., Cuiné, S., Li-Beisson, Y., & Peltier, G. (2022). Alternative photosynthesis pathways drive the algal CO2-concentrating mechanism. Nature 2022 605:7909, 605(7909), 366–371.

Burlacot, A., Richaud, P., Gosset, A., Li-Beisson, Y., & Peltier, G. (2020). Algal photosynthesis converts nitric oxide into nitrous oxide. Proceedings of the National Academy of Sciences of the United States of America, 117(5).

Burnap, R. L., Hagemann, M., & Kaplan, A. (2015). Regulation of CO2 Concentrating Mechanism in Cyanobacteria. Life 2015, Vol. 5, Pages 348-371, 5(1), 348–371.

Burnat, M., Herrero, A., & Flores, E. (2014). Compartmentalized cyanophycin metabolism in the diazotrophic filaments of a heterocystforming cyanobacterium. Proceedings of the National Academy of Sciences of the United States of America, 111(10).

Cabello-Yeves, P. J., Scanlan, D. J., Callieri, ... Puxty, R. J. (2022). α-cyanobacteria possessing form IA RuBisCO globally dominate aquatic habitats. ISME Journal, 16(10), 2421–2432.

Cai, Y., & Wolk, C. P. (1990). Use of a conditionally lethal gene in Anabaena sp. strain PCC 7120 to select for double recombinants and to entrap insertion sequences. Journal of Bacteriology, 172(6).

Callahan, S. M., & Buikema, W. J. (2001). The role of HetN in maintenance of the heterocyst pattern in Anabaena sp. PCC 7120. Molecular Microbiology, 40(4), 941–950.

Calzadilla, P. I., & Kirilovsky, D. (2020). Revisiting cyanobacterial state transitions. In Photochemical and Photobiological Sciences (Vol. 19, Number 5).

Camargo, S., Valladares, A., Flores, E., & Herrero, A. (2012). Transcription activation by NtcA in the absence of consensus NtcA-binding sites in an anabaena heterocyst differentiation gene promoter. Journal of Bacteriology, 194(11), 2939–2948.

Cameron, J. C. (2014). The carboxysome: function, structure and cellular dynamics. Norfolk: Caister Academic Press.

Carr, N. G. (1989). Nitrogen reserves and dynamic reservoirs in cyanobacteria. Clarendon Press.

Carrieri, D., Wawrousek, K., Eckert, C., Yu, J., & Maness, P. C. (2011). The role of the bidirectional hydrogenase in cyanobacteria. Bioresource Technology, 102(18), 8368–8377.

Casanova-Ferrer, P., Muñoz-García, J., & Ares, S. (2022). Mathematical models of nitrogen-fixing cell patterns in filamentous cyanobacteria. Frontiers in Cell and Developmental Biology, 10, 959468.

Chaux, F., Burlacot, A., Mekhalfi, M., Auroy, P., Blangy, S., Richaud, P., & Peltier, G. (2017). Flavodiiron proteins promote fast and transient O2 photoreduction in chlamydomonas. Plant Physiology, 174(3).

Checchetto, V., Segalla, A., Allorent, G., ... Szabò, I. (2012). Thylakoid potassium channel is required for efficient photosynthesis in cyanobacteria. Proceedings of the National Academy of Sciences of the United States of America, 109(27), 11043–11048.

Checchetto, V., Teardo, E., Carraretto, L., Formentin, E., Bergantino, E., …Szabo, I. (2013). Regulation of photosynthesis by ion channels in cyanobacteria and higher plants. Biophysical Chemistry, 182, 51–57.

Chen, X., Schreiber, K., Appel, J., Makowka, A., Fähnrich, B., Roettger, M., ...Gutekunst, K. (2016). The Entner-Doudoroff pathway is an overlooked glycolytic route in cyanobacteria and plants. Proceedings of the National Academy of Sciences of the United States of America, 113(19), 5441–5446.

Cherepanov, D. A., Semenov, A. Y., Mamedov, M. D., …Nadtochenko, V. A. (2022). Current state of the primary charge separation mechanism in photosystem I of cyanobacteria. In Biophysical Reviews (Vol. 14, Number 4).

Christiansen, J., Dean, D. R., & Seefeldt, L. C. (2001). Mechanistic features of the Mo-containing nitrogenase. Annual Review of Plant Biology, 52(Volume 52, 2001), 269–295.

Corrales-Guerrero, L., Tal, A., Arbel-Goren, R., Mariscal, V., Flores, …Stavans, J. (2015). Spatial Fluctuations in Expression of the Heterocyst Differentiation Regulatory Gene hetR in Anabaena Filaments. PLoS Genetics, 11(4).

Cumino, A. C., Marcozzi, C., Barreiro, R., & Salerno, G. L. (2007). Carbon cycling in Anabaena sp. PCC 7120. Sucrose synthesis in the heterocysts and possible role in nitrogen fixation. Plant Physiology, 143(3).

Curatti, L., Flores, E., & Salerno, G. (2002). Sucrose is involved in the diazotrophic metabolism of the heterocyst-forming cyanobacterium Anabaena sp. FEBS Letters, 513(2–3), 175–178.

Daley, S. M. E., Kappell, A. D., Carrick, M. J., & Burnap, R. L. (2012). Regulation of the cyanobacterial CO2-concentrating mechanism involves internal sensing of NADP+ and α-ketogutarate levels by transcription factor CcmR. PLoS ONE, 7(7).

Dangel, A. W., & Tabita, F. R. (2015). CbbR, the Master Regulator for Microbial Carbon Dioxide Fixation. Journal of Bacteriology, 197(22), 3488–3498.

De Araujo, C., Arefeen, D., Tadesse, Y., Long, B. M., Price, G. D., …Espie, G. S. (2014). Identification and characterization of a carboxysomal γ-carbonic anhydrase from the cyanobacterium Nostoc sp. PCC 7120. Photosynthesis Research, 121(2–3).

Deora, S., Deora, G. S., Nigam, S., & Harish. (2025). Hacking heterocysts: advances in the genetic regulation of heterocyst differentiation. Archives of Microbiology 2025 208:1, 208(1), 80-.

Douchi, D., Liang, F., Cano, M., Xiong, W., Wang, B., Maness, P. C., Lindblad, P., & Yu, J. (2019). Membrane-inlet mass spectrometry enables a quantitative understanding of inorganic carbon uptake flux and carbon concentrating mechanisms in metabolically engineered cyanobacteria. Frontiers in Microbiology, 10(JUN).

Dubois, M., Gilles, K. A., Hamilton, J. K., Rebers, P. A., & Smith, F. (1956). Colorimetric Method for Determination of Sugars and Related Substances. Analytical Chemistry, 28(3).

Ducret, A., Sidler, W., Wehrli, E., Frank, G., & Zuber, H. (1996). Isolation, characterization and electron microscopy analysis of a hemidiscoidal phycobilisome type from the cyanobacterium Anabaena sp. PCC 7120. European Journal of Biochemistry, 236(3), 1010–1024.

Eckert, C., Boehm, M., Carrieri, D., Yu, J., Dubini, A., Nixon, P. J., & Maness, P. C. (2012). Genetic analysis of the Hox hydrogenase in the cyanobacterium Synechocystis sp. PCC 6803 reveals subunit roles in association, assembly, maturation, and function. Journal of Biological Chemistry, 287(52), 43502–43515.

Ehira, S., & Ohmori, M. (2006). NrrA Directly Regulates Expression of hetR during Heterocyst Differentiation in the Cyanobacterium Anabaena sp. Strain PCC 7120.Journal of Bacteriology, 188(24), 8520–8525.

Ehira, S., Takeuchi, T., & Higo, A. (2018). Spatial separation of photosynthesis and ethanol production by cell type-specific metabolic engineering of filamentous cyanobacteria. Applied Microbiology and Biotechnology, 102(3), 1523–1531.

Eisenhut, M., Ruth, W., Haimovich, M., Bauwe, H., Kaplan, A., & Hagemann, M. (2008). The photorespiratory glycolate metabolism is essential for cyanobacteria and might have been conveyed endosymbiontically to plants. Proceedings of the National Academy of Sciences, 105(44), 17199–17204.

Elanskaya, I. V., Bulychev, A. A., Lukashev, E. P., & Muronets, E. M. (2021). Deficiency in flavodiiron protein Flv3 promotes cyclic electron flow and state transition under high light in the cyanobacterium Synechocystis sp. PCC 6803. Biochimica et Biophysica Acta - Bioenergetics, 1862(1).

Erdrich, P., Knoop, H., Steuer, R., & Klamt, S. (2014). Cyanobacterial biofuels: New insights and strain design strategies revealed by computational modeling. Microbial Cell Factories, 13(1).

Ermakova, M. (2014). Heterocyst-specific flavodiiron protein Flv3B enables oxic diazotrophic growth of the filamentous cyanobacterium Anabaena sp. PCC 7120. PNAS.

Ermakova, M., Battchikova, N., Allahverdiyeva, Y., & Aro, E. M. (2013). Novelheterocyst-specific flavodiiron proteins in Anabaena sp. PCC 7120. FEBS Letters, 587(1).

Espinosa, J., Forchhammer, K., Burillo, S., & Contreras, A. (2006). Interaction network in cyanobacterial nitrogen regulation: PipX, a protein that interacts in a 2-oxoglutarate dependent manner with PII and NtcA. Molecular Microbiology, 61(2), 457–469.

Espinosa, J., Forchhammer, K., & Contreras, A. (2007). Role of the Synechococcus PCC 7942 nitrogen regulator protein PipX in NtcA-controlled processes. Microbiology, 153(3), 711–718.

Falkowski, P. (2012). Ocean Science: The power of plankton. Nature 2012 483:7387, 483(7387), S17–S20.

Fedorov, V. A., Kovalenko, I. B., Khruschev, S. S., Ustinin, …Rubin, A. B. (2019). Comparative analysis of plastocyanin–cytochrome f complex formation in higher plants, green algae and cyanobacteria. Physiologia Plantarum, 166(1), 320–335.

Figge, R. M., Cassier-Chauvat, C., Chauvat, F., & Cerff, R. (2001). Characterization and analysis of an NAD(P)H dehydrogenase transcriptional regulator critical for the survival of cyanobacteria facing inorganic carbon starvation and osmotic stress. Molecular Microbiology, 39(2).

Flamholz, A. I., Prywes, N., Moran, U., Davidi, D., Bar-On, Y. M., …Milo, R. (2019). Revisiting Trade-offs between Rubisco Kinetic Parameters. Biochemistry, 58(31), 3365–3376.

Flores, E., Arévalo, S., & Burnat, M. (2019). Cyanophycin and arginine metabolism in cyanobacteria. Algal Research, 42, 101577.

Flores, E., Frías, J. E., Rubio, L. M., & Herrero, A. (2005). Photosynthetic nitrate assimilation in cyanobacteria. Photosynthesis Research, 83(2), 117–133.

Flores, E., & Herrero, A. (1994). Assimilatory Nitrogen Metabolism and Its Regulation. In The Molecular Biology of Cyanobacteria.

Flores, E., & Herrero, A. (2010). Compartmentalized function through cell differentiation in filamentous cyanobacteria. In Nature Reviews Microbiology (Vol. 8, Number 1).

Flores, E.; Herrero, A. (2005). Nitrogen assimilation and nitrogen control in cyanobacteria. Biochemical Society Transactions, 33(1), 164–167.

Flores, E., Herrero, A., Forchhammer, K., & Maldener, I. (2016). Septal Junctions in Filamentous Heterocyst-Forming Cyanobacteria. Trends in Microbiology, 24(2), 79–82.

Flores, E., Muro-Pastor, A. M., & Herrero, A. (1999). Cyanobacterial Nitrogen Assimilation Genes and NtcA-Dependent Control of Gene Expression. The Phototrophic Prokaryotes, 463–477.

Flores, E., Picossi, S., Valladares, A., & Herrero, A. (2019). Transcriptional regulation of development in heterocyst-forming cyanobacteria. Biochimica et Biophysica Acta (BBA) - Gene Regulatory Mechanisms, 1862(7), 673–684.

Floß, B., Igloi, G. L., Cassier-Chauvat, C., & Mühlenhoff, U. (1997). Molecular characterization and overexpression of the petF gene from Synechococcus elongatus: Evidence for a second site of electrostatic interaction between ferredoxin and the PS I-D subunit. Photosynthesis Research, 54(1), 63–71.

Forchhammer, K. (2008). PII signal transducers: novel functional and structural insights. In Trends in Microbiology (Vol. 16, Number 2).

Forchhammer, K., & Lüddecke, J. (2016). Sensory properties of the PII signalling protein family. FEBS Journal, 283(3), 425–437.

Forchhammer, K., & Selim, K. A. (2020). Carbon/nitrogen homeostasis control in cyanobacteria. FEMS Microbiology Reviews, 44(1), 33–53.

Forchhammer, K., Selim, K. A., & Huergo, L. F. (2022). New views on PII signaling: from nitrogen sensing to global metabolic control. In Trends in Microbiology (Vol. 30, Number 8).

Frías, J. E., Flores, E., & Herrero, A. (1994). Requirement of the regulatory protein NtcA for the expression of nitrogen assimilation and heterocyst development genes in the cyanobacterium Anabaena sp. PCC7120. Molecular Microbiology, 14(4), 823–832.

Frías, J. E., Flores, E., & Herrero, A. (1997). Nitrate assimilation gene cluster from the heterocyst-forming cyanobacterium Anabaena sp. Strain PCC 7120. Journal of Bacteriology, 179(2).

Frias, J. E., Flores, E., & Herrero, A. (2000). Activation of the Anabaena nir operon promoter requires both NtcA (CAP family) and NtcB (LysR family) transcription factors. Molecular Microbiology, 38(3).

Frías, J. E., Herrero, A., & Flores, E. (2003). Open reading frame all0601 from Anabaena sp. strain PCC 7120 represents a novel gene, cnaT, required for expression of the nitrate assimilation nir operon. Journal of Bacteriology, 185(17).

Gallego, R. P., von Meijenfeldt, F. A. B., Bale, N. J., Sinninghe Damsté, J. S., & Villanueva, L. (2025). Emergence and evolution of heterocyte glycolipid biosynthesis enabled specialized nitrogen fixation in cyanobacteria. Proceedings of the National Academy of Sciences of the United States of America, 122(5), e2413972122.

Galmozzi, C. V., Fernández-Avila, M. J., Reyes, J. C., Florencio, F. J., & Muro-Pastor, M. I. (2007). The ammonium-inactivated cyanobacterial glutamine synthetase I is reactivated in vivo by a mechanism involving proteolytic removal of its inactivating factors. Molecular Microbiology, 65(1), 166–179.

Galmozzi, C. V., Saelices, L., Florencio, F. J., & Muro-Pastor, M. I. (2010). Posttranscriptional regulation of glutamine synthetase in the filamentous cyanobacterium Anabaena sp. PCC 7120: Differential expression between vegetative cells and heterocysts. Journal of Bacteriology, 192(18).

García-Domínguez, M., Reyes, J. C., & Florencio, F. J. (2000). NtcA represses transcription of gifA and gifB, genes that encode inhibitors of glutamine synthetase type I from Synechocystis sp. PCC 6803. Molecular Microbiology, 35(5), 1192–1201.

Gärtner, K., Lechno-Yossef, S., Cornish, A. J., Wolk, C. P., & Hegg, E. L. (2012). Expression of shewanella oneidensis MR-1 [FeFe]-hydrogenase genes in Anabaena sp. strain PCC 7120. Applied and Environmental Microbiology, 78(24), 8579–8586.

Gerotto, C., Alboresi, A., Meneghesso, A., Jokel, M., Suorsa, M., Aro, E. M., & Morosinotto, T. (2016). Flavodiiron proteins act as safety valve for electrons in Physcomitrella patens. Proceedings of the National Academy of Sciences of the United States of America, 113(43).

Gisriel, C. J., Wang, J., Liu, J., Flesher, D. A., Reiss, K. M., Huang, H. L., Yang, K. R., Armstrong, W. H., …Brudvig, G. W. (2022). High-resolution cryo-electron microscopy structure of photosystem II from the mesophilic cyanobacterium, Synechocystis sp. PCC 6803. Proceedings of the National Academy of Sciences of the United States of America, 119(1), e2116765118.

Glauser, M., Bryant, D. A., Frank, G., Wehrli, E., Rusconi, S. S., SidlerI, W., & Zuber, H. (1992). Phycobilisome structure in the cyanobacteria Mastigocladus laminosus and Anabaena sp. PCC 7120. European Journal of Biochemistry, 205(3), 907–915.

Gollan, P. J., Muth-Pawlak, D., & Aro, E. M. (2020). Rapid transcriptional reprogramming triggered by alteration of the carbon/nitrogen balance has an impact on energy metabolism in nostoc sp. Pcc 7120. Life, 10(11).

Gómez, R., Carrillo, N., Morelli, M. P., Tula, S., Shahinnia, F., …Lodeyro, A. F. (2018). Faster photosynthetic induction in tobacco by expressing cyanobacterial flavodiiron proteins in chloroplasts. Photosynthesis Research, 136(2), 129–138.

González, A., Angarica, V. E., Sancho, J., & Fillat, M. F. (2014). The FurA regulon in Anabaena sp. PCC 7120: In silico prediction and experimental validation of novel target genes. Nucleic Acids Research, 42(8).

González, A., Bes, M. T., Valladares, A., Peleato, M. L., & Fillat, M. F. (2012). FurA is the master regulator of iron homeostasis and modulates the expression of tetrapyrrole biosynthesis genes in Anabaena sp. PCC 7120. Environmental Microbiology, 14(12), 3175–3187.

González, A., Valladares, A., Peleato, M. L., & Fillat, M. F. (2013). FurA influences heterocyst differentiation in Anabaena sp. PCC 7120. FEBS Letters, 587(16), 2682–2690.

Grettenberger, C. L., Abou-Shanab, R., & Hamilton, T. L. (2024). Limiting factors in the operation of photosystems I and II in cyanobacteria. Microbial Biotechnology, 17(8), e14519.

Gründel, M., Scheunemann, R., Lockau, W., & Zilliges, Y. (2012). Impaired glycogen synthesis causes metabolic overflow reactions and affects stress responses in the cyanobacterium Synechocystis sp. PCC 6803. Microbiology (United Kingdom), 158(12).

Guío, J., Sarasa-Buisan, C., Velázquez-Campoy, A., Bes, M. T., Fillat, M. F., …Sevilla, E. (2020). 2-oxoglutarate modulates the affinity of FurA for the ntcA promoter in Anabaena sp. PCC 7120. FEBS Letters, 594(2).

Gupta, M., & Carr, N. G. (1981). Enzyme activities related to cyanophycin metabolism in heterocysts and vegetative cells of Anabaena spp. Journal of General Microbiology, 125(1), 17–23.

Gupta, N., Srivastava, A., & Mishra, A. K. (2025). Nitric Oxide Synthases in Cyanobacteria: Diversity, Cellular Implications and Ecological Pertinence. Journal of Plant Growth Regulation, 44(2), 508–528.

Hackenberg, C., Engelhardt, A., Matthijs, H. C. P., Wittink, F., Bauwe, H., ...Hagemann, M. (2009). Photorespiratory 2-phosphoglycolate metabolism and photoreduction of O 2 cooperate in high-light acclimation of Synechocystis sp. strain PCC 6803. Planta, 230(4).

Halinen, K., Fewer, D. P., Sihvonen, L. M., Lyra, C., Eronen, E., & Sivonen, K. (2008). Genetic diversity in strains of the genus Anabaena isolated from planktonic and benthic habitats of the Gulf of Finland (Baltic Sea). FEMS Microbiology Ecology, 64(2).

Hankamer, B., Morris, E., Nield, J., Carne, A., & Barber, J. (2001). Subunit positioning and transmembrane helix organisation in the core dimer of photosystem II. FEBS Letters, 504(3).

Hanson, T. E., Forchhammer, K., Tandeau De Marsac, N., & Meeks, J. C. (1998). Characterization of the glnB gene product of Nostoc punctiforme strain ATCC 29133: glnB or the P(II) protein may be essential. Microbiology, 144(6), 1537–1547.

Happe, T., Schütz, K., & Böhme, H. (2000). Transcriptional and mutational analysis of the uptake hydrogenase of the filamentous cyanobacterium Anabaena variabilis ATCC 29413. Journal of Bacteriology, 182(6).

Harish, & Seth, K. (2020). Molecular circuit of heterocyst differentiation in cyanobacteria. In Journal of Basic Microbiology (Vol. 60, Number 9).

Hauf, W., Schmid, K., Gerhardt, E. C. M., Huergo, L. F., & Forchhammer, K. (2016). Interaction of the nitrogen regulatory protein GlnB (PII) with biotin carboxyl carrier protein (BCCP) controls acetyl-Coa levels in the cyanobacterium synechocystis sp. PCC 6803. Frontiers in Microbiology, 7(OCT).

Havaux, M., Guedeney, G., Hagemann, M., Yeremenko, N., …Jeanjean, R. (2005). The chlorophyll-binding protein IsiA is inducible by high light and protects the cyanobacterium Synechocystis PCC6803 from photooxidative stress. FEBS Letters, 579(11), 2289–2293.

He, M., Santana-Sánchez, A., Tóth, G. S., Ermakova, M., ,… Allahverdiyeva, Y. (2025). Deletion of Flv3A facilitates long-term H2 photoproduction in diazotrophic Anabaena sp. PCC 7120. Physiologia Plantarum, 177(1), e70087.

He, Z., Zheng, F., Wu, Y., Li, Q., Lv, J., Fu, P., & Mi, H. (2015). NDH-1L interacts with ferredoxin via the subunit NdhS in Thermosynechococcus elongatus. Photosynthesis Research 2015 126:2, 126(2), 341–349.

Hebbar, P. B., & Curtis, S. E. (2000). Characterization of devH, a gene encoding a putative DNA binding protein required for heterocyst function in Anabaena sp. strain PCC 7120. Journal of Bacteriology, 182(12), 3572–3581.

Herrero, A., & Flores, E. (2019). Genetic responses to carbon and nitrogen availability in Anabaena. Environmental Microbiology, 21(1), 1–17.

Herrero, A., Muro-Pastor, A. M., & Flores, E. (2001). Nitrogen control in cyanobacteria. Journal of Bacteriology, 183(2), 411–425.

Herrero, Antonia., & Flores, Enrique. (2008). The cyanobacteria : molecular biology, genomics, and evolution (A. 'Herrero & E. 'Flores, Eds.). Caister Academic Press.

Higa, K. C., & Callahan, S. M. (2010). Ectopic expression of hetP can partially bypass the need for hetR in heterocyst differentiation by Anabaena sp. strain PCC 7120. Molecular Microbiology, 77(3), 562–574.

Hisbergues, M., Jeanjean, R., Joset, F., Tandeau De Marsac, N., & Bédu, S. (1999). Protein PII regulates both inorganic carbon and nitrate uptake and is modified by a redox signal in Synechocystis PCC 6803. FEBS Letters, 463(3), 216–220.

Hoare, D. S., & Hoare, S. L. (1966). Feedback Regulation of Arginine Biosynthesis in Blue-Green Algae and Photosynthetic Bacteria. Journal of Bacteriology, 92(2).

Hohmann-Marriott, M. F., & Blankenship, R. E. (2011). Evolution of photosynthesis. Annual Review of Plant Biology, 62.

Hoiczyk, E., & Hansel, A. (2000). Cyanobacterial cell walls: News from an unusual prokaryotic envelope. In Journal of Bacteriology (Vol. 182, Number 5).

Houchins, J. P., & Burris, R. H. (1981). Occurrence and localization of two distinct hydrogenases in the heterocystous cyanobacterium Anabaena sp. Strain 7120. Journal of Bacteriology, 146(1), 209–214.

Huang, W., Yang, Y. J., & Zhang, S. B. (2019). Photoinhibition of photosystem I under fluctuating light is linked to the insufficient ΔpH upon a sudden transition from low to high light. Environmental and Experimental Botany, 160, 112–119.

Hubáček, M., Wey, L. T., Kourist, R., Malihan-Yap, L., Nikkanen, L., & Allahverdiyeva, Y. (2024). Strong heterologous electron sink outcompetes alternative electron transport pathways in photosynthesis. Plant Journal, 119(5), 2500–2513.

Hudson, E. P. (2024). The Calvin Benson cycle in bacteria: New insights from systems biology. In Seminars in Cell and Developmental Biology (Vol. 155).

Huokko, T., Muth-Pawlak, D., Battchikova, N., Allahverdiyeva, Y., & Aro, E. M. (2017). Role of Type 2 NAD(P)H Dehydrogenase NdbC in Redox Regulation of Carbon Allocation in Synechocystis. Plant Physiology, 174(3), 1863–1880.

Jackson, P. J., Hitchcock, A., Brindley, A. A., Dickman, M. J., & Hunter, C. N. (2023). Absolute quantification of cellular levels of photosynthesis-related proteins in Synechocystis sp. PCC 6803. Photosynthesis Research, 155(3).

Jiang, Y. L., Wang, X. P., Sun, H., Han, S. J., Li, W. F., Cui, N., Lin, G. M., Zhang, J. Y., Cheng, W., Cao, D. D., …Zhou, C. Z. (2018). Coordinating carbon and nitrogen metabolic signaling through the cyanobacterial global repressor NdhR. Proceedings of the National Academy of Sciences, 115(2), 403–408.

Jokel, M., Johnson, X., Peltier, G., Aro, E. M., & Allahverdiyeva, Y. (2018). Hunting the main player enabling Chlamydomonas reinhardtii growth under fluctuating light. Plant Journal, 94(5), 822–835.

Jones, K. M., & Haselkorn, R. (2002). Newly Identified Cytochrome c Oxidase Operon in the Nitrogen-Fixing Cyanobacterium Anabaena sp. Strain PCC 7120 Specifically Induced in Heterocysts. Journal of Bacteriology, 184(9), 2491–2499.

Kaneko, T., Nakamura, Y., Wolk, C. P., Kuritz, T., Sasamoto, S., Watanabe, A., Iriguchi, M., … Tabata, S. (2001). Complete Genomic Sequence of the Filamentous Nitrogen-fixing Cyanobacterium Anabaena sp. Strain PCC 7120 (Supplement). DNA Research, 8(5), 227–253.

Kang, R. J., Shi, D. J., Cong, W., Cai, Z. L., & Ouyang, F. (2005). Regulation of CO2 on heterocyst differentiation and nitrate uptake in the cyanobacterium Anabaena sp. PCC 7120. Journal of Applied Microbiology, 98(3).

Kaštovský, J. (2024). Welcome to the jungle!: An overview of modern taxonomy of cyanobacteria. In Hydrobiologia (Vol. 851, Number 4).

Katayama, N., Iwazumi, K., Suzuki, H., Osanai, T., & Ito, S. (2022). Malic Enzyme, not Malate Dehydrogenase, Mainly Oxidizes Malate That Originates from the Tricarboxylic Acid Cycle in Cyanobacteria. MBio, 13(6).

Kato, K., Nagao, R., Jiang, T. Y., Ueno, Y., Yokono, M., Chan, S. K., Watanabe, M., Ikeuchi, M., …Akita, F. (2019). Structure of a cyanobacterial photosystem I tetramer revealed by cryo-electron microscopy. Nature Communications, 10(1).

Kerby, N. W., Musgrave, S. C., Rowell, P., Shestakov, S. V., & Stewart, W. D. P. (1986). Photoproduction of ammonium by immobilized mutant strains of Anabaena variabilis. Applied Microbiology and Biotechnology, 24(1).

Kerfeld, C. A., Melnicki, M. R., Sutter, M., & Dominguez-Martin, M. A. (2017). Structure, function and evolution of the cyanobacterial orange carotenoid protein and its homologs. New Phytologist, 215(3), 937–951.

Khanna, N., & Lindblad, P. (2015). Cyanobacterial Hydrogenases and Hydrogen Metabolism Revisited: Recent Progress and Future Prospects. International Journal of Molecular Sciences 2015, Vol. 16, Pages 10537-10561, 16(5), 10537–10561.

Khetkorn, W., Baebprasert, W., Lindblad, P., & Incharoensakdi, A. (2012). Redirecting the electron flow towards the nitrogenase and bidirectional Hox-hydrogenase by using specific inhibitors results in enhanced H2 production in the cyanobacterium Anabaena siamensis TISTR 8012. Bioresource Technology, 118.

Kieninger, A. K., & Maldener, I. (2021). Cell–cell communication through septal junctions in filamentous cyanobacteria. Current Opinion in Microbiology, 61, 35–41.

Kirilovsky, D. (2015). Modulating energy arriving at photochemical reaction centers: Orange carotenoid protein-related photoprotection and state transitions. Photosynthesis Research, 126(1), 3–17.

Kloft, N., & Forchhammer, K. (2005). Signal transduction protein PII phosphatase PphA is required for light-dependent control of nitrate utilization in Synechocystis sp. strain PCC 6803. Journal of Bacteriology, 187(19).

Klughammer, C., & Schreiber, U. (2016). Deconvolution of ferredoxin, plastocyanin, and P700 transmittance changes in intact leaves with a new type of kinetic LED array spectrophotometer. Photosynthesis Research, 128(2), 195–214.

Knoop, H., Gründel, M., Zilliges, Y., Lehmann, R., Hoffmann, S., Lockau, W., & Steuer, R. (2013). Flux Balance Analysis of Cyanobacterial Metabolism: The Metabolic Network of Synechocystis sp. PCC 6803. PLoS Computational Biology, 9(6).

Kono, M., Noguchi, K., & Terashima, I. (2014). Roles of the Cyclic Electron Flow Around PSI (CEF-PSI) and O2-Dependent Alternative Pathways in Regulation of the Photosynthetic Electron Flow in Short-Term Fluctuating Light in Arabidopsis thaliana. Plant and Cell Physiology, 55(5), 990–1004.

Kosourov, S., Leino, H., Murukesan, G., Lynch, F., Sivonen, K., Tsygankov, A. A., Aro, E. M., & Allahverdiyeva, Y. (2014). Hydrogen Photoproduction by Immobilized N2-Fixing Cyanobacteria: Understanding the Role of the Uptake Hydrogenase in the Long-Term Process. Applied and Environmental Microbiology, 80(18), 5807–5817.

Kotai, J. (1972). Instructions for preparation of modified nutrient solution Z8 for algae. Norwegian Institute for Water Research, Oslo 11.69 (1972): 5.

Kourpa, K., Manarolaki, E., Lyratzakis, A., Strataki, V., Rupprecht, F., Langer, J. D., & Tsiotis, G. (2019). Proteome Analysis of Enriched Heterocysts from Two Hydrogenase Mutants from Anabaena sp. PCC 7120. Proteomics, 19(19).

Kumar, K., Mella-Herrera, R. A., & Golden, J. W. (2010). Cyanobacterial Heterocysts. Cold Spring Harbor Perspectives in Biology, 2(4), a000315.

Kuntz, M. (2004). Plastid terminal oxidase and its biological significance. Planta, 218(6).

Kurio, Y., Koike, Y., Kanesaki, Y., Watanabe, S., & Ehira, S. (2020). The CRP-family transcriptional regulator DevH regulates expression of heterocyst-specific genes at the later stage of differentiation in the cyanobacterium Anabaena sp. strain PCC 7120. Molecular Microbiology, 114(4), 553–562.

Kurkela, J., & Tyystjärvi, T. (2024). Inorganic carbon sensing and signalling in cyanobacteria. In Physiologia Plantarum (Vol. 176, Number 1).

Lang, N. J., Simon, R. D., & Wolk, C. P. (1972). Correspondence of cyanophycin granules with structured granules in Anabaena cylindrica. Archiv Für Mikrobiologie, 83(4), 313–320.

Laughlin, T. G., Bayne, A. N., Trempe, J. F., Savage, D. F., & Davies, K. M. (2019). Structure of the complex I-like molecule NDH of oxygenic photosynthesis. Nature 2019 566:7744, 566(7744), 411–414.

Laurent, S., Chen, H., Bédu, S., Ziarelli, F., Peng, L., & Zhang, C. C. (2005). Nonmetabolizable analogue of 2-oxoglutarate elicits heterocyst differentiation under repressive conditions in Anabaena sp. PCC 7120. Proceedings of the National Academy of Sciences of the United States of America, 102(28).

Laurent, S., Forchhammer, K., Gonzalez, L., Heulin, T., Zhang, C. C., & Bédu, S. (2004). Cell-type specific modification of PII is involved in the regulation of nitrogen metabolism in the cyanobacterium Anabaena PCC 7120. FEBS Letters, 576(1–2), 261–265.

Lea-Smith, D. J., Bombelli, P., Vasudevan, R., & Howe, C. J. (2016). Photosynthetic, respiratory and extracellular electron transport pathways in cyanobacteria. Biochimica et Biophysica Acta (BBA) - Bioenergetics, 1857(3), 247–255.

Lee, H. M., Flores, E., Forchhammer, K., Herrero, A., & Tandeau De Marsac, N. (2000). Phosphorylation of the signal transducer PII protein and an additional effector are required for the PII-mediated regulation of nitrate and nitrite uptake in the cyanobacterium Synechococcus sp. PCC 7942. European Journal of Biochemistry, 267(2), 591–600.

Lee, H.-M., Mari´, M., Fé, M., Va´zquez, L., Va´zquez-Bermu´dez, V., Bermu´dez, B., & Tandeau De Marsac, N. (1999). The Global Nitrogen Regulator NtcA Regulates Transcription of the Signal Transducer PII (GlnB) and Influences Its Phosphorylation Level in Response to Nitrogen and Carbon Supplies in the Cyanobacterium Synechococcus sp. Strain PCC 7942. Journal of Bacteriology, 181(9), 2697–2702.

Leino, H., Kosourov, S. N., Saari, L., Sivonen, K., Tsygankov, A. A., Aro, E. M., & Allahverdiyeva, Y. (2012). Extended H2 photoproduction by N2-fixing cyanobacteria immobilized in thin alginate films. International Journal of Hydrogen Energy, 37(1), 151–161.

Leino, H., Shunmugam, S., Isojärvi, J., Oliveira, P., Mulo, P., Saari, L., Battchikova, N., Sivonen, K., Lindblad, P., Aro, E. M., & Allahverdiyeva, Y. (2014). Characterization of ten H2 producing cyanobacteria isolated from the Baltic Sea and Finnish lakes. International Journal of Hydrogen Energy, 39(17).

Li, B., Wang, X. Q., Li, Q. Y., Xu, D., Li, J., Hou, W. T., Chen, Y., Jiang, Y. L., & Zhou, C. Z. (2024). Allosteric regulation of nitrate transporter NRT via the signaling protein PII. Proceedings of the National Academy of Sciences of the United States of America, 121(11).

Li, J. H., Laurent, S., Konde, V., Bédu, S., & Zhang, C. C. (2003). An increase in the level of 2-oxoglutarate promotes heterocyst development in the cyanobacterium Anabaena sp. strain PCC 7120. Microbiology, 149(11).

Lin, G. M., Zhang, J. Y., Shao, Z. H., Yang, C., Zhao, G. P., Huang, K. Y., & Zhang, C. C. (2025). The LysR-type transcriptional factor PacR controls heterocyst differentiation and C/N metabolism in the cyanobacterium Anabaena PCC 7120. Microbiological Research, 290, 127970.

Lin, S., Zheng, T., Mo, Y., Zhang, G., & Chen, G. (2025). Site-2 protease Sll0528 interacts with RbcR to regulate carbon/nitrogen homeostasis in the cyanobacterium Synechocystis sp. PCC 6803. Frontiers in Microbiology, 16, 1556583.

Lindberg, P. (2003). Cyanobacterial Hydrogen Metabolism - Uptake Hydrogenase and Hydrogen Production by Nitrogenase in Filamentous Cyanobacteria. Uppsala University, Teknisk-naturvetenskapliga vetenskapsområdet, Faculty of Science and Technology, Biology.

Lindblad, P. (2002). A hydrogen-producing, hydrogenase-free mutant strain of Nostoc punctiforme ATCC 29133. International Journal of Hydrogen Energy, 27(11–12), 1291–1296.

Liu, H., Weisz, D. A., Zhang, M. M., Cheng, M., Zhang, B., Zhang, H., Gerstenecker, G. S., Pakrasi, H. B., ...Blankenship, R. E. (2019). Phycobilisomes harbor FNRL in cyanobacteria. MBio, 10(2).

Loll, B., Kern, J., Saenger, W., Zouni, A., & Biesiadka, J. (2005). Towards complete cofactor arrangement in the 3.0 Å resolution structure of photosystem II. Nature, 438(7070).

López-Gomollón, S., Hernández, J. A., Wolk, C. P., Peleato, M. L., & Fillat, M. F. (2007). Expression of furA is modulated by NtcA and strongly enhanced in heterocysts of Anabaena sp. PCC 7120. Microbiology, 153(1), 42–50.

López-Igual, R., Picossi, S., López-Garrido, J., Flores, E., & Herrero, A. (2012). N and C control of ABC-type bicarbonate transporter Cmp and its LysR-type transcriptional regulator CmpR in a heterocyst-forming cyanobacterium, Anabaena sp. Environmental Microbiology, 14(4), 1035–1048.

Lucius, S., & Hagemann, M. (2024). The primary carbon metabolism in cyanobacteria and its regulation. Frontiers in Plant Science, 15, 1417680.

Ludwig, M., Schulz-Friedrich, R., & Appel, J. (2006). Occurrence of hydrogenases in cyanobacteria and anoxygenic photosynthetic bacteria: Implications for the phylogenetic origin of cyanobacterial and algal hydrogenases. Journal of Molecular Evolution, 63(6).

Lyu, H., & Lazár, D. (2017). Modeling the light-induced electric potential difference ΔΨ across the thylakoid membrane based on the **Lindberg, P., Schütz, K., Happe, T., &** transition state rate theory. Biochimica et Biophysica Acta (BBA) - Bioenergetics, 1858(3), 239–248.

Maddocks, S. E., & Oyston, P. C. F. (2008). Structure and function of the LysR-type transcriptional regulator (LTTR) family proteins. Microbiology, 154(12), 3609–3623.

Magnuson, A. (2019). Heterocyst thylakoid bioenergetics. In Life (Vol. 9, Number 1).

Maheswaran, M., Ziegler, K., Lockau, W., Hagemann, M., & Forchhammer, K. (2006). PII-Regulated Arginine Synthesis Controls Accumulation of Cyanophycin in Synechocystis sp. Strain PCC 6803. Journal of Bacteriology, 188(7), 2730–2734.

Makowka, A., Nichelmann, L., Schulze, D., Spengler, K., Wittmann, C., Forchhammer, K., & Gutekunst, K. (2020). Glycolytic Shunts Replenish the Calvin–Benson–Bassham Cycle as Anaplerotic Reactions in Cyanobacteria. Molecular Plant, 13(3).

Malatinszky, D., Steuer, R., & Jones, P. R. (2017). A comprehensively curated genome-scale two-cell model for the heterocystous cyanobacterium Anabaena sp. PCC 7120. Plant Physiology, 173(1).

Malavath, T., Caspy, I., Netzer-El, S. Y., Klaiman, D., & Nelson, N. (2018). Structure and function of wild-type and subunit-depleted photosystem I in Synechocystis. Biochimica et Biophysica Acta - Bioenergetics, 1859(9).

Mallén-Ponce, M. J., Florencio, F. J., & Huertas, M. J. (2024). Thioredoxin A regulates protein synthesis to maintain carbon and nitrogen partitioning in cyanobacteria. Plant Physiology, 195(4).

Mallén-Ponce, M. J., Huertas, M. J., & Florencio, F. J. (2022). Exploring the Diversity of the Thioredoxin Systems in Cyanobacteria. In Antioxidants (Vol. 11, Number 4).

Malone, L. A., Proctor, M. S., Hitchcock, A., Hunter, C. N., & Johnson, M. P. (2021). Cytochrome b6f – Orchestrator of photosynthetic electron transfer. In Biochimica et Biophysica Acta - Bioenergetics (Vol. 1862, Number 5).

Mangan, N. M., Flamholz, A., Hood, R. D., Milo, R., & Savage, D. F. (2016). PH determines the energetic efficiency of the cyanobacterial CO2 concentrating mechanism. Proceedings of the National Academy of Sciences of the United States of America, 113(36), E5354–E5362.

Marques, A. E., Barbosa, A. T., Jotta, J., Coelho, M. C., Tamagnini, P., & Gouveia, L. (2011). Biohydrogen production by Anabaena sp. PCC 7120 wild-type and mutants under different conditions: Light, nickel, propane, carbon dioxide and nitrogen. Biomass and Bioenergy, 35(10), 4426–4434.

Martín-Figueroa, E., Navarro, F., & Florencio, F. J. (2000). The GS-GOGAT pathway is not operative in the heterocysts. Cloning and expression of glsF gene from the cyanobacterium Anabaena sp. PCC 7120. FEBS Letters, 476(3).

Masepohl, B., Schölisch, K., Görlitz, K., Kutzki, C., & Böhme, H. (1997). The heterocyst-specific fdxH gene product of the cyanobacterium Anabaena sp. PCC 7120 is important but not essential for nitrogen fixation. Molecular and General Genetics, 253(6), 770–776.

Masukawa, H., Mochimaru, M., & Sakurai, H. (2002). Disruption of the uptake hydrogenase gene, but not of the bidirectional hydrogenase gene, leads to enhanced photobiological hydrogen production by the nitrogen-fixing cyanobacterium Anabaena sp. PCC 7120. Applied Microbiology and Biotechnology, 58(5).

McDonald, A. E., Amirsadeghi, S., & Vanlerberghe, G. C. (2003). Prokaryotic orthologues of mitochondrial alternative oxidase and plastid terminal oxidase. Plant Molecular Biology, 53(6).

McKinney, R. E. (1953). Staining bacterial polysaccharides. Journal of Bacteriology, 66(4).

Meeks, J. C., & Castenholz, R. W. (1971). Growth and photosynthesis in an extreme thermophile, Synechococcus lividus (Cyanophyta). Archiv Für Mikrobiologie, 78(1), 25–41.

Meeks, J. C., & Elhai, J. (2002). Regulation of Cellular Differentiation in Filamentous Cyanobacteria in Free-Living and Plant-Associated Symbiotic Growth States. Microbiology and Molecular Biology Reviews, 66(1), 94–121.

Meloni, M., Gurrieri, L., Fermani, S., Velie, L., Sparla, F., Crozet, P., Henri, J., & Zaffagnini, M. (2023). Ribulose-1,5-bisphosphate regeneration in the Calvin-Benson-Bassham cycle: Focus on the last three enzymatic steps that allow the formation of Rubisco substrate. In Frontiers in Plant Science (Vol. 14).

Mi, H., Endo, T., Ogawa, T., & Asada, K. (1995). Thylakoid Membrane-Bound, NADPH-Specific Pyridine Nucleotide Dehydrogenase Complex Mediates Cyclic Electron Transport in the Cyanobacterium Synechocystis sp. PCC 6803. Plant and Cell Physiology, 36(4), 661–668.

Miller, N. T., Vaughn, M. D., & Burnap, R. L. (2021). Electron flow through NDH-1 complexes is the major driver of cyclic electron flow-dependent proton pumping in cyanobacteria. Biochimica et Biophysica Acta (BBA) - Bioenergetics, 1862(3), 148354.

Milton, Abdellaoui, Khadka, N., Dean, D. R., Leech D., Seefeldt L. C., Minteer S. D. (2016). Nitrogenase bioelectrocatalysis: heterogeneous ammonia and hydrogen production by MoFe protein. Energy & Environmental Science, 9, 2550–2554.

Mishra, A. K. (2003). MSX-resistant mutants of Anabaena 7120 with derepressed heterocyst development and nitrogen fixation. World Journal of Microbiology and Biotechnology, 19(7).

Mishra, A. K., Kaushik, M. S., & Tiwari, D. N. (2019). Nitrogenase and Hydrogenase: Enzymes for Nitrogen Fixation and Hydrogen Production in Cyanobacteria. Cyanobacteria: From Basic Science to Applications, 173–191.

Mishra, A., Rajput, S., Gupta, S., Goyal, V., Singh, S., Sharma, S., Shukla, S., Singh, A., Shukla, K., Varma, A., …Shukla, K. (2021). Role of Cyanobacteria in Rhizospheric Nitrogen Fixation. 497–519.

Mohan, S. V., & Pandey, A. (2013). Biohydrogen Production: An Introduction. Biohydrogen, 1–24.

Mondal, J., & Bruce, B. D. (2018). Ferredoxin: the central hub connecting photosystem I to cellular metabolism. Photosynthetica, 56(1), 279–293.

Montgomery, B. L., Lechno-Yossef, S., & Kerfeld, C. A. (2016). Interrelated modules in cyanobacterial photosynthesis: The carbon-concentrating mechanism, photorespiration, and light perception. In Journal of Experimental Botany (Vol. 67, Number 10).

Moore, V., & Vermaas, W. (2024). Functional consequences of modification of the photosystem I/photosystem II ratio in the cyanobacterium Synechocystis sp. PCC 6803. Genetics and Molecular Biology

Mullineaux, C. W. (2014). Electron transport and light-harvesting switches in cyanobacteria. In Frontiers in Plant Science (Vol. 5, Number JAN).

Muro-Pastor, A. M., & Hess, W. R. (2012). Heterocyst differentiation: From single mutants to global approaches. Trends in Microbiology, 20(11), 548–557.

Muro-Pastor, A., Olmedo-Verd, E., Flores, E., & Muro-Pastor, A. M. (2006). All4312, an NtcA-regulated two-component response regulator in Anabaena sp. strain PCC 7120.

Muro-Pastor, A. M., Valladares, A., Flores, E., & Herrero, A. (2002). Mutual dependence of the expression of the cell differentiation regulatory protein HetR and the global nitrogen regulator NtcA during heterocyst development. Molecular Microbiology, 44(5).

Muro-Pastor, M. I., Reyes, J. C., & Florencio, F. J. (2001). Cyanobacteria Perceive Nitrogen Status by Sensing Intracellular 2-Oxoglutarate Levels. Journal of Biological Chemistry, 276(41).

Murukesan, G., Lynch, F., Allahverdiyeva, Y., & Kosourov, S. (2019). Acclimation responses of immobilized N 2 -fixing heterocystous cyanobacteria to long-term H 2 photoproduction conditions: carbon allocation, oxidative stress and carotenoid production. Journal of Applied Phycology, 31(1), 131–143.

Mustila, H., Paananen, P., Battchikova, N., Santana-Sánchez, A., Muth-Pawlak, D., Hagemann, M., …Allahverdiyeva, Y. (2016). The Flavodiiron Protein Flv3 Functions as a Homo-Oligomer During Stress Acclimation and is Distinct from the Flv1/Flv3 Hetero-Oligomer Specific to the O2 Photoreduction Pathway. Plant and Cell Physiology, 57(7), 1468–1483.

Nagao, R., Yokono, M., Ueno, Y., Jiang, T. Y., Shen, J. R., & Akimoto, S. (2020). PH-Induced Regulation of Excitation Energy Transfer in the Cyanobacterial Photosystem i Tetramer. Journal of Physical Chemistry B, 124(10).

Nagao, R., Yokono, M., Ueno, Y., Nakajima, Y., Suzuki, T., Kato, K. H., Tsuboshita, N., Dohmae, N., Shen, J. R., Ehira, S., & Akimoto, S. (2022). Excitation-energy transfer in heterocysts isolated from the cyanobacterium Anabaena sp. PCC 7120 as studied by time-resolved fluorescence spectroscopy. Biochimica et Biophysica Acta (BBA) - Bioenergetics, 1863(1), 148509.

Nagao, R., Yokono, M., Ueno, Y., Suzuki, T., Kato, K., Kato, K. H., Tsuboshita, N., Jiang, T. Y., Dohmae, N., Shen, J. R., …Akimoto, S. (2021). Molecular organizations and function of iron-stress-induced-A protein family in Anabaena sp. PCC 7120. Biochimica et Biophysica Acta - Bioenergetics, 1862(1).

Navarro, J. A., Durán, R. V., De La Rosa, M. A., & Hervás, M. (2005). Respiratory cytochrome c oxidase can be efficiently reduced by the photosynthetic redox proteins cytochrome c6 and plastocyanin in cyanobacteria. FEBS Letters, 579(17), 3565–3568.

Nguyen, H. H., Song, Y., Maret, E. L., Silori, Y., Willow, R., Yocum, C. F., & Ogilvie, J. P. (2023). Charge separation in the photosystem II reaction center resolved by multispectral two-dimensional electronic spectroscopy. Science Advances, 9(18).

Nicolaisen, K., Hahn, A., & Schleiff, E. (2009). The cell wall in heterocyst formation by Anabaena sp. PCC 7120. In Journal of Basic Microbiology (Vol. 49, Number 1).

Nicolaisen, K., Mariscal, V., Bredemeier, R., Pernil, R., Moslavac, S., López-Igual, R., Maldener, I., Herrero, A., …Flores, E. (2009). The outer membrane of a heterocyst-forming cyanobacterium is a permeability barrier for uptake of metabolites that are exchanged between cells. Molecular Microbiology, 74(1).

Nieves-Morión, M., Flores, E., Whitehouse, M. J., Thomen, A., & Foster, R. A. (2021). Single-cell measurements of fixation and intercellular exchange of c and n in the filaments of the heterocyst-forming cyanobacterium anabaena sp. Strain pcc 7120. MBio, 12(4).

Nikkanen, L., Santana Sánchez, A., Ermakova, M., Rögner, M., Cournac, L., & Allahverdiyeva, Y. (2020). Functional redundancy between flavodiiron proteins and NDH-1 in Synechocystis sp. PCC 6803. Plant Journal, 103(4).

Nikkanen, L., Solymosi, D., Jokel, M., & Allahverdiyeva, Y. (2021). Regulatory electron transport pathways of photosynthesis in cyanobacteria and microalgae: Recent advances and biotechnological prospects. Physiologia Plantarum, 173(2).

Nikkanen, L., Vakal, S., Hubáček, M., Santana-Sánchez, A., Konert, G., Wang, Y., Boehm, M., Gutekunst, K., ...Allahverdiyeva, Y. (2025). Flavodiiron proteins associate pH-dependently with the thylakoid membrane for ferredoxin-1-powered O2 photoreduction. New Phytologist, 246(5), 2084–2101.

Nishimura, T., Takahashi, Y., Yamaguchi, O., Suzuki, H., Maeda, S. I., & Omata, T. (2008). Mechanism of low CO2-induced activation of the cmp bicarbonate transporter operon by a LysR family protein in the cyanobacterium Synechococcus elongatus strain PCC 7942. Molecular Microbiology, 68(1), 98–109.

Och, L. M., & Shields-Zhou, G. A. (2012). The Neoproterozoic oxygenation event: Environmental perturbations and biogeochemical cycling. In Earth-Science Reviews (Vol. 110, Numbers 1–4).

Ohashi, Y., Shi, W., Takatani, N., Aichi, M., Maeda, S. I., Watanabe, S., Yoshikawa, H., & Omata, T. (2011). Regulation of nitrate assimilation in cyanobacteria. In Journal of Experimental Botany (Vol. 62, Number 4).

Ortega-Martínez, P., Nikkanen, L., Wey, L. T., Florencio, F. J., Allahverdiyeva, Y., & Díaz-Troya, S. (2024). Glycogen synthesis prevents metabolic imbalance and disruption of photosynthetic electron transport from photosystem II during transition to photomixotrophy in Synechocystis sp. PCC 6803. New Phytologist, 243(1), 162–179.

Ow, S. Y., Nolrel, J., Cardona, T., Taton, A., Lindblad, P., Stensjö, K., & Wright, P. C. (2008). Quantitative Overview of N2 Fixation in Nostoc punctiforme ATCC 29133 through Cellular Enrichments and iTRAQ Shotgun Proteomics. Journal of Proteome Research, 8(1), 187–198.

Paz-Yepes, J., Merino-Puerto, V., Herrero, A., & Flores, E. (2008). The amt gene cluster of the heterocyst-forming cyanobacterium Anabaena sp. strain PCC 7120. Journal of Bacteriology, 190(19).

Pereira, I., Moya, M., Reyes, G., & Kramm, V. (2005). A survey of heterocystous nitrogen-fixing cyanobacteria in Chilean rice fields. In Gayana - Botanica (Vol. 62, Number 1).

Perin, G., Fletcher, T., Sagi-Kiss, V., Gaboriau, D. C. A., Carey, M. R., Bundy, J. G., & Jones, P. R. (2021). Calm on the surface, dynamic on the inside. Molecular homeostasis of Anabaena sp. PCC 7120 nitrogen metabolism. Plant Cell and Environment, 44(6).

Pernil, R., & Schleiff, E. (2019). Metalloproteins in the biology of heterocysts. Life, 9(2).

Picossi, S., Flores, E., & Herrero, A. (2014). ChIP analysis unravels an exceptionally wide distribution of DNA binding sites for the NtcA transcription factor in a heterocyst-forming cyanobacterium. BMC Genomics, 15(1), 1–15.

Picossi, S., Flores, E., & Herrero, A. (2015). The LysR-type transcription factor PacR is a global regulator of photosynthetic carbon assimilation in Anabaena. Environmental Microbiology, 17(9), 3341–3351.

Picossi, S., Valladares, A., Flores, E., & Herrero, A. (2004). Nitrogen-regulated Genes for the Metabolism of Cyanophycin, a Bacterial Nitrogen Reserve Polymer: EXPRESSION AND MUTATIONAL ANALYSIS OF TWO CYANOPHYCIN SYNTHETASE AND CYANOPHYCINASE GENE CLUSTERS IN THE HETEROCYST-FORMING CYANOBACTERIUM ANABAENA SP. PCC 7120. Journal of Biological Chemistry, 279(12), 11582–11592.

Pinevich, A. V., & Averina, S. G. (2024). Taxonomy of Cyanobacteria: The Era of Change. Microbiology 2024 93:5, 93(5), 521–536.

Prasanna, R., Kumar, R., Sood, A., Prasanna, B. M., & Singh, P. K. (2006). Morphological, physiochemical and molecular characterization of Anabaena strains. Microbiological Research, 161(3).

Price, G. D., Badger, M. R., Woodger, F. J., & Long, B. M. (2008). Advances in understanding the cyanobacterial CO2-concentrating-mechanism (CCM): functional components, Ci transporters, diversity, genetic regulation and prospects for engineering into plants. Journal of Experimental Botany, 59(7), 1441–1461.

Puerta-Fernández, E., & Vioque, A. (2011). Hfq is required for optimal nitrate assimilation in the cyanobacterium Anabaena sp. strain PCC 7120. Journal of Bacteriology, 193(14).

Rae, B. D., Long, B. M., Badger, M. R., Price, D. G. (2013). Functions, Compositions, and Evolution of the Two Types of Carboxysomes: Polyhedral Microcompartments That Facilitate CO 2 Fixation in Cyanobacteria and Some Proteobacteria . Microbiology and Molecular Biology Reviews, 77(3), 357–379.

Rajaniemi, P., Hrouzek, P., Kaštovská, K., Willame, R., Rantala, A., Hoffmann, L., Komárek, J., & Sivonen, K. (2005). Phylogenetic and morphological evaluation of the genera Anabaena, Aphanizomenon, Trichormus and Nostoc (Nostacales, cyanobacteria). International Journal of Systematic and Evolutionary Microbiology, 55(1), 11–26.

Raleiras, P., Khanna, N., Miranda, H., Mészáros, L. S., Krassen, H., Ho, F., Battchikova, N., Aro, E. M., …Styring, S. (2016). Turning around the electron flow in an uptake hydrogenase. EPR spectroscopy and in vivo activity of a designed mutant in HupSL from Nostoc punctiforme. Energy & Environmental Science, 9(2), 581–594.

Ramos, J. L., Madueño, F., & Guerrero, M. G. (1985). Regulation of nitrogenase levels in Anabaena sp. ATCC 33047 and other filamentous cyanobacteria. Archives of Microbiology, 141(2), 105–111.

Raymond, J., & Blankenship, R. E. (2008). The origin of the oxygen-evolving complex. In Coordination Chemistry Reviews (Vol. 252, Numbers 3–4).

Renström-Keliner, E., Rai, A. N., & Bergman, B. (1990). Correlation between nitrogenase and glutamine synthetase expression in the cyanobacterium Anabaena cylindrical. Physiologia Plantarum, 80(1).

Reyes, J. C., Muro-Pastor, M. I., & Florencio, F. J. (1997). Transcription of glutamine synthetase genes (glnA and glnN) from the cyanobacterium Synechocystis sp. strain PCC 6803 is differently regulated in response to nitrogen availability. Journal of Bacteriology, 179(8), 2678–2689.

Rice, E., Baird, R., Eaton, A., & Clesceri, L. (2012). Standard Methods for the Examination of Water and Wastewater. Standard Methods.

Rizzetto, N., Traverso, E., Sabia, A., Fiorin, F., Francese, C., Trainotti, L., Morosinotto, T., & Alboresi, A. (2025). Flavodiiron Protein Activity Outcompetes Cyclic Electron Transport When Expressed in Angiosperm Nicotiana tabacum. Physiologia Plantarum, 177(4), e70453.

Robles-Rengel, R., Florencio, F. J., & Muro-Pastor, M. I. (2019). Redox interference in nitrogen status via oxidative stress is mediated by 2-oxoglutarate in cyanobacteria. New Phytologist, 224(1).

Roumezi, B., Avilan, L., Risoul, V., Brugna, M., Rabouille, S., & Latifi, A. (2020). Overproduction of the Flv3B flavodiiron, enhances the photobiological hydrogen production by the nitrogen-fixing cyanobacterium Nostoc PCC 7120. Microbial Cell Factories, 19(1), 1–10.

Saenger, W., Jordan, P., & Krauß, N. (2002). The assembly of protein subunits and cofactors in photosystem I. In Current Opinion in Structural Biology (Vol. 12, Number 2).

Sánchez-Baracaldo, P., Bianchini, G., Wilson, J. D., & Knoll, A. H. (2022). Cyanobacteria and biogeochemical cycles through Earth history. In Trends in Microbiology (Vol. 30, Number 2).

Sander, J., Nowaczyk, M., Buchta, J., Dau, H., Vass, I., Deák, Z., Dorogi, M., Iwai, M., & Rögner, M. (2010). Functional characterization and quantification of the alternative PsbA copies in Thermosynechococcus elongatus and their role in photoprotection. Journal of Biological Chemistry, 285(39).

Santabarbara, S., Hastings, G., Tian, L.-R., & Chen, J.-H. (2024). Photosystem I: A Paradigm for Understanding Biological Environmental Adaptation Mechanisms in Cyanobacteria and Algae. International Journal of Molecular Sciences 2024, Vol. 25, Page 8767, 25(16), 8767.

Santamaría-Gómez, J., Mariscal, V., & Luque, I. (2018). Mechanisms for Protein Redistribution in Thylakoids of Anabaena During Cell Differentiation. Plant and Cell Physiology, 59(9).

Santana-Sanchez, A., Solymosi, D., Mustila, H., Bersanini, L., Aro, E. M., & Allahverdiyeva, Y. (2019). Flavodiiron proteins 1–to-4 function in versatile combinations in O2 photoreduction in cyanobacteria. ELife, 8.

Saura, P., & Kaila, V. R. I. (2019). Molecular dynamics and structural models of the cyanobacterial NDH-1 complex. Biochimica et Biophysica Acta (BBA) - Bioenergetics, 1860(3), 201–208.

Schell, M. A. (1993). Molecular biology of the LysR family of transcriptional regulators. Annual Review of Microbiology, 47, 597–626.

Schirrmeister, B. E., De Vos, J. M., Antonelli, A., & Bagheri, H. C. (2013). Evolution of multicellularity coincided with increased diversification of cyanobacteria and the Great Oxidation Event. Proceedings of the National Academy of Sciences of the United States of America, 110(5).

Schirrmeister, B. E., Sanchez-Baracaldo, P., & Wacey, D. (2016). Cyanobacterial evolution during the Precambrian. International Journal of Astrobiology, 15(3).

Schmetterer, G. (2016). The Respiratory Terminal Oxidases (RTOs) of Cyanobacteria.

Schmidt-Rohr, K. (2021). O2 and other high-energy molecules in photosynthesis: Why plants need two photosystems. Life, 11(11).

Schmitz, S., & Böhme, H. (1995). Amino acid residues involved in functional interaction of vegetative cell ferredoxin from the cyanobacterium Anabaena sp. PCC 7120 with ferredoxin:NADP reductase, nitrite reductase and nitrate reductase. BBA - Bioenergetics, 1231(3).

Schmitz, S., Navarro, F., Kutzki, C. K., Florencio, F., & Bohme, H. (1996). Glutamate 94 of [2Fe□2S]-ferredoxins is important for efficient electron transfer in the 1:1 complex formed with

ferredoxin-glutamate synthase (GltS) from Synechocystis sp. PCC 6803. Biochimica et Biophysica Acta (BBA) - Bioenergetics, 1277(1–2), 135–140.

Schrautemeier, B., Böhme, H., & Böger, P. (1984). In vitro studies on pathways and regulation of electron transport to nitrogenase with a cell-free extract from heterocysts of Anabaena variabilis. Archives of Microbiology, 137(1), 14–20.

Schuller, J. M., Birrell, J. A., Tanaka, H., Konuma, T., Wulfhorst, H., Cox, N., Schuller, S. K., …Nowaczyk, M. M. (2019). Structural adaptations of photosynthetic complex I enable ferredoxin-dependent electron transfer. Science, 363(6424), 257–260.

Schuller, J. M., Saura, P., Thiemann, J., Schuller, S. K., Gamiz-Hernandez, A. P., Kurisu, G., Nowaczyk, M. M., & Kaila, V. R. I. (2020). Redox-coupled proton pumping drives carbon concentration in the photosynthetic complex I. Nature Communications 2020 11:1, 11(1), 494-.

Sherman, D. M., Tucker, D., & Sherman, L. A. (2000). HETEROCYST DEVELOPMENT AND LOCALIZATION OF CYANOPHYCIN IN N2-FIXING CULTURES OF ANABAENA SP. PCC 7120 (CYANOBACTERIA). Journal of Phycology, 36(5), 932–941.

Shimakawa, G. (2023). Electron transport in cyanobacterial thylakoid membranes: are cyanobacteria simple models for photosynthetic organisms? In Journal of Experimental Botany (Vol. 74, Number 12).

Shinde, S., Zhang, X., Singapuri, S. P., Kalra, I., Liu, X., Morgan-Kiss, R. M., & Wang, X. (2020). Glycogen Metabolism Supports Photosynthesis Start through the Oxidative Pentose Phosphate Pathway in Cyanobacteria. Plant Physiology, 182(1), 507–517.

Skizim, N. J., Ananyev, G. M., Krishnan, A., & Dismukes, G. C. (2012). Metabolic pathways for photobiological hydrogen production by nitrogenase- and hydrogenase-containing unicellular cyanobacteria Cyanothece. Journal of Biological Chemistry, 287(4).

Solymosi, D., Shevela, D., & Allahverdiyeva, Y. (2022). Nitric oxide represses photosystem II and NDH-1 in the cyanobacterium Synechocystis sp. PCC 6803. Biochimica et Biophysica Acta - Bioenergetics, 1863(1).

Spiller, H., Latorre, C., Hassan, M. E., & Shanmugam, K. T. (1986). Isolation and characterization of nitrogenase-derepressed mutant strains of cyanobacterium Anabaena variabilis. Journal of Bacteriology, 165(2), 412–419.

Stadnichuk, I. N., Krasilnikov, P. M., & Zlenko, D. V. (2015). Cyanobacterial phycobilisomes and phycobiliproteins. In Microbiology (Russian Federation) (Vol. 84, Number 2).

Stal, L. J. (2015). Nitrogen Fixation in Cyanobacteria. Encyclopedia of Life Sciences, 1–9.

Stal, L. J. (2017). The effect of oxygen concentration and temperature on nitrogenase activity in the heterocystous cyanobacterium Fischerella sp. Scientific Reports 2017 7:1, 7(1), 5402-.

Stebegg R. (2011). Heterotrophic growth of the cyanobacterium Anabaena (Nostoc) sp. strain PCC7120 and its dependence on a functional cox1 locus encoding cytochrome c oxidase. PhD Diss., Uniwie.

Steinhauser, D., Fernie, A. R., & Araújo, W. L. (2012). Unusual cyanobacterial TCA cycles: Not broken just different. In Trends in Plant Science (Vol. 17, Number 9).

Stevanovic, M., Hahn, A., Nicolaisen, K., Mirus, O., & Schleiff, E. (2012). The components of the putative iron transport system in the cyanobacterium Anabaena sp. PCC 7120. Environmental Microbiology, 14(7).

Stewart, W. D., Haystead, A., Pearson, H. W. (1996). Nitrogenase Activity in Heterocysts of Blue-Green Algae. Nature, 224, 226–228.

Stewart, W. D. P., & Rowell, P. (1975). Effects of L-methionine-DL-sulphoximine on the assimilation of newly fixed NH3, acetylene reduction and heterocyst production in Anabaena cylindrica. Biochemical and Biophysical Research Communications, 65(3), 846–856.

Storti, M., Puggioni, M. P., Segalla, A., Morosinotto, T., & Alboresi, A. (2020). The chloroplast NADH dehydrogenase-like complex influences the photosynthetic activity of the moss Physcomitrella patens. Journal of Experimental Botany, 71(18).

Su, L., Souaibou, Y., Hôtel, L., Paris, C., Weissman, K. J., & Aigle, B. (2024). Biosynthesis of novel desferrioxamine derivatives requires unprecedented crosstalk between separate NRPS-independent siderophore pathways. Applied and Environmental Microbiology, 90(3).

Sui, S. F. (2021). Structure of Phycobilisomes. Annual Review of Biophysics, 50(Volume 50, 2021), 53–72.

Summerfield, T. C., Toepel, J., & Sherman, L. A. (2008). Low-oxygen induction of normally cryptic psbA genes in cyanobacteria. Biochemistry, 47(49).

Sun, H., Shi, Q., Liu, N. Y., Zhang, S. B., & Huang, W. (2023). Drought stress delays photosynthetic induction and accelerates photoinhibition under short-term fluctuating light in tomato. Plant Physiology and Biochemistry, 196, 152–161.

Tamagnini, P., Axelsson, R., Lindberg, P., Oxelfelt, F., Wünschiers, R., & Lindblad, P. (2002). Hydrogenases and Hydrogen Metabolism of Cyanobacteria. Microbiology and Molecular Biology Reviews, 66(1), 1–20.

Tamagnini, P., Leitão, E., Oliveira, P., Ferreira, D., Pinto, F., Harris, D. J., Heidorn, T., & Lindblad, P. (2007). Cyanobacterial hydrogenases: Diversity, regulation and applications. In FEMS Microbiology Reviews (Vol. 31, Number 6).

Tanigawa, R., Shirokane, M., Maeda, S. I., Omata, T., Tanaka, K., & Takahashi, H. (2002). Transcriptional activation of NtcA-dependent promoters of Synechococcus sp. PCC 7942 by 2-oxoglutarate in vitro. Proceedings of the National Academy of Sciences, 99(7), 4251–4255.

Theune, M. L., Hildebrandt, S., Steffen-Heins, A., Bilger, W., Gutekunst, K., & Appel, J. (2021). In-vivo quantification of electron flow through photosystem I – Cyclic electron transport makes up about 35% in a cyanobacterium. Biochimica et Biophysica Acta - Bioenergetics, 1862(3).

Thomas, J. (1970). Absence of the pigments of photosystem II of photosynthesis in heterocysts of a blue-green alga. Nature, 228(5267), 181–183.

Thomas, J., Meeks, J. C., Wolk, C. P., Shaffer, P. W., Austin, S. M., & Chien, W.-S. (1977). Formation of glutamine from [13n]ammonia, [13n]dinitrogen, and [14C]glutamate by heterocysts isolated from Anabaena cylindrica. Journal of Bacteriology, 129(3), 1545–1555.

Thoré, E. S. J., Muylaert, K., Bertram, M. G., & Brodin, T. (2023). Microalgae. Current Biology, 33(3), R91–R95.

Torrado, A., Ramírez-Moncayo, C., Navarro, J. A., Mariscal, V., & Molina-Heredia, F. P. (2019). Cytochrome c6 is the main respiratory and photosynthetic soluble electron donor in heterocysts of the cyanobacterium Anabaena sp. PCC 7120. Biochimica et Biophysica Acta - Bioenergetics, 1860(1).

Tsujii, M., Kobayashi, A., Kano, A., Kera, K., Takagi, T., Nagata, N., Kojima, S., Hikosaka, K., Oguchi, R., Sonoike, K., …Uozumi, N. (2024). Na + -driven pH regulation by Na+/H+ antiporters promotes photosynthetic efficiency. in cyanobacteria. Plant Physiology, 197(1), 562

Tsygankov, A. A. (2007). Nitrogen-fixing cyanobacteria: A review. Applied Biochemistry and Microbiology, 43(3), 250–259.

Tumer, N. E., Robinson, S. J., & Haselkorn, R. (1983). Different promoters for the Anabaena glutamine synthetase gene during growth using molecular or fixed nitrogen. Nature, 306(5941), 337–342.

Valladares, A., & Herrero, A. (2025). ThyD Is a Thylakoid Membrane Protein Influencing Cell Division and Acclimation to High Light in the Multicellular Cyanobacterium Anabaena sp. Strain PCC 7120. Molecular Microbiology, 123(1), 31–47.

Valladares, A., Herrero, A., Pils, D., Schmetterer, G., Flores, E., & Vespucio, A. (2003). Cytochrome c oxidase genes required for nitrogenase activity and diazotrophic growth in Anabaena sp. PCC 7120. Molecular Microbiology, 47(5), 1239–1249.

Valladares, A., Maldener, I., Muro-Pastor, A. M., Flores, E., & Herrero, A. (2007). Heterocyst development and diazotrophic metabolism in terminal respiratory oxidase mutants of the cyanobacterium Anabaena sp. strain PCC 7120. Journal of Bacteriology, 189(12).

Valladares, A., Rodríguez, V., Camargo, S., Martínez-Noël, G. M. A., Herrero, A., & Luque, I. (2011). Specific role of the cyanobacterial pipX factor in the heterocysts of Anabaena sp. strain PCC 7120. Journal of Bacteriology, 193(5).

van Stokkum, I. H. M., Niedzwiedzki, D. M., Akhtar, P., Biswas, A., Lambrev, P. H., & Liu, H. (2025). Cyanobacteria dynamically regulate phycobilisome-to-photosystem excitation energy transfer. IScience, 28(6).

Vega-Palas, M. A., Flores, E., & Herrero, A. (1992). NtcA, a global nitrogen regulator from the cyanobacterium Synechococcus that belongs to the Crp family of bacterial regulators. Molecular Microbiology, 6(13), 1853–1859.

Vicente, J. B., Carrondo, M. A., Teixeira, M., & Frazão, C. (2008). Structural Studies on Flavodiiron Proteins. In Methods in Enzymology (Vol. 437).

Vicente, J. B., Gomes, C. M., Wasserfallen, A., & Teixeira, M. (2002). Module fusion in an A-type flavoprotein from the cyanobacterium Synechocystis condenses a multiple-component pathway in a single polypeptide chain. Biochemical and Biophysical Research Communications, 294(1).

Videau, P., Cozy, L. M., Young, J. E., Ushijima, B., Oshiro, R. T., Rivers, O. S., Burger, A. H., & Callahan, S. M. (2015). The trpE Gene Negatively Regulates Differentiation of Heterocysts at the Level of Induction in Anabaena sp. Strain PCC 7120.

Videau, P., Rivers, O. S., Hurd, K., Ushijima, B., Oshiro, R. T., Ende, R. J., O'Hanlon, S. M., & Cozy, L. M. (2016). The heterocyst regulatory protein HetP and its homologs modulate heterocyst commitment in Anabaena sp. strain PCC 7120. Proceedings of the National Academy of Sciences of the United States of America, 113(45), E6984–E6992.

Vignais, P. M. (2005). H/D exchange reactions and mechanistic aspects of the hydrogenases. In Coordination Chemistry Reviews (Vol. 249, Numbers 15-16 SPEC. ISS.).

Viola, S., Bailleul, B., Yu, J., Nixon, P., Sellés, J., Joliot, P., & Wollman, F. A. (2019). Probing the electric field across thylakoid membranes in cyanobacteria. Proceedings of the National Academy of Sciences of the United States of America, 116(43).

Volgusheva, A., Kosourov, S., Lynch, F., & Allahverdiyeva, Y. (2019). Immobilized heterocysts as microbial factories for sustainable nitrogen fixation. Journal of Biotechnology: X, 4.

Wada, S., Yamamoto, H., Suzuki, Y., Yamori, W., Shikanai, T., & Makino, A. (2018). Flavodiiron Protein Substitutes for Cyclic Electron Flow without Competing CO2 Assimilation in Rice. Plant Physiology, 176(2), 1509–1518.

Walsby, A. E. (2007). Cyanobacterial heterocysts: terminal pores proposed as sites of gas exchange. Trends in Microbiology, 15(8).

Walter, J., Lynch, F., Battchikova, N., Aro, E. M., & Gollan, P. J. (2016). Calcium impacts carbon and nitrogen balance in the filamentous cyanobacterium Anabaena sp. PCC 7120. Journal of Experimental Botany, 67(13).

Wan, N., DeLorenzo, D. M., He, L., You, L., Immethun, C. M., Wang, G., Baidoo, E. E. K., Hollinshead, W., …Tang, Y. J. (2017). Cyanobacterial carbon metabolism: Fluxome plasticity and oxygen dependence. Biotechnology and Bioengineering, 114(7).

Wang, H. L., Postier, B. L., & Burnap, R. L. (2004). Alterations in Global Patterns of Gene Expression in Synechocystis sp. PCC 6803 in Response to Inorganic Carbon Limitation and the Inactivation of ndhR, a LysR Family Regulator. Journal of Biological Chemistry, 279(7), 5739–5751.

Wang, K., Mahbub, M., Mastroianni, G., Valladares, A., & Mullineaux, C. W. (2024). mRNA localization and thylakoid protein biogenesis in the filamentous heterocyst-forming cyanobacterium Anabaena sp.PCC 7120. Journal of Bacteriology, 206(10).

Watanabe, M., Kubota, H., Wada, H., Narikawa, R., & Ikeuchi, M. (2011). Novel Supercomplex Organization of Photosystem I in Anabaena and Cyanophora paradoxa. Plant and Cell Physiology, 52(1), 162–168.

Watzer, B., Spät, P., Neumann, N., Koch, M., Sobotka, R., MacEk, B., Hennrich, O., & Forchhammer, K. (2019). The signal transduction protein PII controls ammonium, nitrate and urea uptake in cyanobacteria. Frontiers in Microbiology, 10(JUN).

Wegelius, A., Li, X., Turco, F., & Stensjö, K. (2018). Design and characterization of a synthetic minimal promoter for heterocyst-specific expression in filamentous cyanobacteria. PLOS ONE, 13(9), e0203898.

Wei, T. F., Ramasubramanian, T. S., & Golden, J. W. (1994). Anabaena sp. strain PCC 7120 ntcA gene required for growth on nitrate and heterocyst development. Journal of Bacteriology, 176(15), 4473–4482.

Wilson, S. T., Caffin, M., White, A. E., & Karl, D. M. (2021). Evaluation of argon-induced hydrogen production as a method to measure nitrogen fixation by cyanobacteria. Journal of Phycology, 57(3), 863–873.

Wolk, C. P. (1973). Physiology and cytological chemistry blue-green algae. In Bacteriological reviews (Vol. 37, Number 1).

Wolk, C. P., Thomas, J., Shaffer, P. W., Austin, S. M., & Galonsky, A. (1976). Pathway of nitrogen metabolism after fixation of 13N labeled nitrogen gas by the cyanobacterium, Anabaena cylindrica. Journal of Biological Chemistry, 251(16), 5027–5034.

Xing, W. Y., & Zhang, C. C. (2019). Preventing accidental heterocyst development in cyanobacteria. Journal of Bacteriology, 201(17).

Yamamoto, H., & Shikanai, T. (2019). PGR5-Dependent Cyclic Electron Flow Protects Photosystem I under Fluctuating Light at Donor and Acceptor Sides. Plant Physiology, 179(2), 588–600.

Yamamoto, H., Takahashi, S., Badger, M. R., & Shikanai, T. (2016). Artificial remodelling of alternative electron flow by flavodiiron proteins in Arabidopsis. Nature Plants, 2(3).

Yang, Q. Y., Wang, X. Q., Yang, Y. J., & Huang, W. (2024). Fluctuating light induces a significant photoinhibition of photosystem I in maize. Plant Physiology and Biochemistry, 207, 108426.

Yi, S., Guo, X., Lou, W., Mao, S., Luan, G., & Lu, X. (2024). Structure, Regulation, and Significance of Cyanobacterial and Chloroplast Adenosine Triphosphate Synthase in the Adaptability of Oxygenic Photosynthetic Organisms. Microorganisms 2024, Vol. 12, Page 940, 12(5), 940.

Yoon, H. S., & Golden, J. W. (1998). Heterocyst Pattern Formation Controlled by a Diffusible Peptide. Science, 282(5390), 935–938.

Yoon, H. S., & Golden, J. W. (2001). PatS and Products of Nitrogen Fixation Control Heterocyst Pattern. Journal of Bacteriology, 183(8), 2605–2613.

You, D., Rasul, F., Wang, T., & Daroch, M. (2024). Insufficient Acetyl-CoA Pool Restricts the Phototrophic Production of Organic Acids in Model Cyanobacteria. International Journal of Molecular Sciences, 25(21), 11769.

Yutthanasirikul, R., Kurdrid, P., Saree, S., Senachak, J., Saelee, M., & Hongsthong, A. (2024). Increasing activity of the GS-GOGAT cycle highlights the compensation of N-assimilation in the absence of nitrogen and its metabolic effects in cyanobacteria. Algal Research, 79, 103490.

Zeng, X., & Zhang, C. C. (2022). The Making of a Heterocyst in Cyanobacteria. In Annual Review of Microbiology (Vol. 76).

Zeth, K., Fokinas, O., & Forchhammers, K. (2014). Structural basis and target-specific modulation of ADP sensing by the Synechococcus elongatus PII signaling protein. Journal of Biological Chemistry, 289(13), 8960–8972.

Zhang, C. C., Zhou, C. Z., Burnap, R. L., & Peng, L. (2018). Carbon/Nitrogen Metabolic Balance: Lessons from Cyanobacteria. Trends in Plant Science, 23(12), 1116–1130.

Zhang, C., Shuai, J., Ran, Z., Zhao, J., Wu, Z., Liao, R., Wu, J., Ma, W., & Lei, M. (2020). Structural insights into NDH-1 mediated cyclic electron transfer. Nature Communications 2020 11:1, 11(1), 888-.

Zhang, H., Liu, Y., Nie, X., Liu, L., Hua, Q., Zhao, G. P., & Yang, C. (2018). The cyanobacterial ornithine-ammonia cycle involves an arginine dihydrolase article. Nature Chemical Biology, 14(6).

Zhang, H., & Yang, C. (2019). Arginine and nitrogen mobilization in cyanobacteria. In Molecular Microbiology (Vol. 111, Number 4).

Zhang, L. C., Chen, Y. F., Chen, W. L., & Zhang, C. C. (2008). Existence of periplasmic barriers preventing green fluorescent protein diffusion from cell to cell in the cyanobacterium Anabaena sp. strain PCC 7120. Molecular Microbiology, 70(4).

Zhang, P., Allahverdiyeva, Y., Eisenhut, M., & Aro, E. M. (2009). Flavodiiron proteins in oxygenic photosynthetic organisms: Photoprotection of photosystem II by FIv2 and FIv4 in Synechocystis sp. PCC 6803. PLoS ONE, 4(4).

Zhang, P., Eisenhut, M., Brandt, A. M., Carmel, D., Silén, H. M., Vass, I., Allahverdiyeva, Y., Salminen, T. A., & Aro, E. M. (2012). Operon flv4-flv2 provides cyanobacterial photosystem ii with flexibility of electron transfer. Plant Cell, 24(5).

Zhang, S. (2011). The tricarboxylic acid cycle in cyanobacteria. Science.

Zhang, S., Zou, B., Cao, P., Su, X., Xie, F., Pan, X., & Li, M. (2023). Structural insights into photosynthetic cyclic electron transport. In Molecular Plant (Vol. 16, Number 1).

Zhang, Y., Pu, H., Wang, Q., Cheng, S., Zhao, W., Zhang, Y., & Zhao, J. (2007). PII is important in regulation of nitrogen metabolism but not required for heterocyst formation in the cyanobacterium Anabaena sp. PCC 7120. Journal of Biological Chemistry, 282(46), 33641–33648.

Zhang, Y., & Zhao, J. D. (2008). PII, the key regulator of nitrogen metabolism in the cyanobacteria. Science in China, Series C: Life Sciences, 51(12).

Zhou, J. X., Zhou, J., Yang, H. M., Chen, M., & Huang, F. (2008). Characterization of two glutaminases from the filamentous cyanobacterium Anabaena sp. PCC 7120. FEMS Microbiology Letters, 289(2), 241–249.

Zhu, J., Kong, R., & Wolk, C. P. (1998). Regulation of hepA of Anabaena sp. strain PCC 7120 by elements 5' from the gene and by hepK. Journal of Bacteriology, 180(16), 4233–4242.

Zulkefli, N. S., & Hwang, S. J. (2020). Heterocyst Development and Diazotrophic Growth of Anabaena variabilis under Different Nitrogen Availability. Life, 10(11), 279.

TURUN
YLIOPISTO
UNIVERSITY
OF TURKU

Painosalama, Turku, Finland 2026

ISBN 978-952-02-0695-6 (PRINT)
ISBN 978-952-02-0696-3 (PDF)
ISSN 0082-7002 (Print)
ISSN 2343-3175 (Online)